DESIGN AND DEVELOPMENT OF A WATER OBSERVATORY: AN AUTONOMOUS ENVIRONMENTAL SAMPLING SYSTEM FOR IN-SITU SENSING OF LAKES AND RIVERS.

By

MUWANIKA JDIOBE

Bachelor of Science in Mechanical and Aerospace Engineering
Oklahoma State University
Stillwater, OK
2019

Submitted to the Faculty of the
Graduate College of the
Oklahoma State University
in partial fulfillment of
the requirements for
the Degree of
Master of Science
December, 2020

DESIGN AND DEVELOPMENT OF A WATER OBSERVATORY:
AN AUTONOMOUS ENVIRONMENTAL SAMPLING SYSTEM
FOR IN-SITU SENSING OF LAKES AND RIVERS.

Thesis Approved:

Dr. Jamey D. Jacob

Thesis Advisor

Dr. Brian R. Elbing

Dr. David J. Lampert

ACKNOWLEDGMENTS

I thank my adviser, Dr. Jamey Jacob, who has mentored and supported me during my undergraduate and graduate endeavours. My academic committee Dr. David Lampert and Dr. Brian Elbing, thank you for the significant role you played in making me a successful graduate student. Thank you to the Oklahoma State University Unmanned System Research Institute (USRI) and the United States Bureau of Reclamation for supporting and sponsoring this project. My family and friends have been supportive through this process and therefore, I am appreciative for their unconditional support. Special thanks to Pamula Abriham for collaborating with me during the data collection, and Levi Ross for the tremendous support and guide with MATLAB programming.

Acknowledgments reflect the views of the author and are not endorsed by committee members or Oklahoma State University.

Name: MUWANIKA JDIOBE

Date of Degree: DECEMBER, 2020

Title of Study: DESIGN AND DEVELOPMENT OF A WATER OBSERVATORY: AN AUTONOMOUS ENVIRONMENTAL SAMPLING SYSTEM FOR IN-SITU SENSING OF LAKES AND RIVERS.

Major Field: MECHANICAL AND AEROSPACE ENGINEERING

Abstract:

This project focuses on the design, development, and implementation of an autonomous system, or unmanned surface vessel (USV), known as MANUEL (Mobile Autonomously Navigable USV for Evaluation of Lakes). MANUEL is an autonomous boat that can monitor water quality in lakes, rivers, and reservoirs to monitor modern-day pollution from industries and run off from agricultural farmlands into lakes and rivers. The USV can be coupled with an unmanned aircraft system (UAS) to collect data and enhance the water quality sensing capabilities. The surface vehicle is a single meshed W-V-shaped hull for improved stability and operability in all weather and wave conditions including turbulent water and strong winds. MANUEL is powered by two electric driven thrusters providing enhanced maneuverability and it is controlled using an Orange Cube Pixhawk V.2.0. as the autopilot.

MANUEL measures water quality parameters using its embedded sensor probes that are in direct contact with the water. Critical water quality parameters include water temperature, dissolved oxygen, chlorophyll, pH, turbidity, conductivity, salinity, and depth as well as nutrients of the body of water. The data collected is stored on board. Using digital maps and GPS, MANUEL can autonomously map an entire lake with no human intervention, even in conditions unsuitable for humans such as high winds or storms. After the autonomous mission, the data is retrieved from MANUEL, analyzed using MATLAB to map the observed parameters, and builds prediction models for the water quality of the body of water and the corresponding water shed. Boomer Lake, Lake McMurtry, and Grand Lake in Oklahoma have been used as test sites. In Grand Lake MANUEL is currently monitoring and surveying the water quality to better understand and prevent Harmful Algal Blooms (HABs).

TABLE OF CONTENTS

LIST OF TABLES

LIST OF FIGURES

CHAPTER I

INTRODUCTION

1.1 Background

As Unmanned Systems are increasingly becoming popular, they are used in more numerous ways than ever before. Both in military and civilian applications such as, environmental observation, search and recuse, and research on land, water and in air. However, the use of surface water Unmanned Automated System (UAS) has not been greatly explored. Water surface UAS has a higher endurance,and range compared to Unmanned Aerial Vehicles (UAVs) such as multi rotor. The Water surface UAS can also operate in extreme environments that are not easily accessible by both UAVs and human. Therefore, the Water Surface Autonomous System supplements the already existing platforms and systems hence offering an all-around survey, and environmental observations both in air, at the water surface and under water. Surface water UAS are safe, inexpensive and easy to use for water monitoring and research compared to the use of the manned systems.

Previously at Oklahoma State University's Unmanned System Research Institute (USRI), the first prototype of a Water Surface Autonomous System was designed and used to collect data from different lakes and creeks around Oklahoma, namely Boomer Lake, Lake McMurtry in Stillwater and Salina Creek in Tulsa. However, the system experienced some challenges and limitations during its missions such as poor turn radius, low speed, and difficulty in maneuvering under strong winds above 15 mph. The designed Water Surface Autonomous System collected temperature, depth, pH and conductivity of water data. Figure 1 was the first Water Surface Autonomous System prototype known as Aquarius 1.

Figure 1: A picture of Aquarius 1

1.2 Motivation

Three percent of the water in the world is fresh and only one half of one percent of fresh water is available for our use, according to the U.S. Bureau of Reclamation [25]. Due to modern-day pollution from industries and run off from agricultural farmlands, natural water sources such as lakes, when not properly maintained, can be harmful to our life by exposing us to polluted drinking water, contaminated food sources, and can even be harmful when swimming. For example, recently Grand Lake was shut down on July 4th, it's busiest day of the year, due to harmful algal blooms, severely impacting the local economy.

This research focuses on the design, development, and implementation of an autonomous system known as MANUEL, an autonomous boat that monitors water quality such as temperature of water, dissolved oxygen, chlorophyll, pH, turbidity, conductivity, salinity, depth and nutrients of the lakes, rivers, and reservoirs. The water quality parameters determine whether the water is safe for drinking, cooking, swimming, and how well it can support aquatic life such as fish and amphibians. The autonomous boat will be coupled with an autonomous aerial vehicle to collect data and enhance the water quality sensing capabilities as demonstrated in figure 2.

Figure 2: UAS for water quality monitoring

MANUEL measures water quality parameters using its embedded sensor probes that are in direct contact with the water. The data collected is stored on board. Using digital maps, programs such as mission planner and GPS, MANUEL can autonomously map an entire lake with no human intervention, even in conditions unsuitable for humans such as high winds or storms. After the autonomous mission, the data is retrieved from MANUEL, analyzed using MATLAB to map the pollution levels, and build prediction models for the water quality of the water shed.

MANUEL provides a fast, inexpensive, efficient, and more accurate method for water monitoring by health officials, scientists, and environmental monitoring agencies. The designed system will help the planet by increasing public health and water quality awareness, helping to save lives. Every year millions of dollars are spent to monitor and maintain our natural water sources. MANUEL provides a more cost-efficient way to create a safe world with clean water for all. The mission to save lives has started with Lake McMurtry and Grand Lake where MANUEL is currently monitoring and surveying the water quality, but this system will be deployed across the state, nation, and world.

1.3 Mission CONOPs/Profile

MANUEL's mission of monitoring and surveying the lakes, rivers, and reservoirs involves following a predefined path set in mission planner. The path followed is in a lawnmower pattern while measuring different water quality parameters as shown in figure 3..

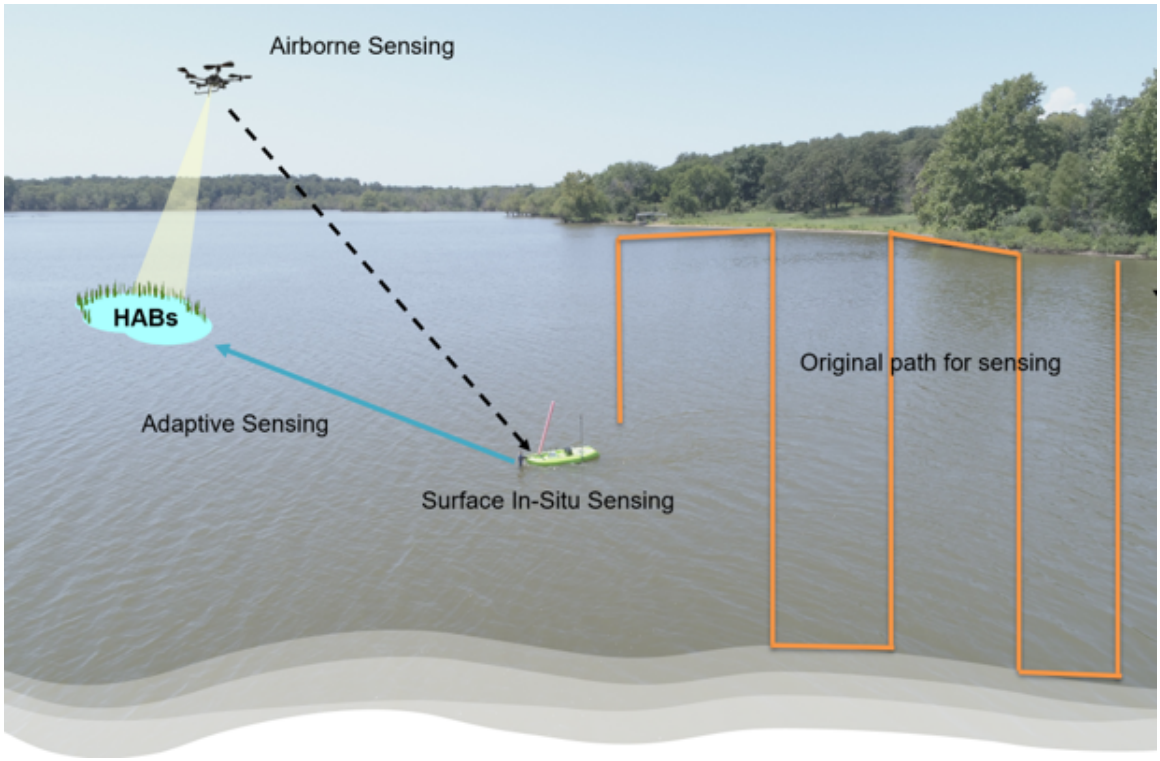

Figure 3: MANUEL's CONOPs

However, when the unmanned aerial vehicle identifies or spots any active Harmful Algae Blooms (HABs) as MANUEL is executing the regular mission, the UAV communicates with MANUEL, which then responds by heading to direction of the HABs to collect a high resolution data in the process known as adaptive sensing.

1.4 Goal

The main goal of this thesis is to design, evaluate and analyze a water surface autonomous system that can be used for environmental water observations and in-situ sensing. The objectives of the thesis are as follows.

1.4.1 Objective 1

Design and build of the Water Surface Autonomous Vehicle; A detailed design and analysis of the Water Surface Autonomous Vehicle, includes the vehicle platform and its automatic control unit. The functions, capabilities, potentials of the platform and control limitations, and challenges clearly identified and explained with possible strategies to mitigate the challenges.

1.4.2 Objective 2

Sensor integration and programming; Identify the necessary water quality sensors that will be incorporated within the Water Surface Autonomous System; this involves identifying the

capabilities and the limitations. It also involves the integration of the sensors into the overall system and programming the micro programmable board to store the data collected.

1.4.3 Objective 3

Calibration and Validation of Sensors collecting data; The sensors integrated within the system can only be valuable if well calibrated and the data collected can be validated. The sensors are calibrated with the information provided by the manufacturer. Furthermore, the data collected using the sensors will be compared to data collected by other means hence validated.

1.4.4 Objective 4

Testing the integrated system and real-world application; The fully integrated system involving the sensors and the Water Surface Autonomous System is tested at Boomer Lake, Grand Lake, and Lake McMurtry in Stillwater. The system is also used in the field to collect data for practical application.

1.5 Thesis Outline

Chapter 1; includes the background and motivation for this research, chapter 2 addresses the literature review about the approaches taken in surveying of lakes and rivers; as well the previous work done by USRI in terms of methods for water monitoring. Chapter 3 details the design and development of MANUEL. Chapter 4; gives a detailed account of data acquisition: water quality parameters of interest, calibration, sensor selection, and sensor vehicle integration. Chapter 5 documents the test, implementations and results. Finally, this report includes a conclusion and future works and plans.

CHAPTER II

Literature Review and Previous Work

2.1 Literature Review

According to Becq, defining and understanding water quality parameters is critical. Water quality parameters are classified in three different classes. The first category is parameters that can be measured by in-situ probes such as turbidity, temperature, pH, conductivity, dissolved oxygen, chlorophyll-a and redox among others. The in-situ probes are easy to maintain, calibrate, affordable and install [8]. The second category is parameters that require the use of analyzers because they cannot be measured with the use of in-situ probes. However, the analyzers can be automated. These parameters include Ammonia, Phosphates, Nitrates, among others. Unlike in-situ probes, the use of analyzers involve the using chemical reactants and pumping system to filter. Analyzers are difficult to automate, maintain and expensive. Lastly, there are water quality parameters such as metals and ecotoxicology that can neither be analyzed by in-situ probes nor analyzers and hence require the use of sophisticated laboratory analysis.

Becq further discusses, that in order to have many water quality parameters measured and analyzed, there is need to design automated laboratories that include probes and analyzers. However, this methodology and approach is expensive. To reduce the cost, a group of scientists, authorities and industries in Europe and France worked together to determine minimum possible parameters measured by in-situ probe and still deliver sufficient data to evaluate lakes, and rivers. According to the collaboration between scientists, authorities and industries, 80 percent considered parameters such as temperature, pH, dissolved oxygen, Redo, conductivity, nitrates measured by in-situ probes sufficient to monitor the overall quality of water.

Jones et al 2017 designed and implemented a real time observatory for aquatic and terrestrial stations to monitor the water quality [22]. However, for the purpose of this thesis, the focus is on the aquatic station. They designed water monitoring stations to collect fundamental water quality parameters including specific conductance, dissolved oxygen, pH, turbidity and water temperature; They further investigated/studied more parameters identified as enhanced variables required in addition to the fundamental to provide a better understanding of the water qualities. The enhanced variables are the biological constituents such as chlorophyll-a, nutrients such as nitrates and other fluorescent dissolved organic matters. They used the multi-parameter Sonde equipped with sensors to measure the water variables.

Jones et al 2017 Investigated the dissolved oxygen using a Sonde sensor model YSI EXO2 599100-01 to measure the amount of oxygen dissolved in the water. This is critical because

oxygen supports living organisms and aquatic ecosystem. Temperature affects the growth and biological activities of an organism, and specific conductance measures the concentration of dissolved constituents, temperature. Specific conductance is a good water quality parameter and it was measured using a Sonde sensor model YSI EXO2 599870-01. They measured pH using a Sonde sensor model YSI EXO2 599795-02 to determine the biological availability and solubility of chemical constituents in water [22].

Turbidity is a measure of water clarity using optical instruments. This tells the total concentration of suspended solids in water: Turbidity was measured using the Forest Technology Systems DTS-12. The enhanced biological constituents which include fluorescent dissolved organic matter such as carbon cycle that are critical for the food webs are measured with sensor model YSI EXO2 599101-01. Jones et al 2017 measured chlorophyll-a using sensor model YSI EXO2 599102-01; this is crucial for determining the concentration of the green photosynthetic pigments in algae and cyanobacteria. Lastly, they measured the critical macro nutrients such as nitrate using the Satlantic SUNA V.2 [22].

The real time water observatory designed and implemented by Jones et al 2017 are four different stations placed at four different watersheds in Utah including Red Butte, Provo River, and Logan River. The stations collected the water quality parameters discussed earlier and with the aid of a mixed telemetry system with both spread-spectrum radio and cellular technology to overcome communication challenges associated with mountainous topography, the data from the stations is communicated in real time. The sensors are powered by solar energy for extended periods. Jones et al 2017 protected the sensors from debris and high-water flow using acrylonitrile butadiene styrene (ABS) housing built around the sensors while ensuring accurate measurements [22].

Wang et al 2009, designed an autonomous surface vehicle for marine environment monitoring; the vehicle used a catamaran for improved stability and exploited the shape of a high-speed ship to reduce the resistance from water [35]. Their Autonomous Surface Vehicle (ASV) has optimized electric motor and propeller designs to optimize power and have a long endurance. The ASV uses a local wireless loop for effective extended communication and remote control of the vehicle. The main design requirement of the ASV hull included sole weight of 60kg, a payload of 60kg, maximum speed of 6kt and an endurance of 2 hours at 4kt

Wang et 2009 designed the hull using aluminum alloy with length of 2.7m, width of 1.48m and depth of 0.36m. The overall design is presented in the figure below. During the experiment, the ASV had a maximum speed of 6.2kt and endurance of 136 minutes at a speed between 3 and 4 kt.

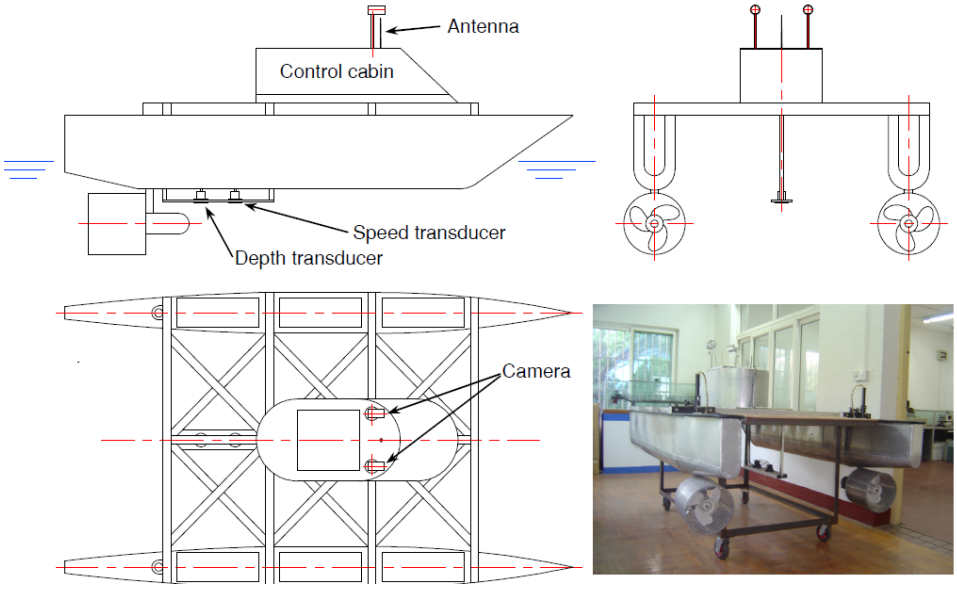

Figure 4: Wang's Design of the ASV

The remote-control system uses a wireless LAN and consists of the ASV and the ground station as shown in the figure below Wang et 2009. The command instructions are sent from the base station, also known as the ground control, to the ASV. The communication distance of the Wang et 2009 ASV was 10 nautical miles when tested at sea.

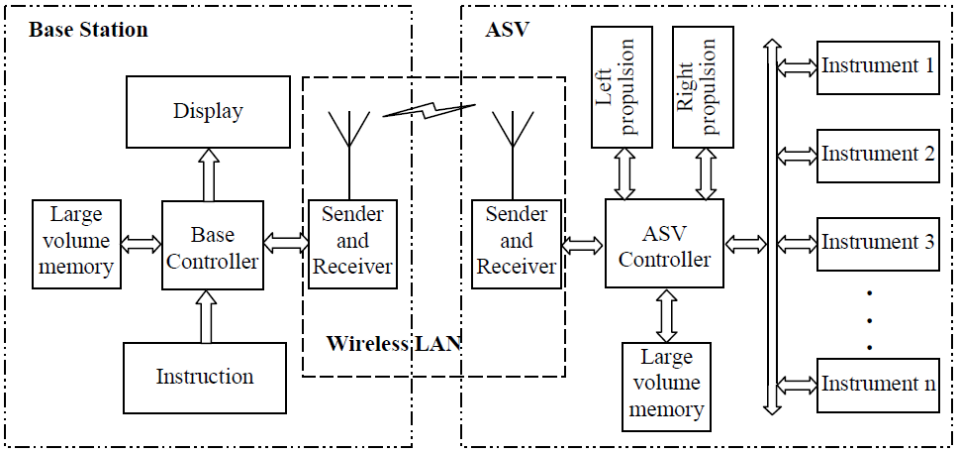

Figure 5: Wang's Remote control system for the ASV

Dun and Grinham designed and developed an autonomous surface vehicle for water quality and greenhouse gas emission monitoring [11, 12]. They designed an autonomous system capable of circumnavigating complex water-bodies while measuring different water qualities and greenhouse emissions. Their autonomous system is based on a catamaran platform, which is 16 feet long and powered by solar energy. The system provides unique capabilities of profiling the water column while in motion. It is paired with a sensor network on a water reservoir at Lake Wivenhoe in Queensland, Australia, where it is implemented.

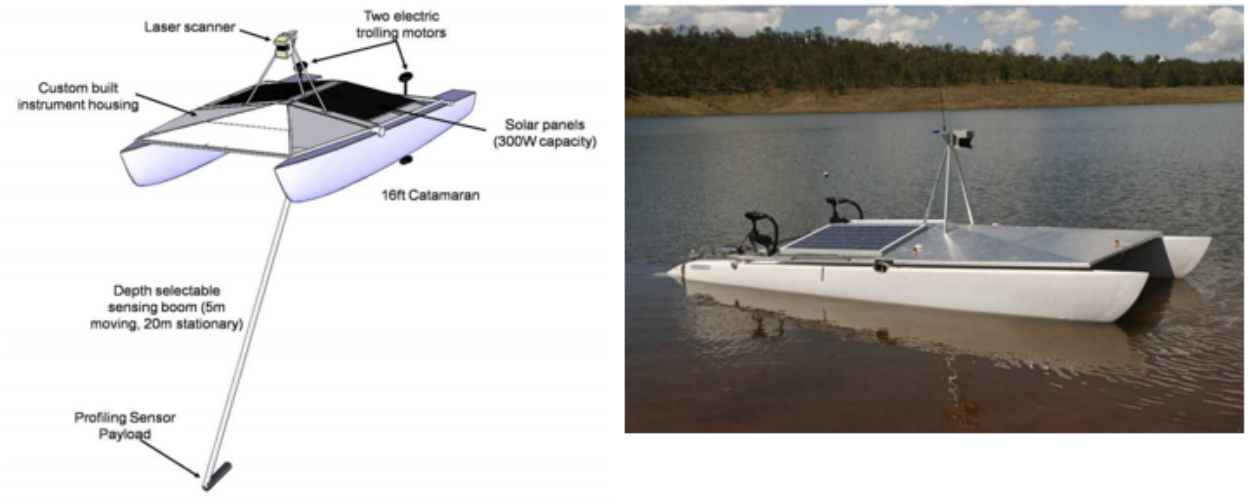

Figure 6: Dun and Grinham autonomous system design [11]

Bikram et al 2018 developed a UAV-mounted system to remotely collect water samples from mining operations [6].The developed system provided rapid capabilities for acquiring water from hazardous water environments in timely manner without causing risk to humans. The water samples collected are examined in the laboratory for accurate testing of water quality parameters: pH, dissolved oxygen, conductivity, etc. Their system is an Unmanned aerial vehicle integrated with a electromechanical pneumatic system that extracts the sample. The electromechanical pneumatic system consists of a servo, syringe, teflon tube, a receiver and transmitter; the system is assembled as showed in figure 7.

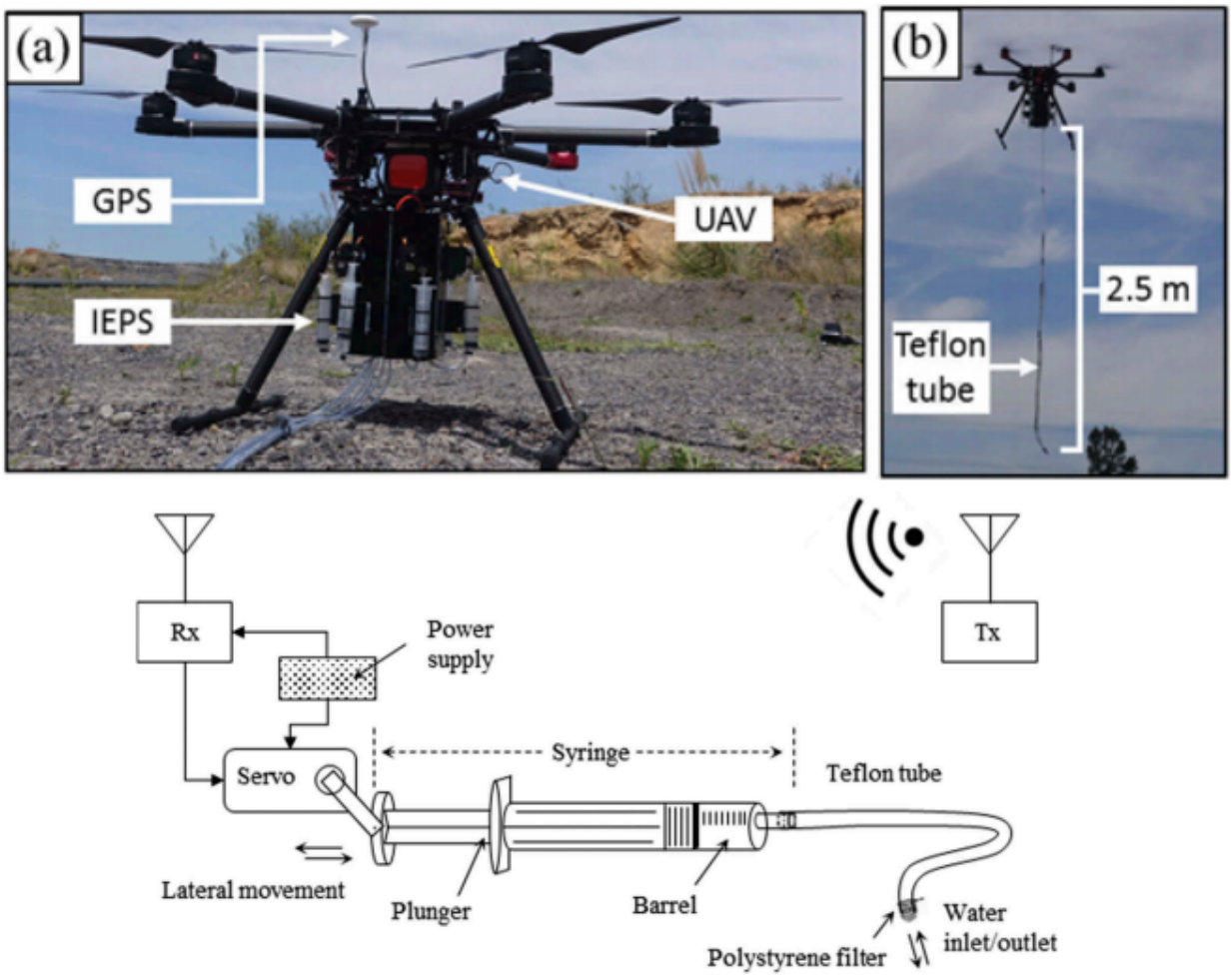

Figure 7: Bikram et al 2018's autonomous system design [6]

Koparan et al 2018, designed and implemented the use of a multirotor UAV to actively collect water samples for water quality analysis in the laboratory [23]. They designed a custom water collection mechanism called thief-style water sampler [14] in the figure 8, which was mounted on the UAV to collect the water autonomously. The electronics were waterproofed to avoid water damage. When the UAV is at the pre-planned location and altitude, the autopilot triggers the UAV to release the water collector to pick the water sample from the lake. The captured sample is taken to the laboratory for analysis.

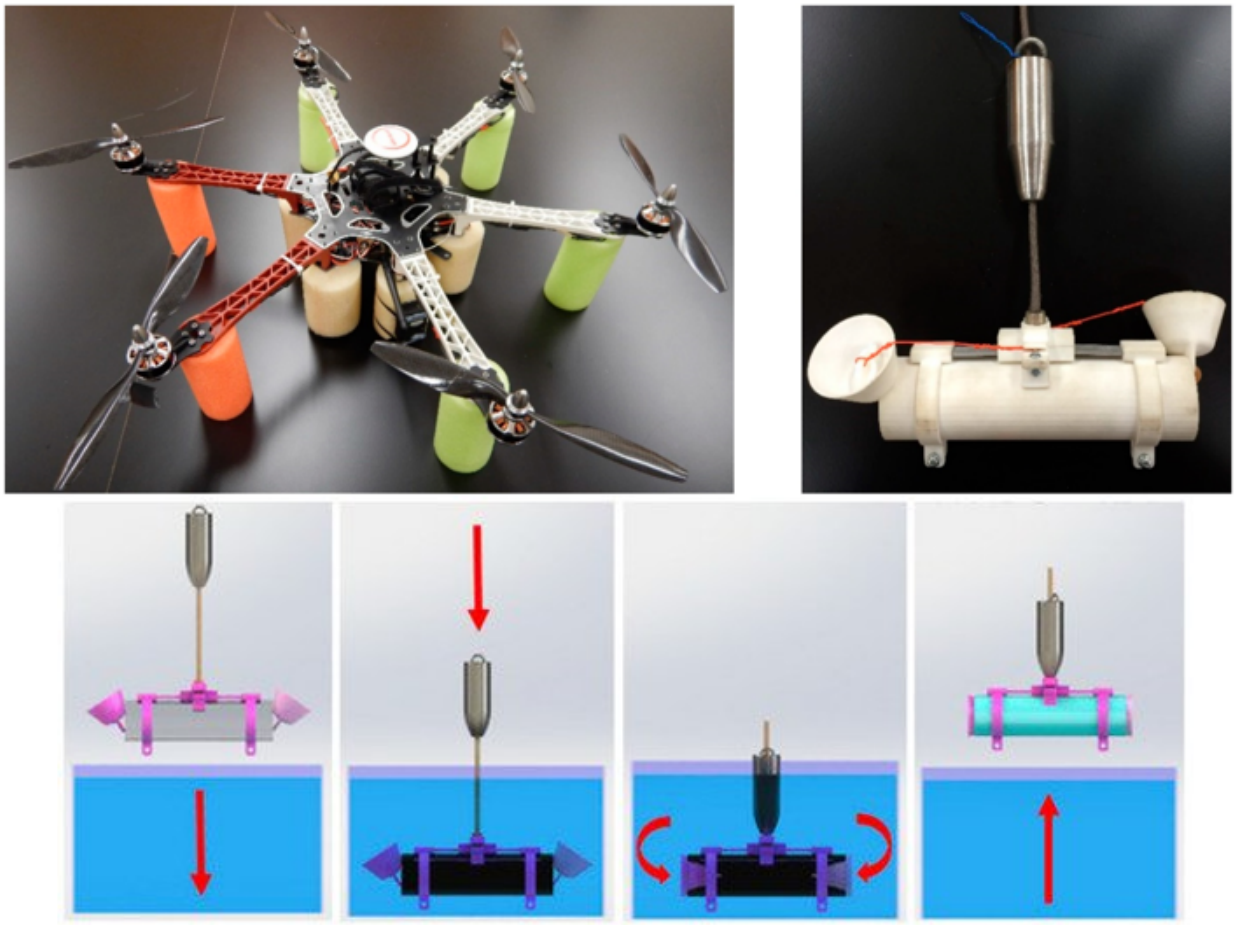

Figure 8: Koparan et al 2018 design for water sampling [23]

Prempraneerach and Kulvanit 2019, developed an autonomous robotic boat for environmental water sampling [27]. The robotic boat is fitted with an auto water sampler in figure 9. The water auto sampler uses a pump to pull water from the lake into the bottles in the water sampler, the system is designed to avoid mixing of different water samples and cross contamination. The auto water sampler can obtain water samples within 6 meters deep of the lakes and rivers, the boat is fitted with 12 bottles that can be filled with 1 liter of water each. It takes one minute for the auto sampler to fill a one litter bottle. The auto boat can be operated by an operator and it is capable of operating autonomously. The auto boat has an enabled GPS to geo-tag water samples collected from different parts of the lake. The collected water samples are further analyzed in the laboratory.

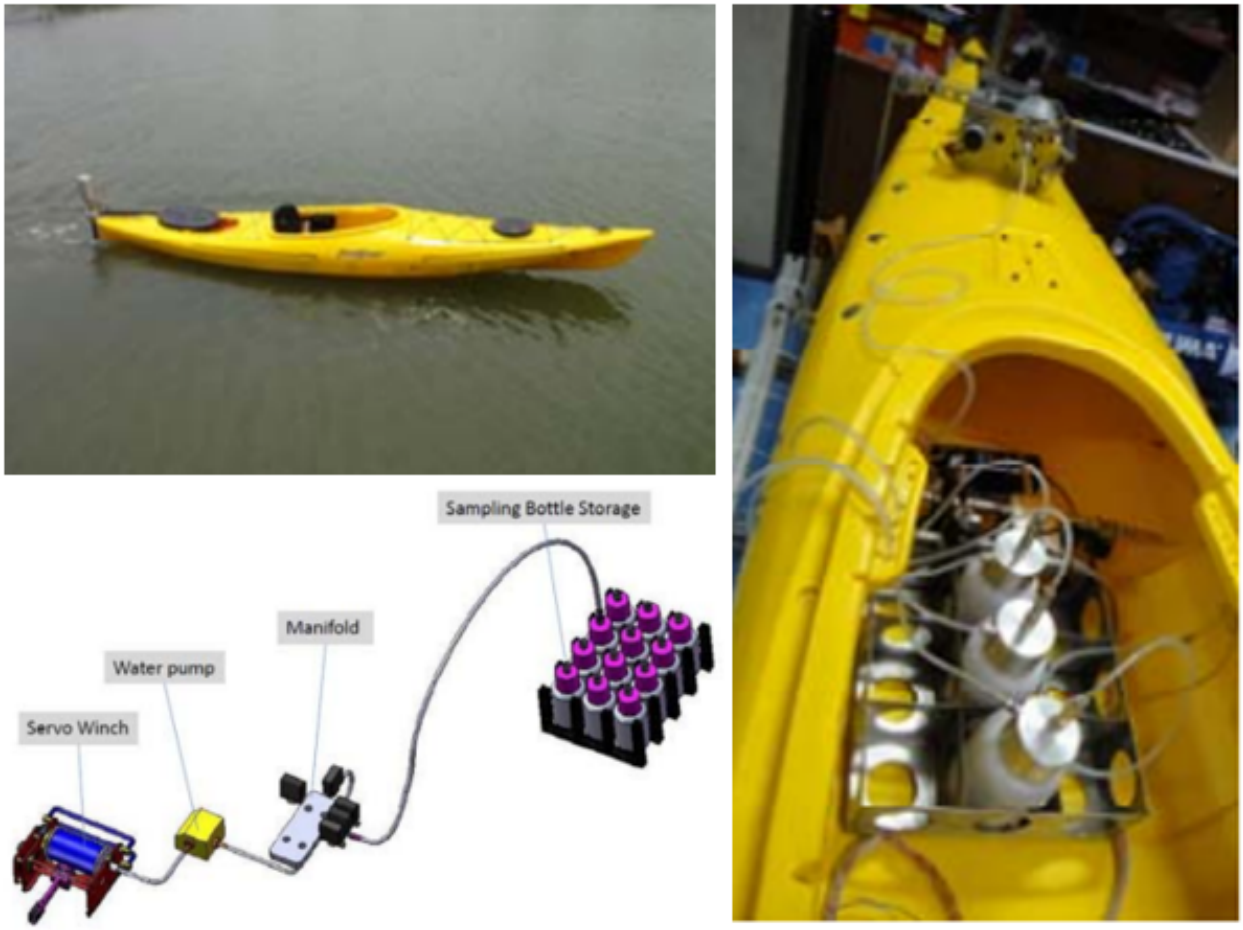

Figure 9: Robotic Boat & Auto water sampler by Prempraneerach and Kulvanit 2019 [27]

Water Quality Monitoring at Oklahoma State University USRI

The first attempt to water monitoring and in-situ sensing using autonomous systems at Oklahoma State University involved using an autonomous surface system known as Aquarius 1. Aquarius 1 is a remotely controlled surface vehicle with a system that collects data while fusing it with global positioning system (GPS). Aquarius 1 is built with two pontoons, with a combination of electric brushless motor and propeller. It uses a rudder to control direction and steering. Aquarius 1 uses a Pixhawk v2.1 flight controller loaded with the rover mode software working with GPS and telemetry capabilities enabling autonomous missions for accurate and replicable data collection.

The on-board data logger system used is an Enviro-Mayfly Data Logger board, using an Arduino programmable with Enviro libraries to collect GPS fused water quality parameters such as temperature, and depth. The data is collected at a rate of 2 Hz for accuracy reasons and stored as a csv file. It is crucial to state the cruising speed of Aquarius 1 to be 4 kts and maximum speed of 10 kts. Aquarius 1 has been used for water observatory in Boomer lake, Lake McMurtry and the Salina Creek in Oklahoma. The figure below shows latest modifications to Aquarius 1.

2.2 Lessons Learned from Prototype 1 (Aquarius 1)

Aquarius 1, is the first prototype implemented for water monitoring. However, there are a few lessons learned during its implementation as below:

1. During strong winds and turbulent water, Aquarius 1 experienced difficulties to operate and maneuver; It was challenging to perform autonomous missions when speeds above 10mph.

2. The pontoon materials used for building Aquarius 1 were deteriorating and decaying therefore a different material was required for longer missions.

3. Steering and mobility was a challenge. Aquarius 1 was only capable of moving forward, turning left and right but not capable of reversing in times when the functionality was required. For example, in cases where it got stuck a few times while on missions, the vehicle Could not be reversed.

4. The time of operation was extremely short with a maximum operation time of 15 minutes. This was a challenge when monitoring/surveying large water bodies.

The lessons learned, are implemented in the design leading prototype II(MANUEL 2.0). MANUEL stands for Movable Autonomously Navigable USV for Evaluating Lakes.

CHAPTER III

Vehicle Design

3.1 Hull and Structure

The hull and structure section discusses the design choices and factors considering the number of hulls, shape and how effective the choices are in testing and implementing in real environmental applications.

Hull Shapes and Design Choice

One of the major design considerations for the Water Surface UAS, is between a single or two hulls for the flotation. The double hull has a greater stability because of its wide beam, which provides more room for the payloads. The manufacturing process is easier because any minor errors in the design does not result in inherent instability. However, it has a major disadvantage of requiring a large area when turning. A single hull has advantages such as easy maneuverability in shallow waters. However, it is not as stable when compared to the double hull. It also has a tendency of rolling and banking in sharp turns and it is difficult to manufacture. Therefore, to build a coherently stable Water Surface UAS, a design choice made to proceed with the double hull design.

The different shapes for the pontoon that were considered were flat-bottomed, Round-bottomed, and V-shaped as shown in figure 10. The flat-bottomed are very stable in calm water environments, and easy to manufacture. However, they are not stable in turbulent waters and strong winds. The V-shaped hull is a commonly used type of hull for powered boats. V-shaped require higher speeds to achieve a smooth maneuver through turbulent waters, strong winds and rough waters. Lastly the round bottomed hulls work well at slow speeds; However, they tend to roll and require stabilizing surfaces.

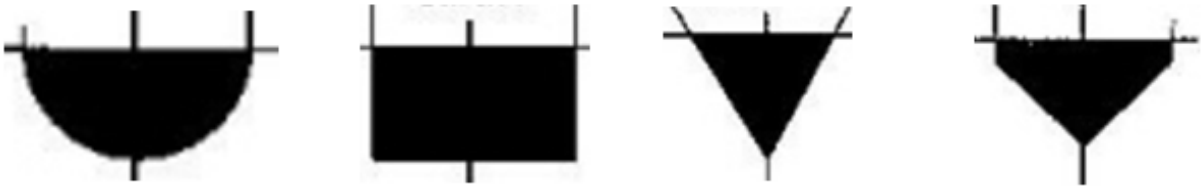

Figure 10: Different shapes of hulls

The shape hull in figure 11 is readily available on the market as a kayak, it provides enhanced stability, and flip resistant in highly turbulent water conditions because of it's

reverse chine and stable hull design. Therefore, the hull in 11 is the platform on which MANUEL is designed and built.

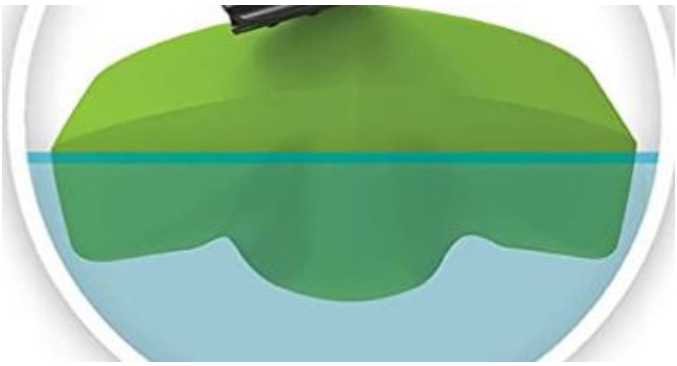

Figure 11: Front view of the hull shape

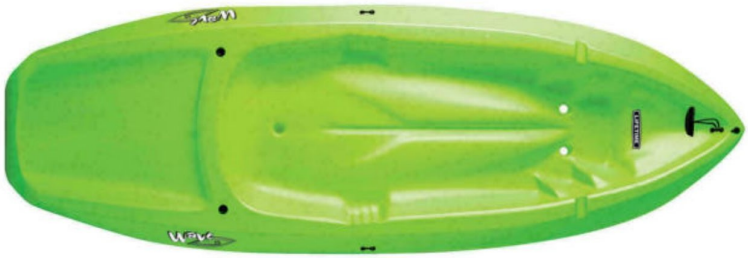

Figure 12: Top view of the hull

Figure 13: Bottom view of the hull

Drag Estimation

Water is a highly viscous fluid hence, the water surface vehicle experiences drag as it maneuvers from one point to another. However, the two major drags are categorized as wave and viscous drag. The drag as the vehicle maneuvers on water through air is negligible because the air is less viscous compared to water. The drag is a factor of speed of the boat, water property and the hull form. In order to analyze the total drag, there are two major non-dimensional terms used to analyze the boat drag: Reynolds numbers and the Froude number. The Reynolds numbers relates to the viscous flow and frictional drag while the

Froude number relates to the wave drag [12]. The Reynolds numbers and Froude number of the boat are determined as indicated below.

$$Re = \frac{LV}{v} \tag{3.1.1}$$

Where Re is the Reynolds numbers, L is the length of the boat in contact with water, V is the velocity of the boat and v is the kinematic viscosity of water.

$$Fr = \frac{V}{\sqrt{gL}} \tag{3.1.2}$$

Where Fr is the Froude numbers, L is the length of the boat in contact with water, V is the velocity of the boat and g is the acceleration due to gravity.

The total drag by the surface vehicle is estimated using the expressions as below.

$$D_{Total} = D_{Wave} + D_{Viscous} \tag{3.1.3}$$

$$D_T = \frac{1}{2}\rho_w V^2 S_p C_T \tag{3.1.4}$$

Where ρw is the density of the water, V is the speed of the vehicle, and Sp is the area of the pontoon submerged and CT is the total drag/resistance coefficient.

$$C_{Total} = C_{Wave} + C_{Viscous} \tag{3.1.5}$$

Where CW is the wave drag coefficient and CV is the viscous drag coefficient.

To determine the total drag experienced by the boat, is a challenge and therefore, the experimental approach presented better means to estimate the total drag by the boat. However, the experimental approach of determining the drag does not specify the individual component of drag such as wave and skin friction drag.

Experiment Setup and Procedure to determine the Total Drag

The total drag experienced by the boat is determined experimentally by determining the drag experienced by a model boat submerged in the water tunnel. Two dimensioned 4 by 4 by 12 inch pontoon designed hulls, held together for stability reasons were tested in the water tunnel in Endeavor lab at Oklahoma State University to experimentally determine the drag it experiences. The wetted surface area is fully determined by how heavy the boat; Because of Archimedes' Principle, the heavier the boat, the more surface area of the pontoon gets submerged. The pontoon, is placed in a water tunnel secured with a load cell, as shown in the figure below. Conducting the experiment in the water tunnel presents an advantage of altering the flow velocity of the water. During the experiment there is a wide range of velocities from 5 to 50 ft/s.

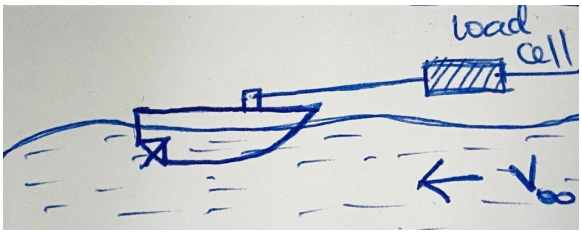

Figure 14: Estimating the total drag on MANUEL

The load cell measures the drag force exerted onto the specimen pontoon boat as the velocity is changed. The data recorded i.e drag force and velocity, is plotted. From the data, the total drag coefficient CT, is obtained and used to calculate the total drag on the boat at any speed and weight using the equation as shown

3.2 Propulsion

The propulsion system produces the force to overcome the drag acting on the boat, and provide the maneuvering capabilities to the boat. For the size of the boat designed, two different propulsion systems are considered: air propulsion and water propulsion system.

3.2.1 Propulsion Down Selection

Air propulsion

Air propulsion system involves powering the boat through air; the propulsion system is fully in air without any water. The air propulsion system would include a propeller driven type of system in air as showed in figure 15 from the first prototype Aquarius 1.

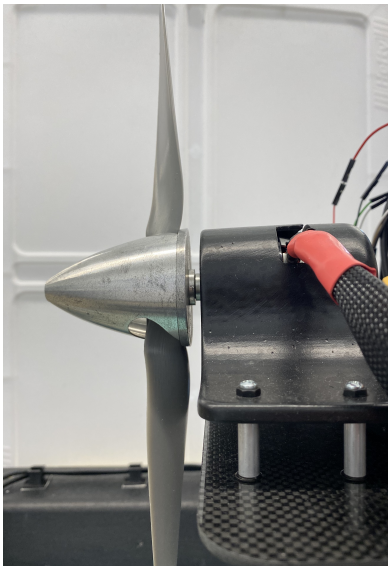

Figure 15: Air propulsion of Aquarius 1

Water propulsion

Water propulsion system involves powering the boat through water. The propulsion system is fully immersed under water for a better efficiency. A water propulsion system would include systems such as thrusters and water jet engines.

3.2.2 Propulsion Analysis

Thruster Description

A T100 thruster is a 4in and 3.9in in length and diameter respectively with a 3in diameter 3-bladed propeller manufactured by BlueRobotics. According to the manufacturer, the T100 produces a maximum forward thrust of 5.2 lb f, maximum reverse thrust of 4.1 lb f and minimum thrust of 0.02 lb f. The T100 has a an operating voltage range between 6 to 16 volts and a maximum current of 12.5 amps. Therefore, T100 has a maximum required power of 135 watts at full throttle setting [29].

The T200 thruster has a length of 4.45in and diameter of 3.9in with a 3in diameter 3-bladed propeller manufactured by the same company BlueRobotics. The published data by the manufacturer states the operating voltage range is from 7 to 20 voltages. At the full throttle settings with a 20 Voltage power supply, the T200 produces a maximum forward and reverse thrust of 14.8 and 11.1 lb f respectively. The T200 has minimum thrust of 0.05 lb f. The full throttle at 20 voltages has a required maximum current of 32 amps and maximum power of 645 watts. However, the T200 is designed to operate efficiently at 16 volts and produces a maximum forward and reverse thrust of 11.6 and 9.0 lb f respectively at the full throttle setting. At a nominal 16 volts and full throttle setting, the T200 requires a maximum of 24 amps and 390 watts [30].

Figure 16: T200 Thruster from BlueRobitics [30]

The T100 and T200 thrustes can operate with a 30 amp Electronic Speed Controller (ESC) that runs BLHelis firmware. The Basic ESC is capable of forward and reverse rotation direction to produce forward and revere thrust and requires minimal cooling, hence high efficiency. The BlueRobotics basic ESC operates with the range of voltages from 7 to 26 volts with a maximum constant current of 30 amps [28].

The T200 thruster provides more capabilities, power and thrust compared to the T100 thruster. Therfore, the T200 increases the operating conditions and ranges, producing stronger winds and highly turbulent waters. Therefore, it was decided to proceed with the T200 thruster and its compatible basic ESC.

Power Source

Different power sources were considered for MANUEL, including Lithium-Polymer (LiPo) Battery, lead-acid battery, solar energy and fuel cell energy. It was decided to proceed with the Lithium-Polymer (LiPo) Battery because of its light weight, high energy density, great discharge rates and has a higher capacity, translating to more power. However, the LiPo batteries are very sensitive to high temperatures, exceeding the recommended high and low voltage will damage the battery. Lastly, they are prone to explode when exposed to high heat or charged improperly.

Figure 17: A LiPo Battery

MANUEL is currently powered by 4 Lithium-Polymer batteries each rated 22.44 volts (6S), 14,000mah and producing up to 314.16watts. The LiPo batteries are connected in series to increase the capacity (mah) of the battery up to 56,000mah hence increasing endurance for MANUEL. During AUTO missions, MANUEL cruises at 4.5 ft/s and 35 percent of the throttle setting and an endurance of 3.5 hours.

A major decision was made to use 6S batteries rather than the optimal 4S because it increases the over all mission efficiency rather than electrical efficiency as recommended by the manufacturer of the thrusters. The 6S therefore increases the power available and endurance for MANUEL

3.3 Stability and Control

MANUEL is based on an already existing frame of a 6 feet long and 2 feet wide kayak. The kayak is designed for a maximum of 130 pounds. It is designed with twin fins, reverse chines to enhance stability, tracking and resist flips. Therefore, the kayak provided a stable platform for MANUEL.

3.3.1 Down Selection of Controls

There are two different ways to control the direction and turning of the boat: use of rudder and differential thrust.

Use of Rudder

The use of the rudder for controlling the direction of the boat is efficient for use in systems operating in relatively calm water. However, as learned from the first prototype, using the rudder to control and steer presents limitations on the operational environment and conditions. For example, the turning/steering is slow, steering is slow sue to the larger radius, hence Aquarius 1 would not operate in narrow environments thus it was difficult to have accurate and narrow paths to collect the data from the lakes. The rudder was not effective in highly turbulent waters limiting when the water bodies were surveyed.

Differential Thrust

Differential Thrust involves the use of a thruster to control the direction of the boat. This is achieved by reducing the thrust produced by one thruster while increasing the thrust produced by the other thruster of the same system. Differential thrust provides better steering and turning capabilities compared to the use of the rudder. Steering the direction using the differential thrust is faster, tighter and effective in all conditions: calm, choppy, and highly turbulent waters compared to the use of the rudder.

Having considered the use of the rudder and differential thrust as possible means for steering the boat, the use of differential thrust presented better maneuverability and controllability in all environmental conditions.

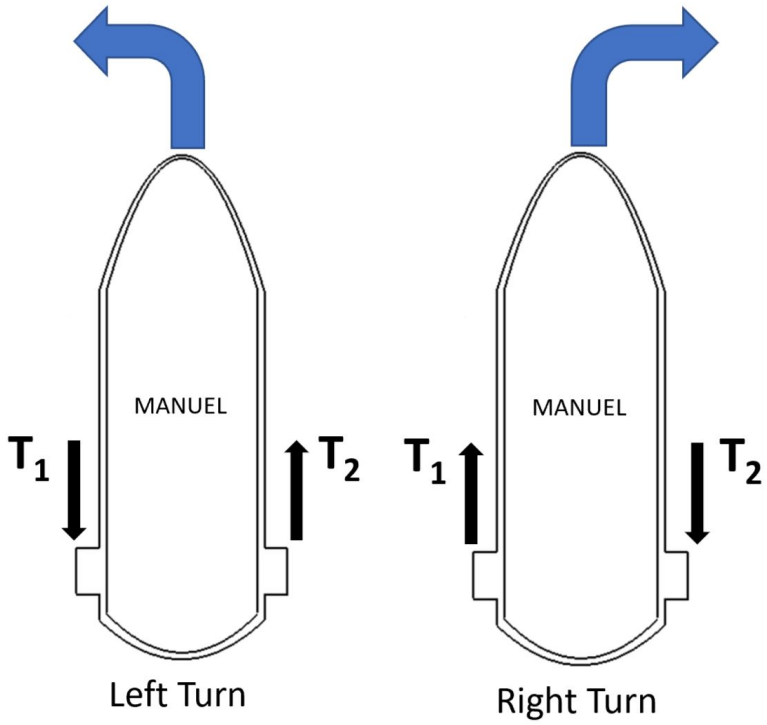

Figure 18: Differential thrust demonstration

To turn left, MANUEL reduces the rate at which it turns thruster 1 compared to thruster 2 resulting to attendance of turning left as demonstrated in figure 18. Turning

right, MANUEL reduces the rate at which it turns thruster 2. However, the steering rate is determined by how slow the respective thrusters turn. In order to maintain a straight forward or revese movement, both thrusters T1 and T2 spin/turn at the same rate as demonstrated in figure 19.

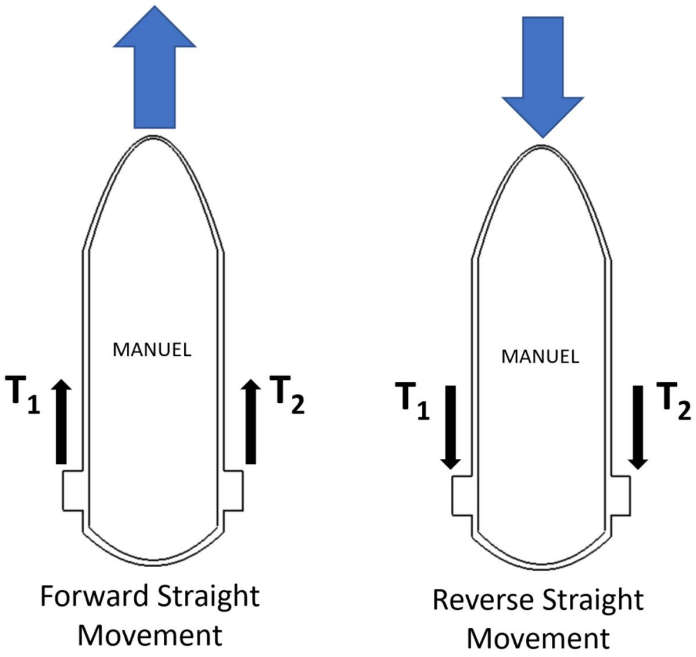

Figure 19: Movement by dual thrusters

3.4 Avionics and Autopilot

3.4.1 Avionics

The avionics includes the Pixhawk, GPS, Electronic Speed Controller (ESC), Receiver, Transmitter, and Telemetry.

Pixhawk

An orange cubic Pixhawk 2.0 autopilot was added to MANUEL. A Pixhawk is popular and common autopilot used to support numerous vehicles including planes, multicopters, ground vehicles, water surface vehicles and submersible systems. The pixhawk is securely fastened inside the avionics box of MANUEL.

Receiver and Transmitter

For a communication to be established between an unmanned system and the operator, a receiver and transmitter are required. Range of operation is one of the major requirements considered when deciding the right choice of a transmitter and receiver. A transmitter is a device that transmits a signal such as data, video, and audio using an antenna to broadcast

the signal in air. A receiver is a device that deciphers transmitted information using an antenna to receive signals from air.

Two options were considered, the Futaba and Spektrum which offer better software performances compared to other brands. The initial decision was using a Spektrum DX8 8-Channel DSMX transmitter and receiver. However, MANUEL kept loosing the signal 700 feet away from the operator, triggering a fail-safe and return home. When switched from the Spektrum combination to the Futaba T8J 2.4GHz S-FHSS and raising the height at which the receiver was mounted on MANUEL, this increased the range of operation up to approximately 1 mile for MANUEL without triggering a fail-safe.

Telemetry

Telemetry provides mechanisms and a link of a two way communication between MANUEL and the ground station. Different telemetry options were considered for use with MANUEL including Radio Frequency (RF), and Global System for Mobile (GSM).

The radio frequencies operate in a relatively lower range compared to the GSM. Data communicated through radio frequencies is transferred directly from the sender to the receiver and vice verse, without a third system involved. While for the GSM data transfer, the data from the sender is sent first to the cloud before to the receiver and vice verse. However, in situations without a cellular network coverage, data can be transferred using GSM. Using GSM is expensive due to subscription fees involved. Therefore, a radio frequency telemetry is considered and implemented in the design of MANUEL.

The RFD 900X telemetry is an encrypted long range operating between 902 and 928 MHz ISM band at a transmission power of one watt. The manufacturer published RFD 900X telemetry is capable of a data link of up to 40km RFD. Compared to other radio frequency telemetry considered, the RFD 900X stands out for its ultra long range and compatibility with the Pixhawk. However, during the testing, due to many activities happening on the lake including change in topography, and a lot of vegetation, the data link between MANUEL and the ground station held up to 1.5 miles and lost thereafter.

Avionics Integration

The GPS, Futaba receiver, RFD 900X ultra long radio modem telemetry and ESCs are connected to the Pixhawk and closely secured into a water tight container to protect the electronics from water damage. The ESC's are also connected to the battery and thrusters control the direction and rate at which the trushters turn. The receiver is not enclosed in the avionic casing to reduce the magnetic and electrical interference from other electronics, such as the ESCs and RFD that draw large currents that cause magnetic induction and electric interference.

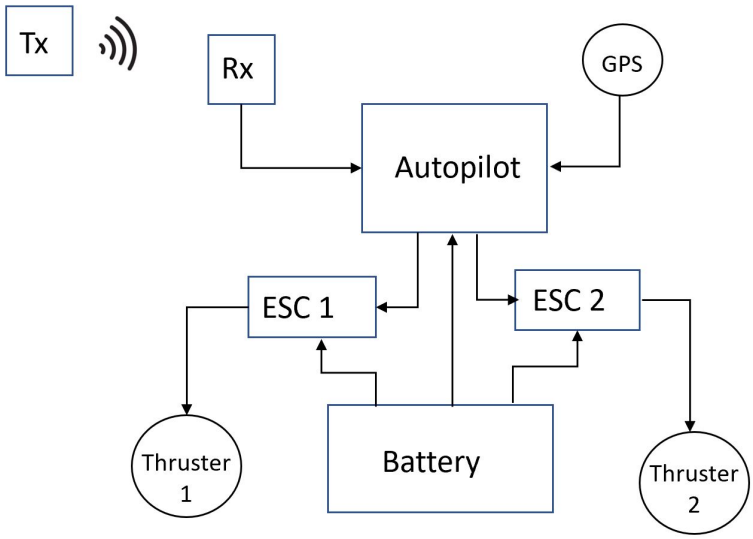

Figure 20: MANUEL Avionics wiring and setup

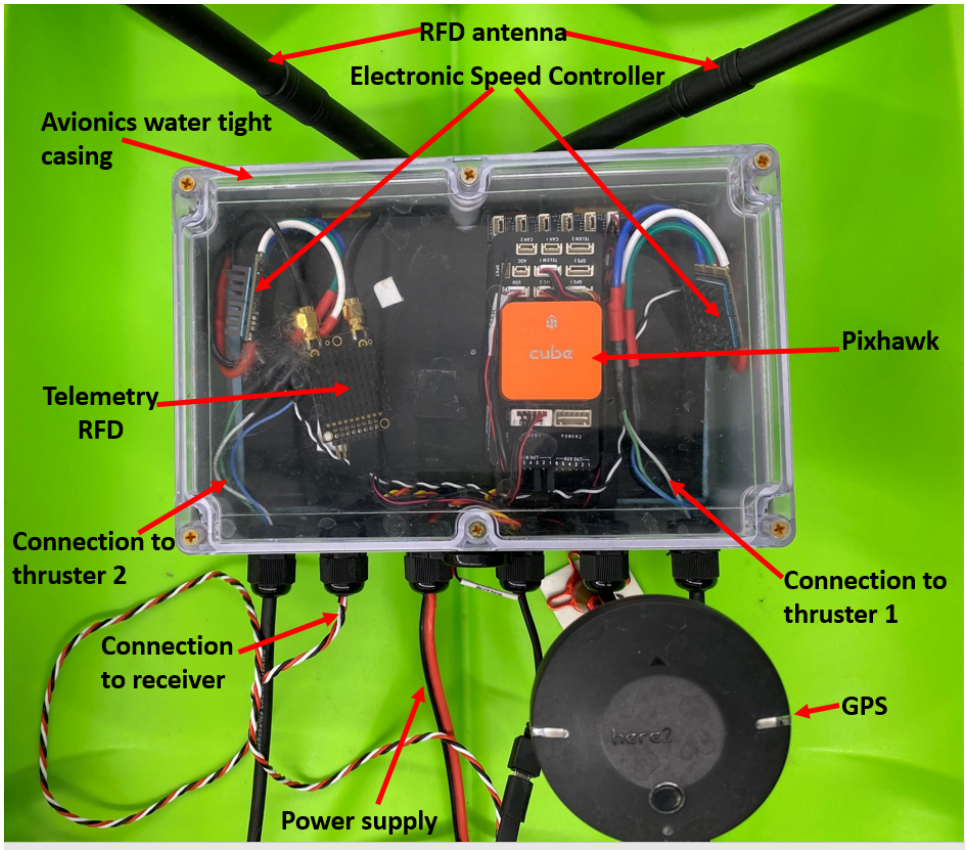

Figure 21: MANUEL Avionics Function block diagram

During testing, the avionics water tight casing had accumulated sweat as shown in the figure below. This was resolved with tightening the wiring covers and installing the humidity

remover to keep the avionic compartment dry during the operations.

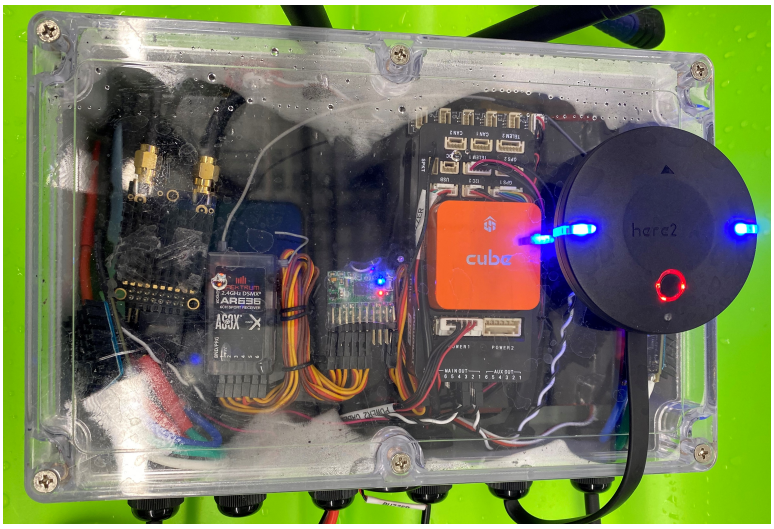

Figure 22: Showing sweat in the Avionic sealed casing

3.4.2 Navigation and Path Planning

MANUEL is designed just like an Unmanned Aerial Vehicle (UAV) and therefore its navigation and path planning is the same. However, the difference between the operation of UAV and MANUEL is the altitude, and therefore the altitude at which MANUEL is always operating at is 0 ft.

Mission planner, an open source software, is compatible with the autopilot installed in MANUEL. For the mission planner to function accordingly with MANUEL, a few initial settings were implemented.

An open source rover firmware from the Ardupilot was uploaded to the Pixhawk through mission planner and detailed parameters were adjusted as indicated in the parameter files attached in the appendix. The vehicle configuration was changed and tuned to a boat by setting the frame-class parameter to 2 autopilot. Differential thrust, and three modes of operations: Auto, Manual, and SmartRTL were enabled through changing and enabling the parameters in the paramfiles in appendix. Differential thrust provided control and steering of MANUEL during operations. The different models of operation offered different capabilities. Auto model, enables operations autonomously following an already predetermined path or mission. Manual model, enables the operator to directly control and operate MANUEL. Lastly, the SmartRTL is enabled in MANUEL for situations in which a fail safe is triggered hence returning MANUEL safely to home (launch point) by following the same exact path taken.

For MANUEL to operate in AUTO mode, first the mission is created using mission planner loaded on the ground station by selecting the mission way points, and speed. Every time before any mission is started, a home position is set; this is usually the position where the system is armed and therefore, when a fail safe is triggered or when switched to SmartRTL, MANUEL will always return to that particular location. When the mission is set and ready to be executed, it is written and sent to the Pixhawk. A screen shot of MANUEL's path in

mission planner for one of the lakes is below.

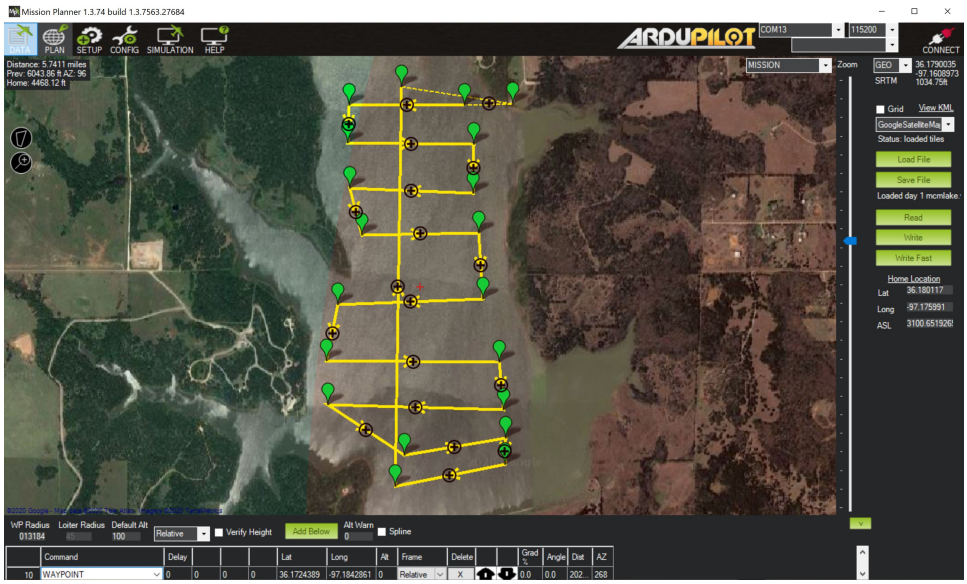

Figure 23: Mission planner screen shot

3.5 Surface Vehicle Integration

The kayak as described earlier is 6 ft long and 2 ft wide as shown in the figure below. The integration approach was for it to be simple and functional.

Figure 24: Kayak before transformation

To install the thrusters on the kayak, a distance of 2 ft between the two thrusters to enable effective steering was considered. The thrusters are securely tightened to Aluminium bar indicated in the figures below. Aluminium is highly resistant to rusting hence the appropriate material to build MANUEL.

Figure 25: Thruster mounting technique

The avionics are securely tightened in the a waterproof casing and placed at the center top of the kayak. The battery casing is designed to protect the batteries from getting wet to ensure circulation of air and cool off the LiPo batteries.

MANUEL v2.0 Specifications

Table 1: MANUEL Specification.

Vehicle Structure	Single Hull Kayak, 6 ft by 2 2ft
Steering type	Thrust differential
Propulsion System	Dual Thrusters
Powered	4 6S LiPo 14,000 mAh
Endurance	3.5 hours at cruising speed
Cruise Speed	4.5 ft/s
Maximum Speed	9 ft/s
Maximum weight	130 lbs.
Maximum thrust	24 lbs.
Autopilot	Pixhawk 2.0 Orange Cubic
Operation Modes	Auto, Manual and SmartRTL
Maximum range manuel operation	$<$ 1 mile

Figure 26: MANUEL 2.0

CHAPTER IV

Sensor Selection and Data Acquisition

4.1 Water Quality Parameters

Turbidity

Turbidity is the total amount of suspended solids in water. Turbidity is reported and measured in Nephelometric Turbidity Unit (NTU) with an output ranging from 400 to 680 nm wavelength or a Jackson Turbidity Unit (JTU). Turbidity is an indication of photosynthesis of plants underwater, soil erosion from the water body banks, contamination and pollution with pollutants such as pathogens and dissolved metals [17].

Turbidity of the water is influenced by numerous factors such as weather and water flow. Turbidity is related to flow rate of the water as shown in the graph of figure 27. The higher the flow rate of water, the higher number of suspended particles in water. Heavy rains affect the flow of water and increase the amount of suspended particles due to overflow therefore increasing turbidity of water streams [17]. Turbidity is also influenced by other factors such as waste discharge, soil erosion and resuspenses.

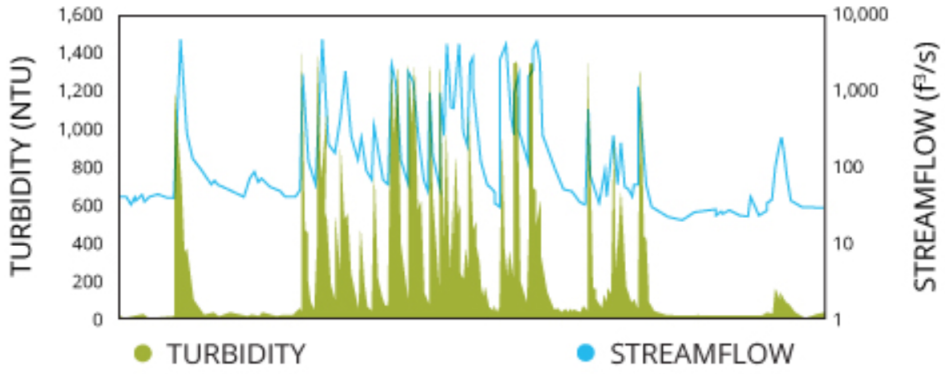

Figure 27: A graph of Turbidity and flow rate of water [17].

High levels of turbidity have consequential effects, such as reducing the visibility for the aquatic organisms, such as fish, which use light to get their food hence reducing their feeding behaviors. This physically harms the aquatic life. Highly turbid water holds pathogens that are harmful to both humans and aquatic lives.

Temperature of water

The temperature of water, a physical property, is the degree of hotness or coldness of water [18]. Temperature of water is a crucial water quality parameter because it affects the living organisms and other water quality parameters. The temperature affects conductivity, salinity, pH, dissolved oxygen, photosynthesis of plants in water and the rate of metabolism for the living organisms in aquatic environment [18].

Temperature affects the biological activities and rate of metabolism for the aquatic organisms. Studies have shown a correlation between temperature and the rate of metabolism of aquatic life. For example, the rate of metabolism in aquatic organisms increases with the increase in the temperature of water. However, at higher temperature, metabolic rate of organisms decreases as demonstrated in figure 28.

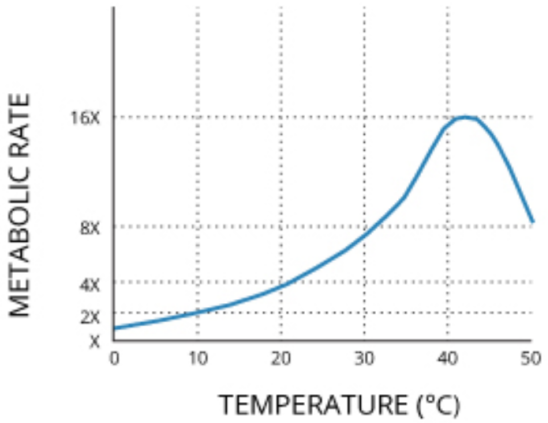

Figure 28: A graph showing effect of temperature on metabolic rate [18].

Temperature affects the amount of oxygen dissolved in water. The increase in the temperature of water, decreases the oxygen dissolved in water as showed in figure 29. When the water is warm, it holds less oxygen hence it can not support life for aquatic organisms.

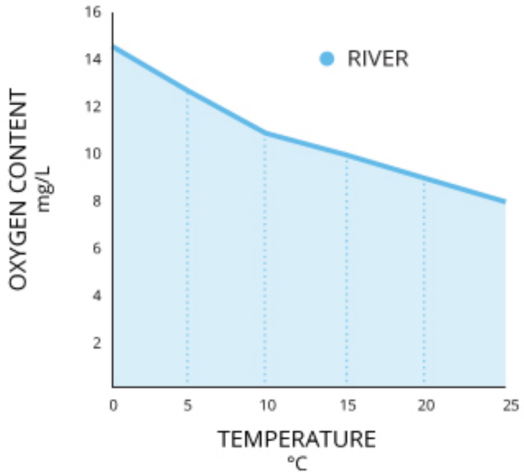

Figure 29: A graph showing effect of temperature on oxygen content [18].

The increase in the temperature of water increases the conductivity of water and vice versa. Conductivity is the measure of electrical potential of ions in water. The increase of conductivity is lower in pure water. The change in the temperature leads to a change in the ion concentration hence changing the pH of the water as shown in the graph of figure 30. However, the change in pH due to temperature is not significant.

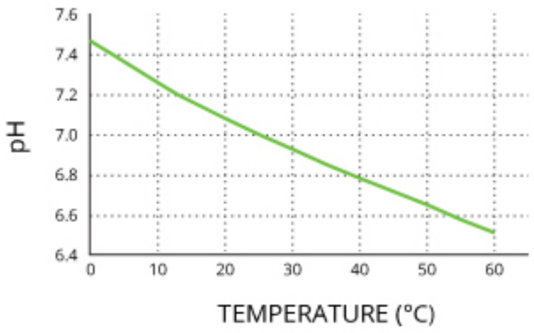

Figure 30: A graph showing effect of temperature on the pH level of water[18].

The temperature of the water is influenced by sunlight, atmosphere, and turbidity. When the sunlight rays hit the water, it heats up the water leading to the temperature increase. Heat from the atmosphere also contributes to the increase of the water temperature. The increase in turbidity levels increases the temperature of the water [18].

PH of water

The pH of water is a chemical parameter that is measured as a concentration. The logarithmic pH scale is between 0 and 14 shown in figure 31. This indicates the acidic and alkaline levels of water [3]. Water is considered neutral when its pH scale reads 7, numbers less than 7 would be considered acidic and numbers greater than 7 on the scale indicates water is alkaline [3, 26]. The pH of the water can be measured using sensor probes without transporting the water to the laboratory for analysis. Majority of aquatic organisms live within a pH range of 6.5 to 9.0 [16, 26].

A too high or too low pH affects (kills/harms) living organisms that live within water bodies. For example, Amphibians are endangered by low pH. The pH also affects the toxicity and solubility of chemicals in water such as lead, cadmium and chromium [website][3, 26]. The pH of water is influenced by various activities like releasing waste into water. Chemicals from agriculture and discharges from the industries including heavy metals. Hence measuring the pH of water is critical for the living organisms in water and the environmental monitoring [16].

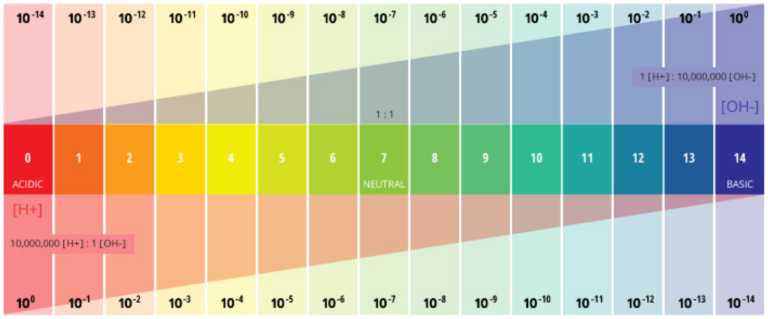

Figure 31: A pH Scale [16]

Dissolved oxygen

Dissolved oxygen (DO) is the amount of oxygen dissolved in water or the concentration of the oxygen in the water. DO is a critical water quality parameter that indicates the water pollution levels, a higher dissolved oxygen is an indicator of good water quality. The concentration of dissolved oxygen is affected by the temperature, salinity, and pressure of the water. Dissolved oxygen affects living organisms in water. For example, a fish requires 5 milligrams per liter of oxygen concentration to breath in water. However, the dissolved oxygen has no direct impact on the human health other than tasting unpleasant [5].

Chlorophyll

Chlorophyll is a color pigment in plants, algae and phytoplankton [15]. There are four different types of chlorophyll including a, b, c, d, e and f with different green wavelengths as shown in the figure below. Chlorophyll-a is a green pigment responsible for photosynthesis in both plants and algae[15].

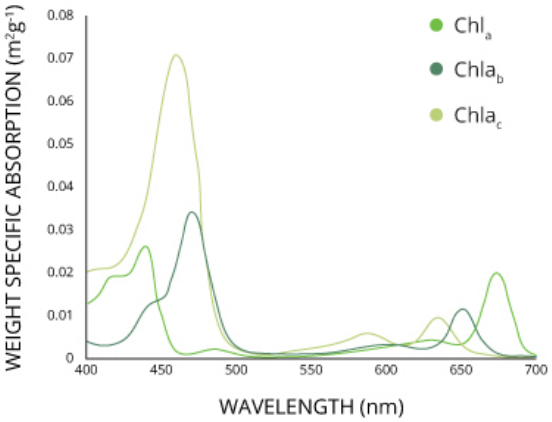

Figure 32: Different chlorophyll absorb different wavelengths of for photosynthesis [15].

Chlorophyll can be measured using in-situ sensors by exposing it to a high energy wavelength of 470 nm hence emitting a lower energy light between 650 to 700 nm; this process is known as fluorescence[20]. Chlorophyll has units of micrograms per liter. Chlorophyll is

an indicator of the nutrients and health of the water body and tracks the growth of algae blooms. When the bloom of algae dies due to sudden change in the temperature and other environmental conditions, it reduces the amount of oxygen in the water, affecting living organisms in water such as fish and and in some cases, directly affecting human health [20].

Conductivity

Conductivity of the water is the measure of the ability of water to conduct an electric current [33]. Conductivity has a U.S. units of microohms/cm. Conductivity is the flow of ions therefore, the increase in the ion concentration, increases the conductivity of the water[5]. Conductivity of water determines the suitability of using the water for putting out a fire and irrigation. Conductivity of water can also be used to estimate the TDS value of water; Pure, drinking water and sea water have a conductivity of 5.5 x 10exp-6, 0.005 - 0.05, and 5 S/m respectively [5, 33]

Salinity

Salinity is the amount of salts dissolved in water. Any slight change of salinity in water impacts aquatic lives, humans and wild life. Salinity is affected by precipitation, evaporation and chemical wastes coming from industries and agricultural farmlands. Salinity can be measured using sensor probes that measure the electrical current moving through water. The higher the concentration of salts, the faster the current flows through the water [37].

Nitrates

Nitrates are common elements in fertilizers, many of the nitrates are soluble in water. Increased levels of nitrate lead to harmful algae brooms (HABs), which is why we want to measure it. Nitrates are tasteless in water and cannot be smelled. High concentration of nitrates and nitrites in water is harmful to human life and aquatic organisms. The nitrates in lakes and rivers are mainly from agricultural runoff, wastewater treatment plant discharge, industrial runoff, and urban runoff [2]. High concentration of nitrates in water bodies promotes algae and bacterial growth. The nitrates in the lake are measured using an optional ion specific electrodes (ISE) with a nitrate probe. Nitrates affect the electric potential and the change is measured by the nitrate probe [36].

Bathymetry

Bathymetry is the measure of the the depth of a water source. The methods for collecting bathymetric data include the use of "the Ecomapper Autonomous Underwater Vehicle, multi-beam and single-beam surveys, ADCPs, and sub-bottom profilers." [31]. However, in this research, the interest is between multi-beam and single-beam surveys. In a single-beam bathymetry, an echo sounder is attached to the bottom of a boat sending out a narrow beam of arrays to the basin/floor of the waterbody that bounce back hence measuring the depth of the water directly under the boat as shown in figure 33. Single-beam surveys are popular and commonly used for small water bodies.

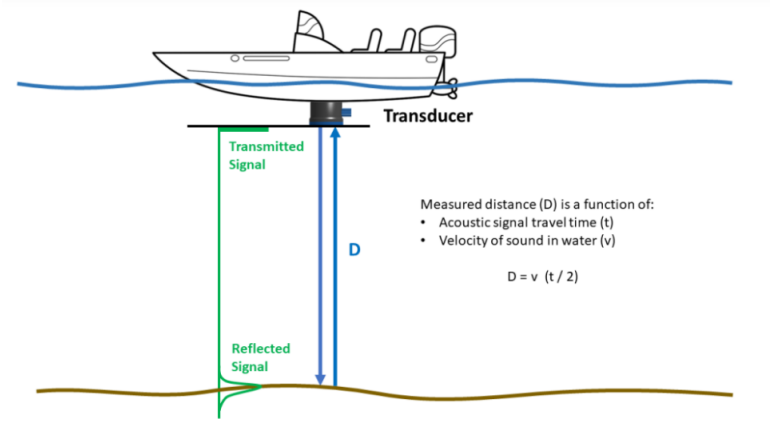

Figure 33: Bathymetry Sonar System[9]

The multi beam survey works using the same principle as the single beam echo sounder, except it produces larger beams of array and used for larger water bodies as shown in figure 34 [31]. Bathymetric data is critical for water quality studies, and detecting leakages to the water bodies,

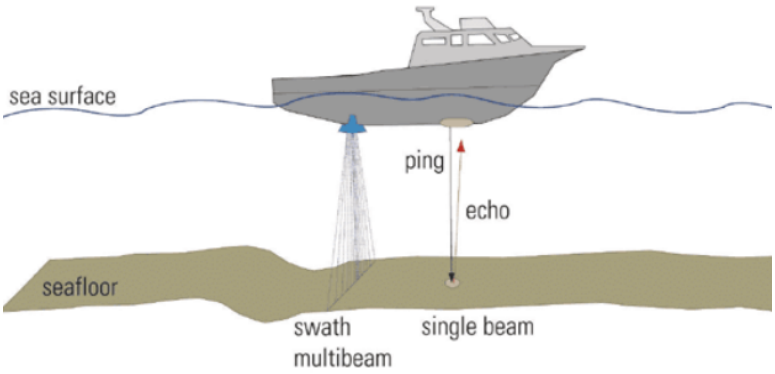

Figure 34: Bathymetry Sonar System[24]

4.2 Sensor Selection

Water quality parameters such as pH, temperature, dissolved oxygen, turbidity, salinity, conductivity, chlorophyll, and phycocyanin are critical for monitoring the lakes and rivers. The need for measuring and monitoring these water qualities is critical in deciding the type of sensors to consider. During the bench marking, numerous options were considered. However, the YSI EXO3 water quality Sonde was more effective than other sensors.

The YSI EXO3 water quality Sonde is designed and built using titanium sensors with 5 general sensor ports allowing the sensors to be switched with different sensors and a water proofed battery casing. The EXO3 is capable of SDI-12 communication, bluetooth connection and has 5 titanium smart sensors including conductivity/temperature, dissolved oxygen, pH, total algae (chlorophyll and phycocyanin) and turbidity for monitoring the

water temperature, dissolved oxygen, pH, turbidity, salinity, conductivity, chlorophyll and phycocyanin [19].

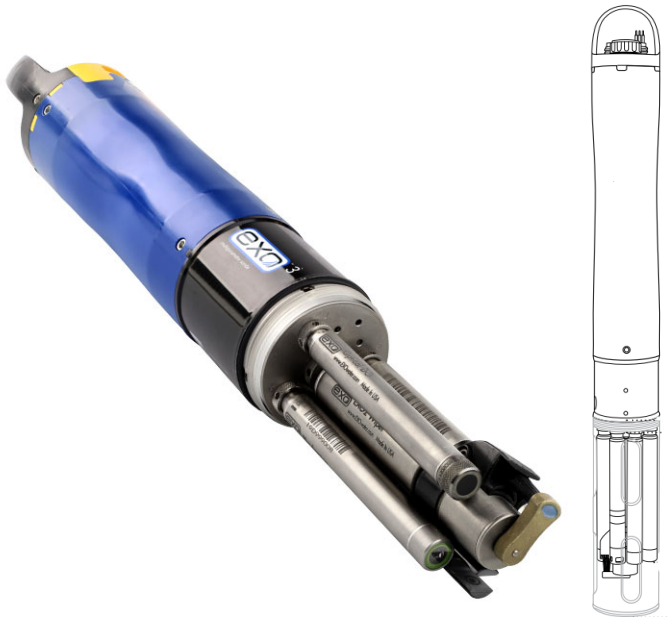

Figure 35: A picture of the YSI EXO3 multiparameter Sonde [19]

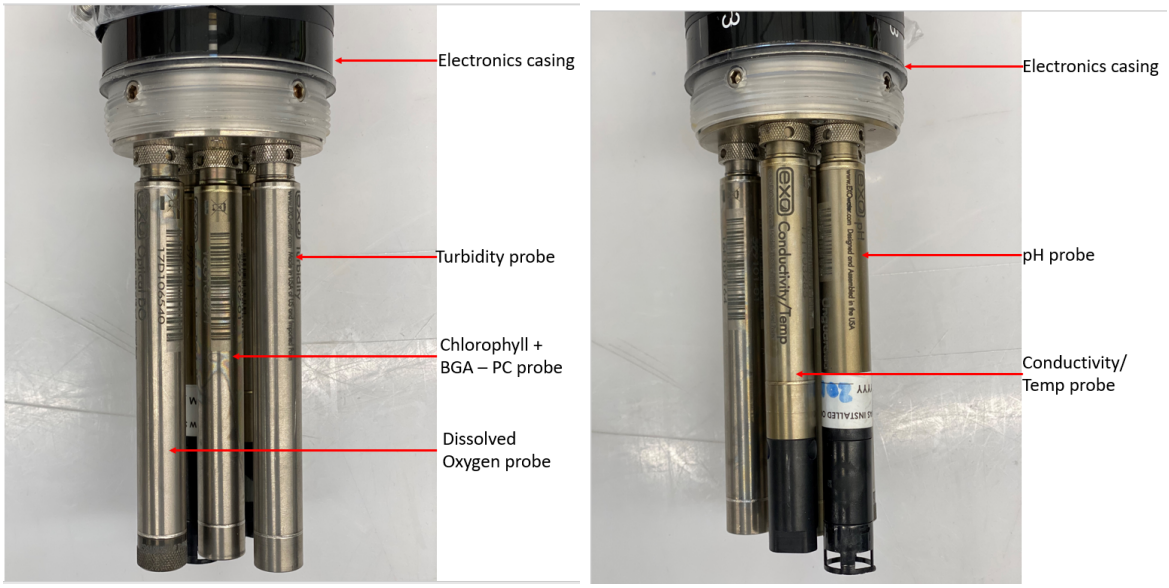

Figure 36: Sonde sensor probes

Table 2: Temperature sensor Probe Specifications.

Sensor Type	Thermistor
Units	Celsius
Operating Temperature	-5 to 50°C
Range	20
Response	T63< 1 seconds
Resolution	0.001 ° C
Accuracy	-5 to 35°C: ± 0.01°C and 35 to 50°C: ± 0.05°C

Table 3: Conductivity sensor Probe Specifications.

Sensor Type	4-electrode nickel cell
Units	microSiemens/centimeter
Operating Temperature	-5 to 50 °C
Range	20
Response	T63<2 seconds
Resolution	0.0001 to 0.01 mS/cm
Accuracy	0-100 mS/cm: ±0.5% and 100-200 mS/cm: ±1%

Table 4: pH sensor Probe Specifications.

Sensor Type	electrode Glass combination
Units	pH units
Operating Temperature	-5 to 50 °C
Range	0 to 14
Response	T63 < 3 seconds
Resolution	0.01
Accuracy	±0.01

Table 5: Chlorophyll sensor Probe Specifications.

Sensor Type	Fluorescence, Optical
Units	μg/L
Operating Temperature	-5 to 50 °C
Range	0 - 400 μg/L
Response	T63 < 2 seconds
Resolution	0.01 μg/L
Accuracy	0.01 μg/L

Table 6: Dissolved Oxygen sensor Probe Specifications.

Sensor Type	Optical
Units	mg/L
Operating Temperature	-5 to 50 °C
Range	0 to 50 mg/L
Response	T63 <5 seconds
Resolution	±0.1 mg/L
Accuracy	0-20 mg/L: ±0.1 mg/L

Table 7: Turbidity sensor Probe Specifications.

Sensor Type	Optical, 90° scatter
Units	FNU
Operating Temperature	-5 to 50 °C
Range	0 - 4000 FNU
Response	T63 <2 seconds
Resolution	0.01 FNU
Accuracy	0.3 FNU

Bathymetry is the measurement of the lake or river depth. It is critical to measure the depth of the lakes and rivers as discussed earlier in this chapter. The YSI EXO3 water quality Sonde is capable of measuring the depth and was considered for the application. However, the EXO3 uses pressure transducers to determine the depth. In order for the EXO3 to measure the depth, the tethered EXO3 is required to be dropped to the base of the lake. This would present enormous difficulty for the mission conducted by MANUEL.

Having determined that the Sonde could not measure the depth, we decided to use sonar sensor(see figure 37) to measure the depth. A ping sonar measures up to a maximum distance of 100 ft under the water using a single beam echosounder. The ping sonar produces a beam width of 30 degrees providing accurate measurements and physical temperature operating range between 32 to 86 Fahrenheit.The ping sonar has other applications including obstacle avoidance. The ping is connected to a microcontroller, Arduino programmed using Arduino software.

Figure 37: A picture of the Ping Echosounder [21]

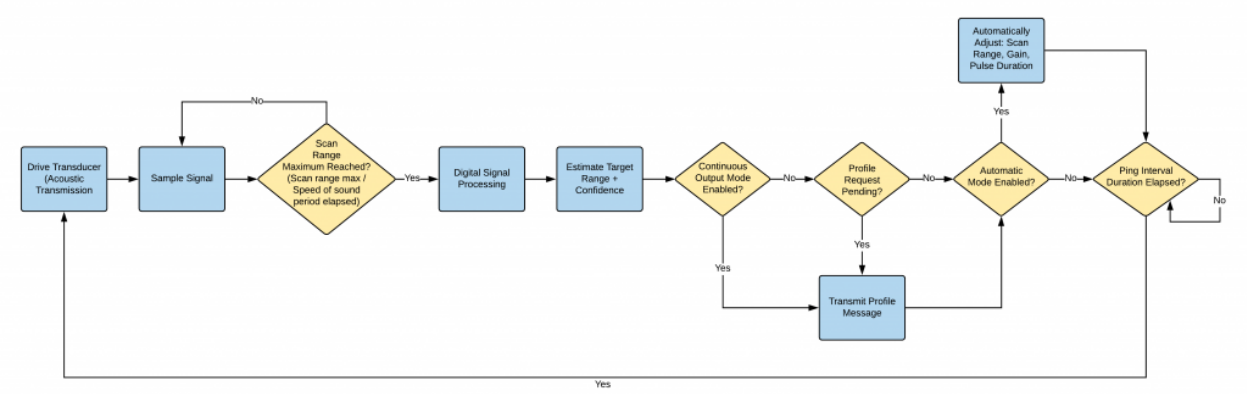

Figure 38: Ping internal functional diagram [21]

The ping measures the depth of the lakes by emitting acoustic pulse from the transducer at 115 kHz; it listens to the acoustic pulses back to the ping. The ping calculates the distance from its position to the bottom of the lake using equation 4.2.1. Where D is the depth, c is the speed of sound in water and t is the time measured for the echo to return [21].

$$D = c\frac{t}{2} \tag{4.2.1}$$

Table 8: Ping Sonar Specifications.

Sensor Type	Optical, 90° scatter
Units	ft, mm
Operating Temperature	0 to 30 °C
Range	1.6 - 100 ft
Response	T63 <2 seconds
Resolution	0.5% of Range
Accuracy	0.5% of Range

4.3 Sensor Calibration

4.3.1 EXO3 Sonde

For accurate calibration results, the calibration cup was filled with deionized water for rinsing all the sensors. All the sensors were rinsed three times before calibration. After rinsing, the probes were air-dried and connected to a personal computer to access KOR software. The detailed procedure for calibrating each sensor is as follows:

1. Conductivity calibration

   In a pre-rinsed EXO calibration cup, a conductivity standard of 1000 /muS/cm was poured. Based on the YSI recommendation, the calibration standard was filled until the second marked line. Air-dried probes were inserted into the calibration solution and gently moved to remove any air bubbles in the conductivity cell. In the calibration menu of KOR software, the calibrating conductivity option was selected, and the standard value of 1000 was entered. After calibration, the QC score was checked to ensure that the calibration was within the factory-defined limits. This procedure calibrates multiple water quality parameters, including conductivity, specific conductance, salinity, and Total Dissolved Solids (TDS).

2. Temperature calibration

   Based on the YSI manual, the temperature sensor cannot be user calibrated, but it was checked periodically with a thermometer for comparison at several reference points. This periodical check was suggested by the manufacturer and considered as the best management practice.

3. Dissolved Oxygen (DO) calibration

   The tap water was saturated with air for an hour. The Sonde with Dissolved Oxygen (DO) sensor was placed into the air-saturated water for five minutes, such that temperature and oxygen pressure reach an equilibrium. In the calibration menu, ODO was selected, and ODO% was set to 100%. This calibration for ODO% automatically calibrates DO (mg/L). Finally, the QC score was checked to ensure that the calibration result was within the factory defined limits.

4. pH calibration

   1-point calibration was done for the pH sensor using a pH 7 buffer. Later the pH probe was tested using known pH buffer solutions of 4, 7, and 10.

5. Total Algae calibration (CHLa and Phycocyanin)

   For Total Algae calibration, solutions used included clean water and 625 micro gram per litre Rhodamine WT dye solution based on the recommendation by YSI. Therefore, a two-point calibration was performed to calibrate the total algae sensor to measure both CHLa and Phycocyanin. First deionized water was poured into the calibration cup, and value '0' was entered as standard in the calibration. Similarly, with Rhodamine dye solution, a known fluorescence value of 66 was entered for calibration.

6. Turbidity calibration

   Clean and air dried probes were calibrated using formazin with 0, 10, and 100 NTU calibration standards. By placing the air-dried probes in the standard solutions, 3-point calibration was performed by entering the standard values in the KOR software's calibration menu. After calibration, the QC score was checked to ensure that the readings by turbidity sensor were within factory defined limits.

4.3.2 Ping Sonar

Calibrating the ping sonar involved using the ping-viewer an open source GUI application. calibrating the ping sonar requires changing the speed of sound in the particular situation. The speed of sound in fresh and salty water are 1435, 1500 m/s respectively. Therefore, the speed of sound for the ping sonar was set to be 1435 m/s because all the lakes in Oklahoma where MANUEL is implemented are dominantly fresh water. The ping sonar has error percentage of 0.5.

4.4 Sensor-Vehicle Integration

4.4.1 EXO3 Sensor Attachment

The EXO3 weights 4.4 pounds and has a diameter and length of 3 inches and 2 feet, respectively. Therefore, to mount the Sonde on MANUEL, a holding cup was designed and 3D printed, the holding cup in the figure below has a diameter of 3.25 inches. The Sonde is securely tightened in the holding cup with screws, a carbon fiber rod is screwed in to the holding arm(holding cup) which is secured on MANUEL.

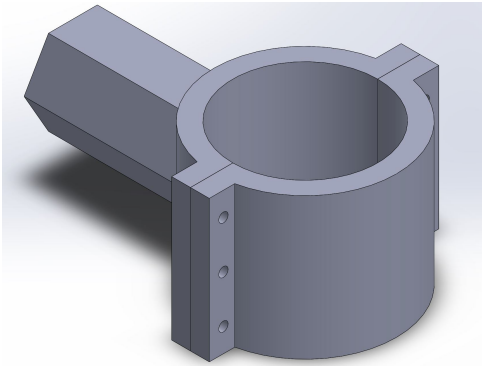

Figure 39: Holding arm of the Sonde

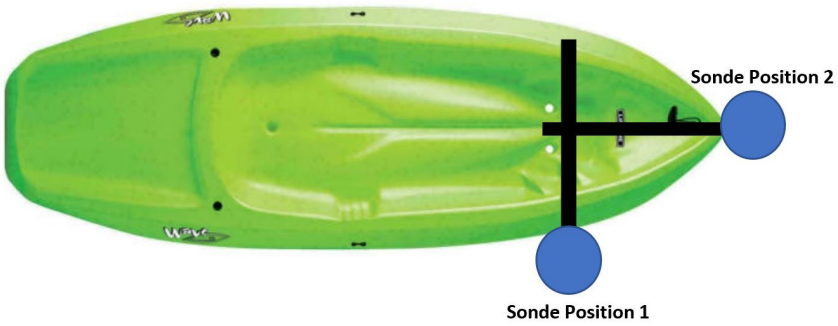

Figure 40: Top view of MANUEL showing Sonde placement

The initial approach of securing the Sonde on the side as indicated in the figure 41 was considered. However, placing the Sonde on either the left or right side of MANUEL presented unique challenges. The flow in contact with Sonde at either side of the placement was disturbed which affects the measurements of parameters such as dissolved oxygen, temperature among others. The disturbance in the flow is due to the wake caused by the front point of MANUEL. Secondly, this approach of attachment created a tendency of MANUEL to drift to the side that the Sonde was placed.

Figure 41: Side position of the Sonde

Clearly the initial approach of placing the Sonde on either side of MANUEL hindered the performance and measurements of the water quality parameters. Therefore, the position of the Sonde was shifted to the front position as shown in the figure 42. The front position enabled clean flow measurements since the Sonde interacted with the flow before any disturbances. The boat was more stable with the Sonde at that position making this the best position of placement.

Figure 42: Front position of the Sonde

4.4.2 Sonar Sensor Attachment

The ping sonar is attached to MANUEL at the base mounted in the middle section of the aluminum bar using two screws as shown in the figure 43 and 44. The sonar is directly placed under the same position as the batteries; this keeps the sonar fully immersed and leveled accurate depth measurement.

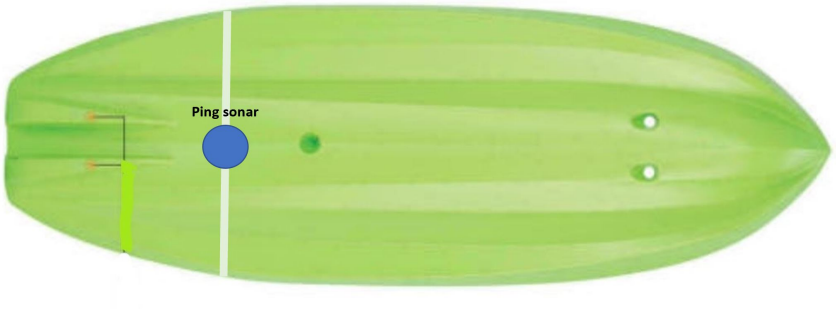

Figure 43: Bottom view showing Ping sonar placement

Figure 44: Sonar placement

4.5 Data Collection

The Sonde is programmed using the KorEXO software (screenshot 45). Through the KorEXO software, a sketch of water quality parameters are selected including the rate at which data is logged. KorEXO software enables different units to be selected for the water quality parameters, deploys and un-deployed the Sonde downloads the CSV data from the Sonde for further processing. The data is collected at 1 Hz.

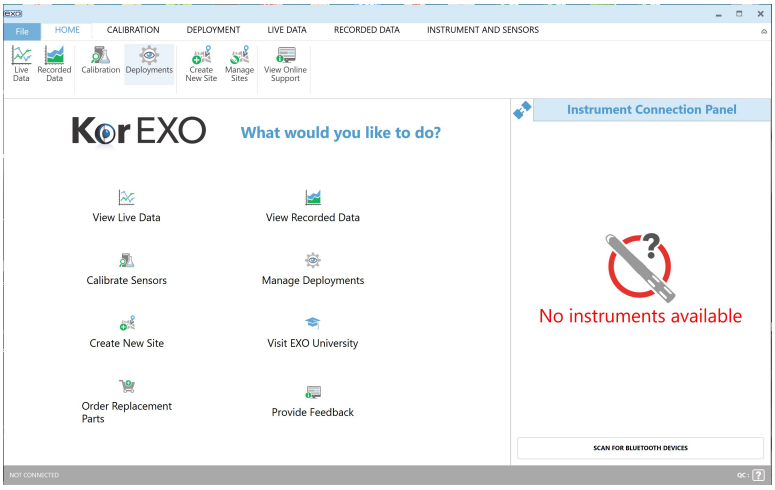

Figure 45: KorEXO software screenshot

Using the auto pilot Pixhawk cubic to collect latitude, longitude, and coordinated time, the data collected is merged with that from the Sonde EXO3 using a MATLAB algorithm in appendix that matches the time stamps from both, this was tested intensively to ensure proper merge of the data. The final CSV data file consists of the Date, Time Latitude, Longitude, Phytoplankton and Chlorophyll-a, Depth, Dissolved Organic Material, Conductivity, Salinity, Dissolved Oxygen, pH of water, Turbidity, and Water Temperature.

The ping sonar is connected to a micro controller, Enviro Mayfly data logger (see figure 46) programmed using the Arduino software to collect the depth measurements. The data collected from the sonar is geo-tagged with the GPS coordinates from the pixhawk and then stored into a log line in a CSV file on a micro SD card for post processing. The data is logged at 2 Hz. The sketch for logging the data, geo-tagging and storing it on the micro SD card is included in the appendix.

Figure 46: Enviro Mayfly Data Logger [13]

CHAPTER V

Results

5.1 Boomer Lake: Testing of MANUEL

The testing of MANUEL involved tuning, learning her capabilities and pushing her to the limits. The majority of the testing was conducted at Boomer lake because it is closer to our lab facilities Unmanned Systems Research Institute (USRI). The testing was conducted in phases 1, 2 and 3.

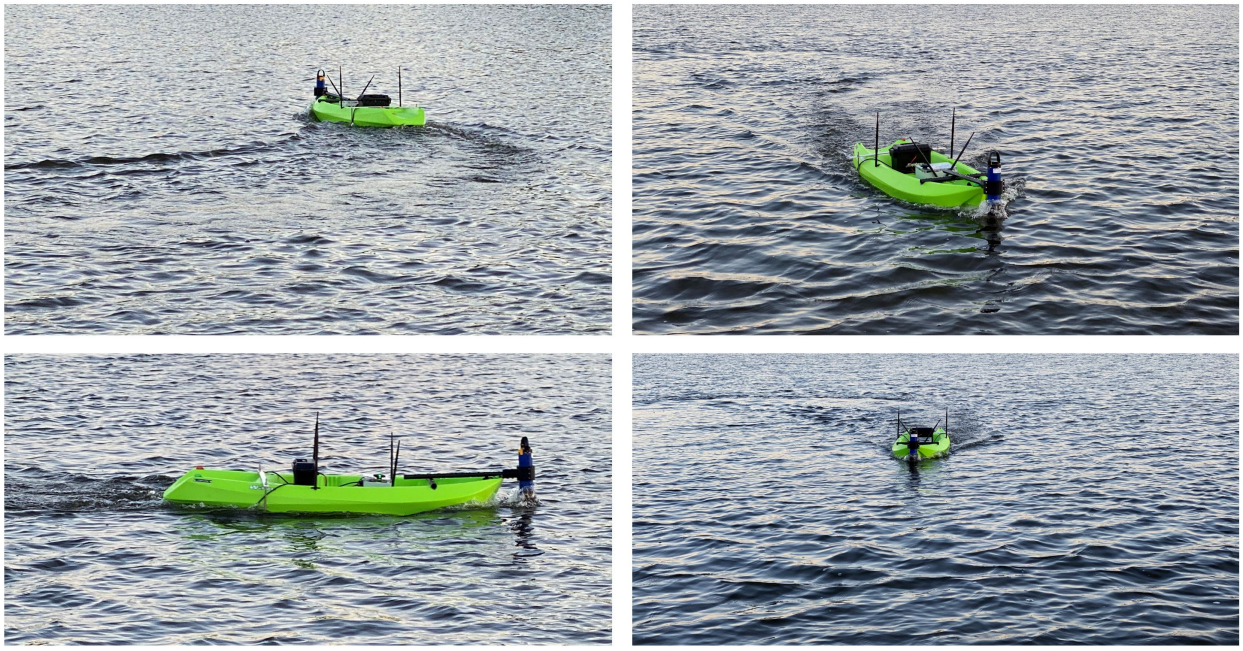

Figure 47: MANUEL test at Boomer Lake

1. Phase 1

   Phase 1 was to test the basic functions of MANUEL. Objectives for phase 1 included testing the propulsion system, steering capabilities using thrust differential, and manual operation. Phase 1 testing enabled the troubleshooting of issues faced during the testing of the particular characteristics of MANUEL. Before moving to phase 2, all the objectives were addressed, resolved and approved.

2. Phase 2

Phase 2 was to test the autonomous capabilities of MANUEL. During this phase, the PIDs of MANUEL were tuned, a working communication between MANUEL and the ground control station was established through telemetry, and numerous AUTO missions were performed. The figure below shows the path taken by MANUEL during its one of many AUTO missions performed. The path in the figure below is obtained by plotting the GPS coordinates from the autopilot using MATLAB.

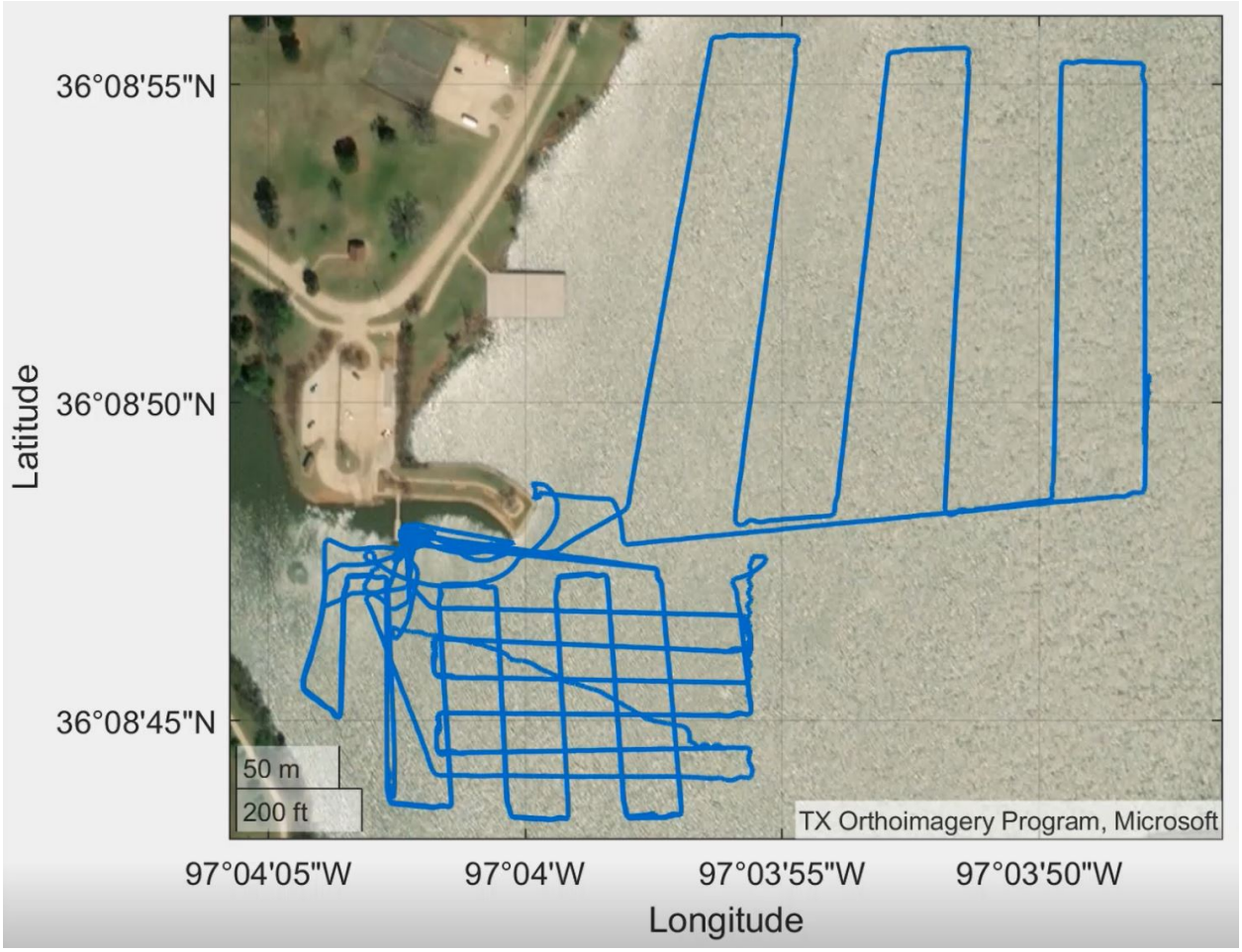

Figure 48: MANUEL's different auto mission paths during test at Boomer lake

Simultaneously, the data acquisition system went through multiple testing phases. The maximum cruising speed, endurance and range of operation of MANUEL testing of the integration, and sampling rate of the data acquisition system were assessed.

3. Phase 3

Figure 49: Phase 3: MANUEL long range test at Boomer Lake

During phase 3, MANUEL was pushed to it's limit; this involved performing an autonomous mission from one end of boomer lake to the other end approximately 1.06 miles apart (see fig 50). During the test, MANUEL had telemetry until approximately 1 mile and lost connection to the ground station thereafter. However, the loss of telemetry connection was due to the high vegetation around the lake.

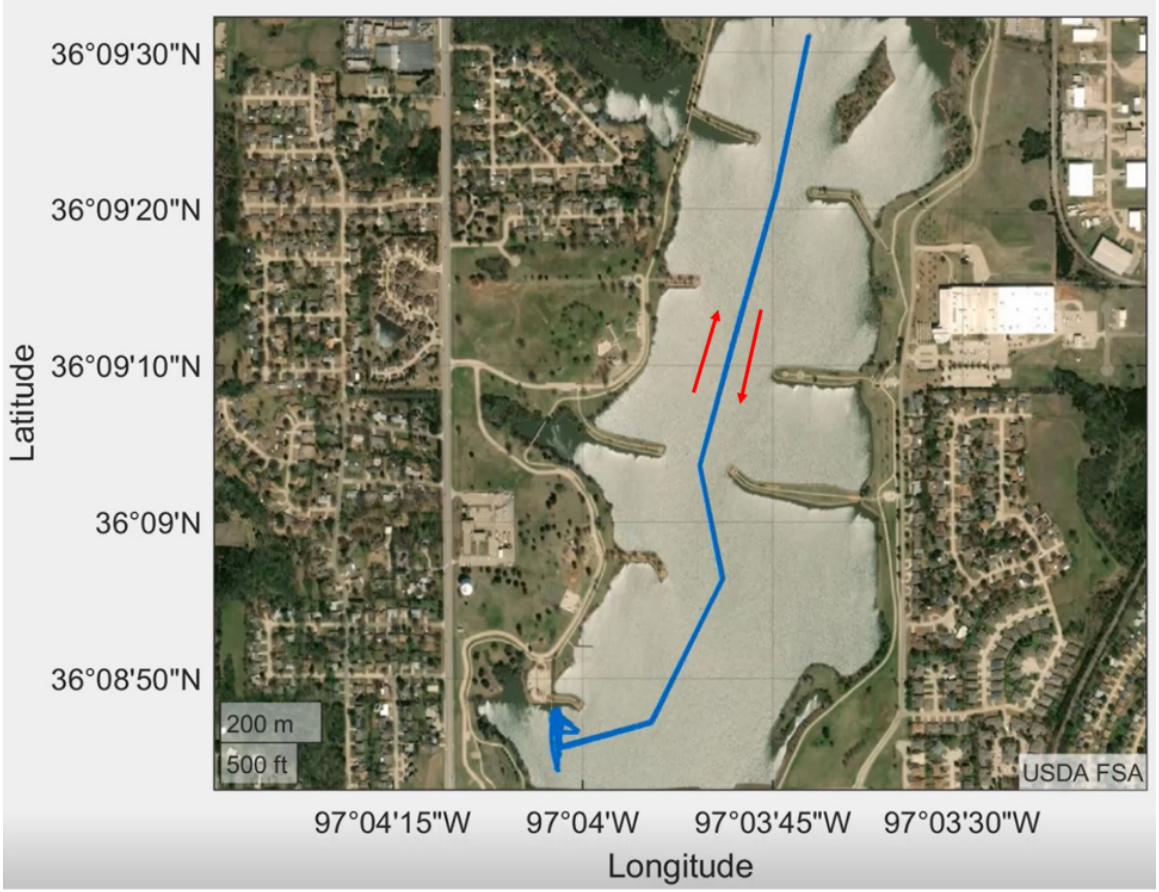

Figure 50: MANUEL path from South end of Boomer lake to the North end.

5.2 Implementation

5.2.1 Horse Creek Cove at The Grand Lake O' the Cherokees (Grand Lake)

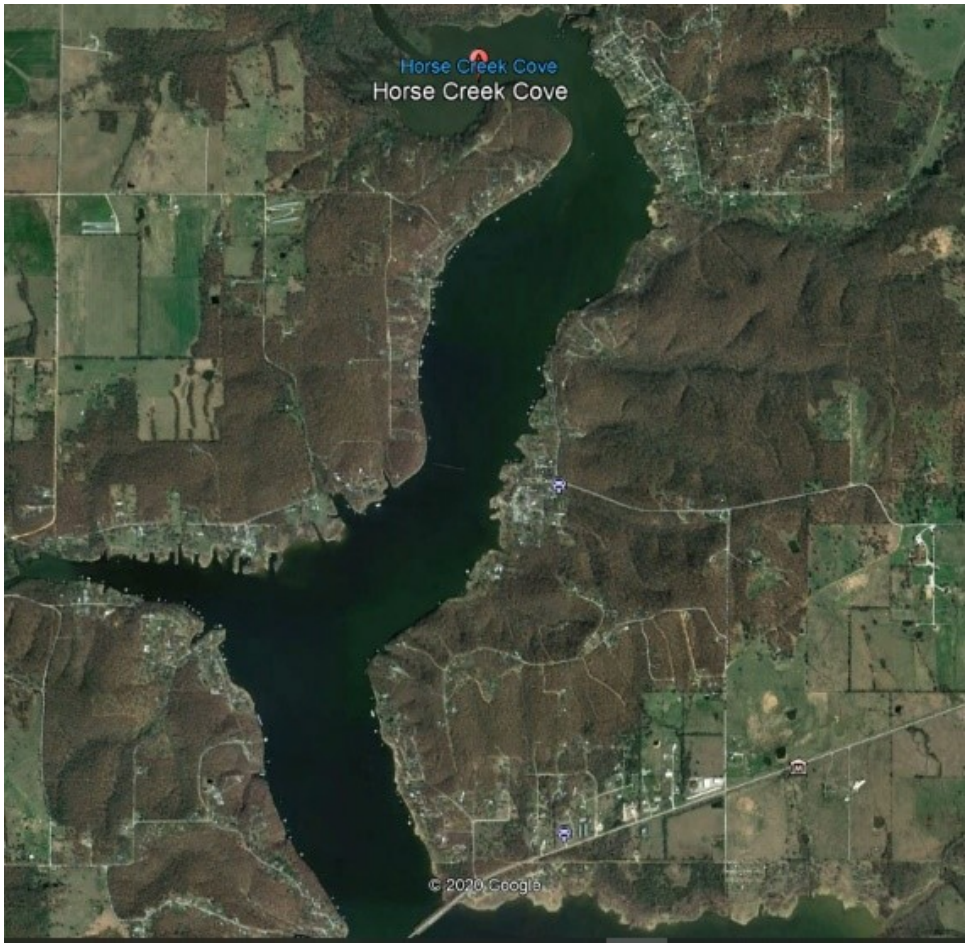

Figure 51: A map of Horse Creek Cove

Horse Creek Cove in figure 51 is one of the feeding arms to the main Grand Lake. The Grand Lake has a total surface area of 169.07 kilometers squared of water. The Horse Creek Cove is part of the Grand Lake. The Grand Lake serves more than 10,000 people with fresh water for drinking, irrigation for the agricultural farmland and industrial use.

Grand lake in the Northeastern part of Oklahoma in Delaware county has been faced with Harmful Algae Brooms (HABs), sedimentation, and eutrophication. HABs is a quick growth of algae that are harmful to humans, animals, and the community ecology. Since 2011, HABs have invaded the Horse Creek Cove on numerous occasions. Nutrients that flow in the creek such as fertilizers from the agricultural lands surrounding the creek support the growth of HABs when the condition are favorable; mostly during drought. The Horse Creek Cove was severely flooded in 2015 and 2019, carrying sediments into Grand Lake. The floods are due to heavy rainfalls. The sediments carried into the lake reduce the water storage capacity of the reservoir, hence affecting the drinking water supply, ecosystem and

recreation activities at the lake which has had a negative impact on the economy of the local community and numerous bans on swimming.

Having described the challenges facing Grand lake, it is critical to forecast sedimentation and HABs formation in the reservoir. The data collected during the forecast will be used to create predication models, equip scientists with information to make better decisions to preserve the water reservoir. MANUEL is equipped to provide the capabilities to forecast the formation of HABs and sedimentation hence it is implemented at the Horse Creek Cove.

Figure 52: MANUEL monitoring Horse Creek Cove at Grand Lake.

During the implementation of MANUEL at the Horse Creek Cove, MANUEL autonomously surveyed along the path in the blue lines as indicated in figure 53 while taking water quality parameters and bathymetry. The blue lines indicate the path taken during the survey; the data plotted to achieve the paths is downloaded from the log files of MANUEL's Pixhawk.

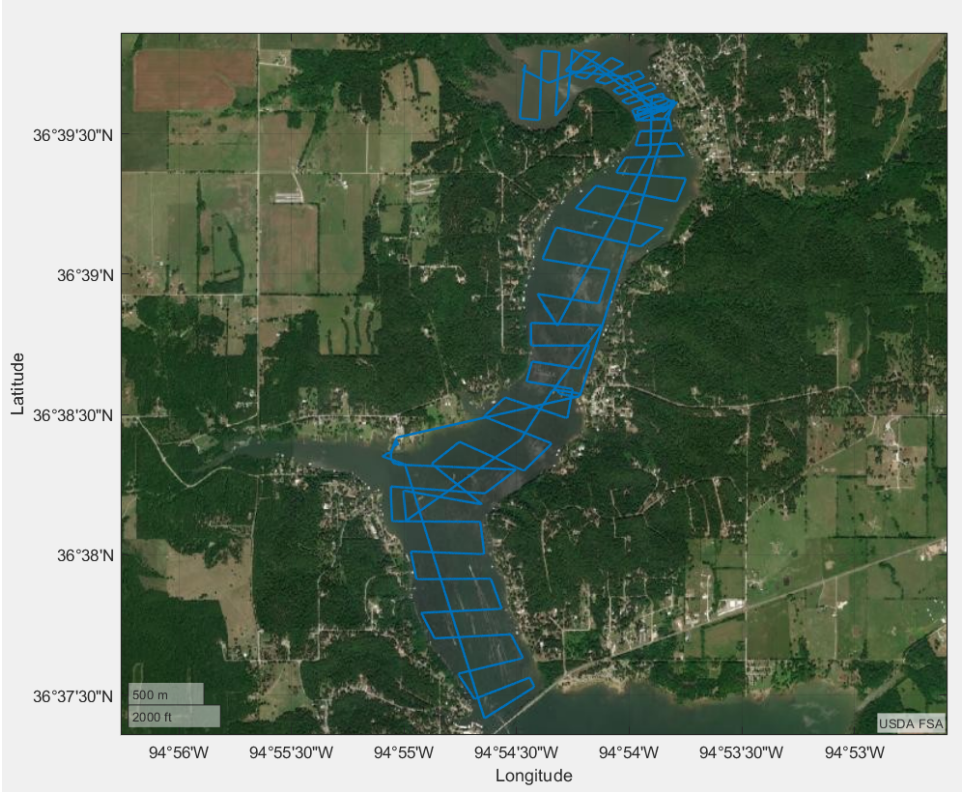

Figure 53: MANUEL's path followed at Horse Creek Cove

The sampling at the Horse Creek Cove was conducted in 4 different days with 2 hours long AUTO mission. In figure 54, each color represents the different days the sampling was conducted. The data was collected during the survey as discussed in chapter **??** in the data collection section. Red represents day 1, green day 2, blue day 3 and yellow is day 4.

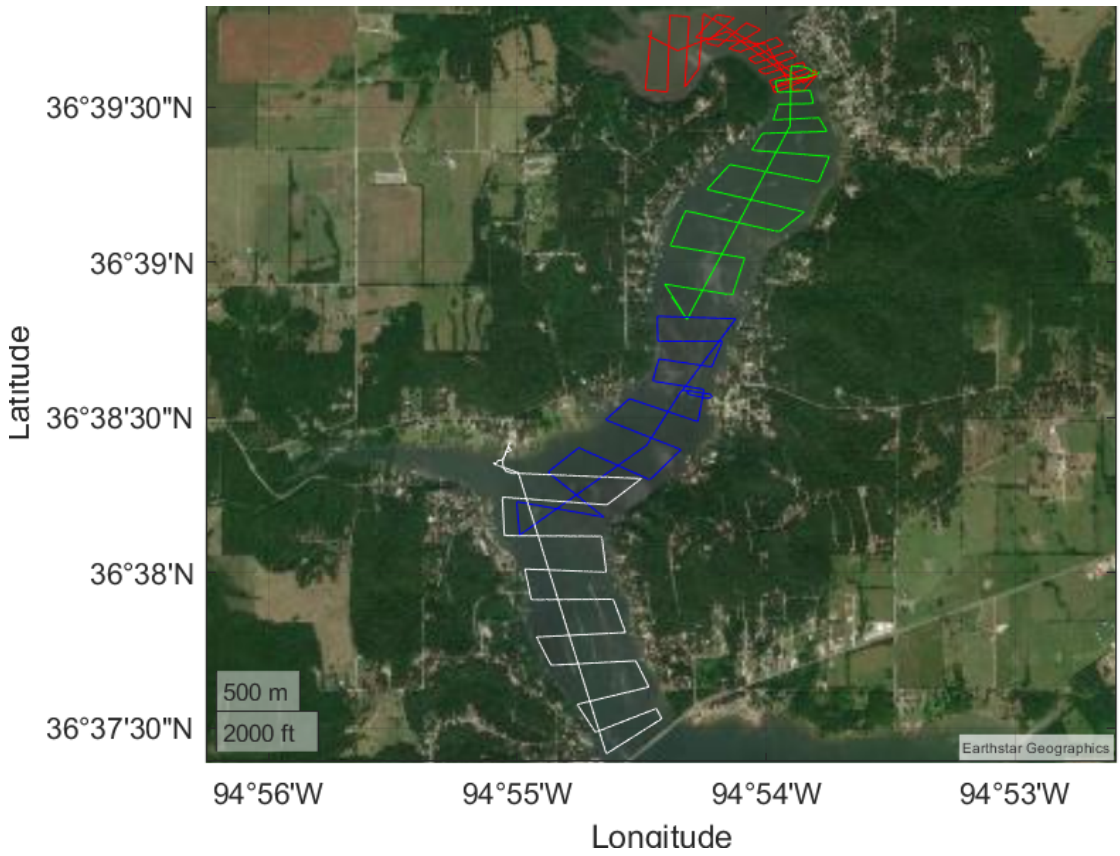

Figure 54: Color coding of MANUEL's entire mission on Horse Creek Cove

Ambient Conditions

The conditions of the respective days were recorded, this included the temperature, wind speed and the time when sampling started and stopped. The ambient conditions affect the measurements collected such temperature of the water, and dissolved oxygen. The ambient conditions are recorded in the table 9. During data collection, on day 4, there was a heavy rainfall as data was collected and similarly on day 3, there had been a heavy rainfall the night before.

Table 9: Ambient Conditions during the survey at Horse Creek Cove.

Day	Date	Start Time	End Time	Temp oC	Wind Speed (mph)
1	8/19/2020	11:32:22	13:10:06	27.8	5
2	7/23/2020	10:38:41	12:12:59	32.2	5
3	7/28/2020	17:04:44	18:06:04	30	10
4	7/29/2020	11:36:15	13:04:14	25.3	12

5.2.2 Data Processing

During the data processing, the collected data was parsed to remove the data considered as noise such as the data recorded before the start of the AUTO mission, all this was to be removed because it was undesired data. The data collected as MANUEL returned to the

launch point was rejected because it created noisy data, this included the data that was time sensitive such as temperature, dissolved oxygen and among others. The parsed data was then plotted and discussed below.

Bathymetry

The bathymetry data included the latitude, and longitude from the Pixhawk GPS unit merged with the depth measurements from the sonar. The data is loaded in the MATLAB where the latitude, and longitude are initialized and the mesh grid created. However, during the plotting, it was observed when interpolating data, the mesh grid execuded from the water to land hence interpolating the land as part of the lake. To resolve the interpolation over land as part of the lake, the boundary of the lake was created using mission planner which generated a way-point file. The generated way-point file is imported into MATLAB which then creates a polygon hence interpolating and generating a mesh grid only over the water surface.

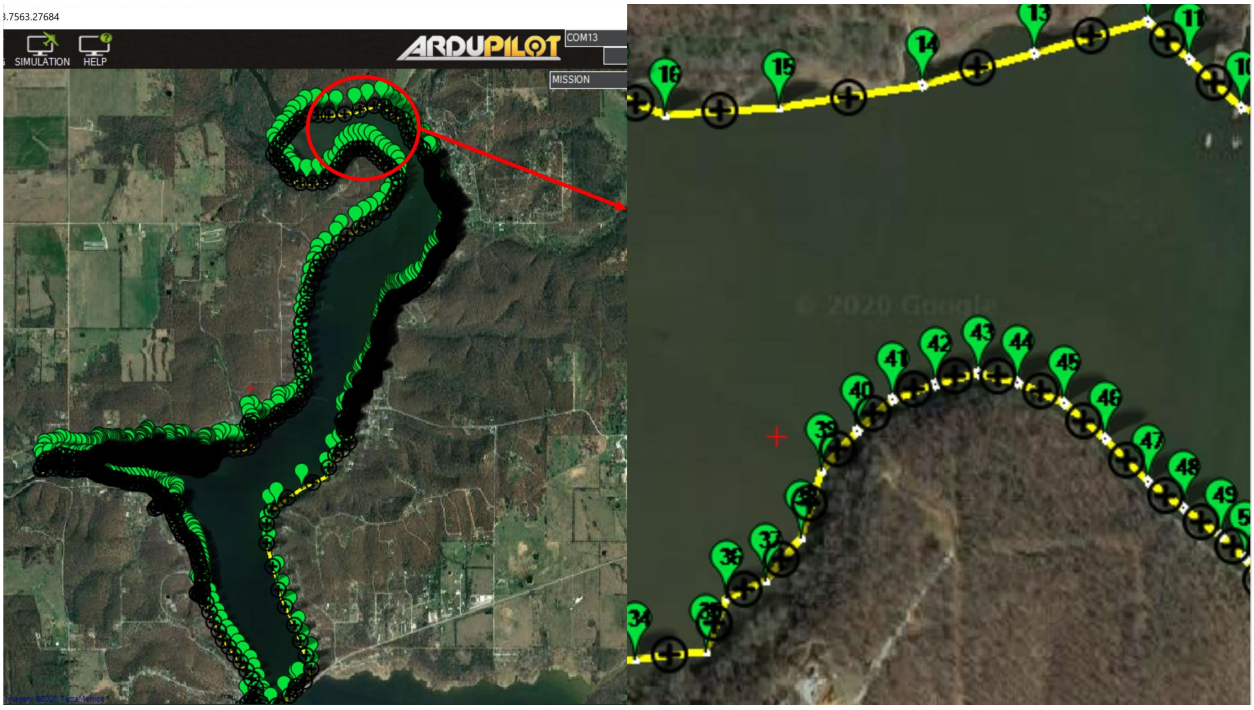

Figure 55: Generating a boundary of Horse Creek Cove in mission planner

Plotting the bathymetry data, two different interpolation approaches were considered. The first interpolation was the standard linear interpolation where the data interpolation followed the lawn mower pattern. The results from the plotting are shown in figure 56. However, the plot produced was not a smooth plot.

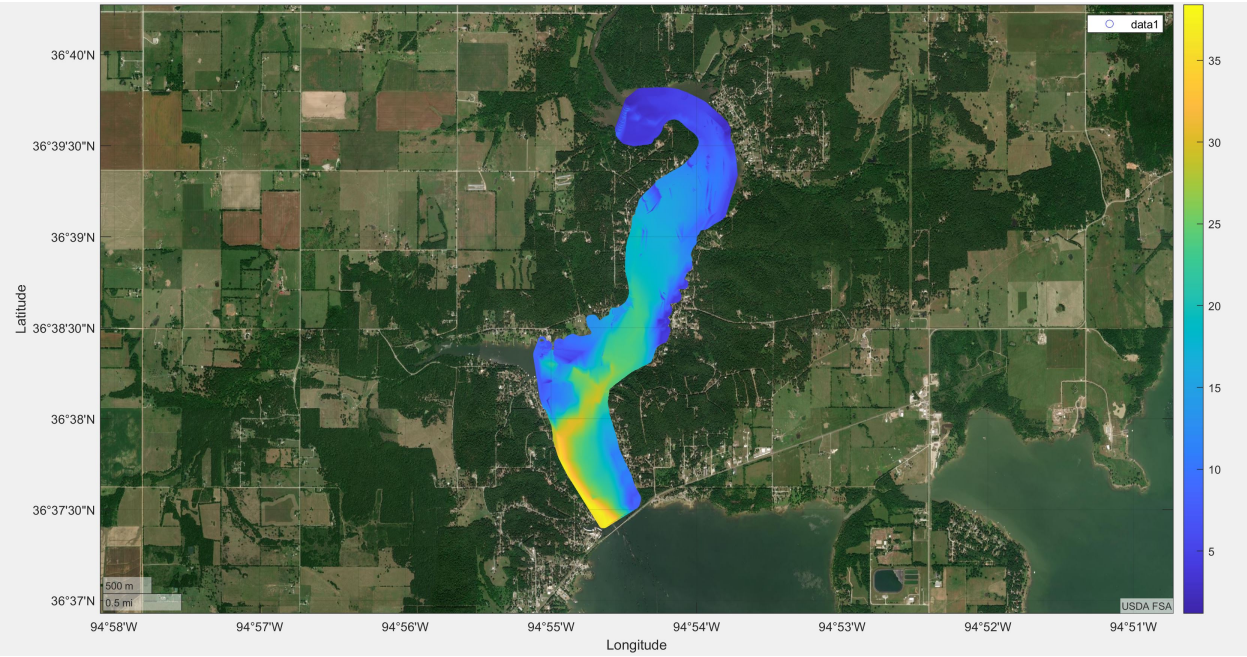

Figure 56: Depth Map of Horse Creek Cove

A different interpolation approach was taken; the linear interpolation using the immediate neighbour data points, this approach produce a plot smoother than the previous plot of the same exact data in figure 56. The data plotted using the neighbour linear interpolation technique is as shown in the figure 57.

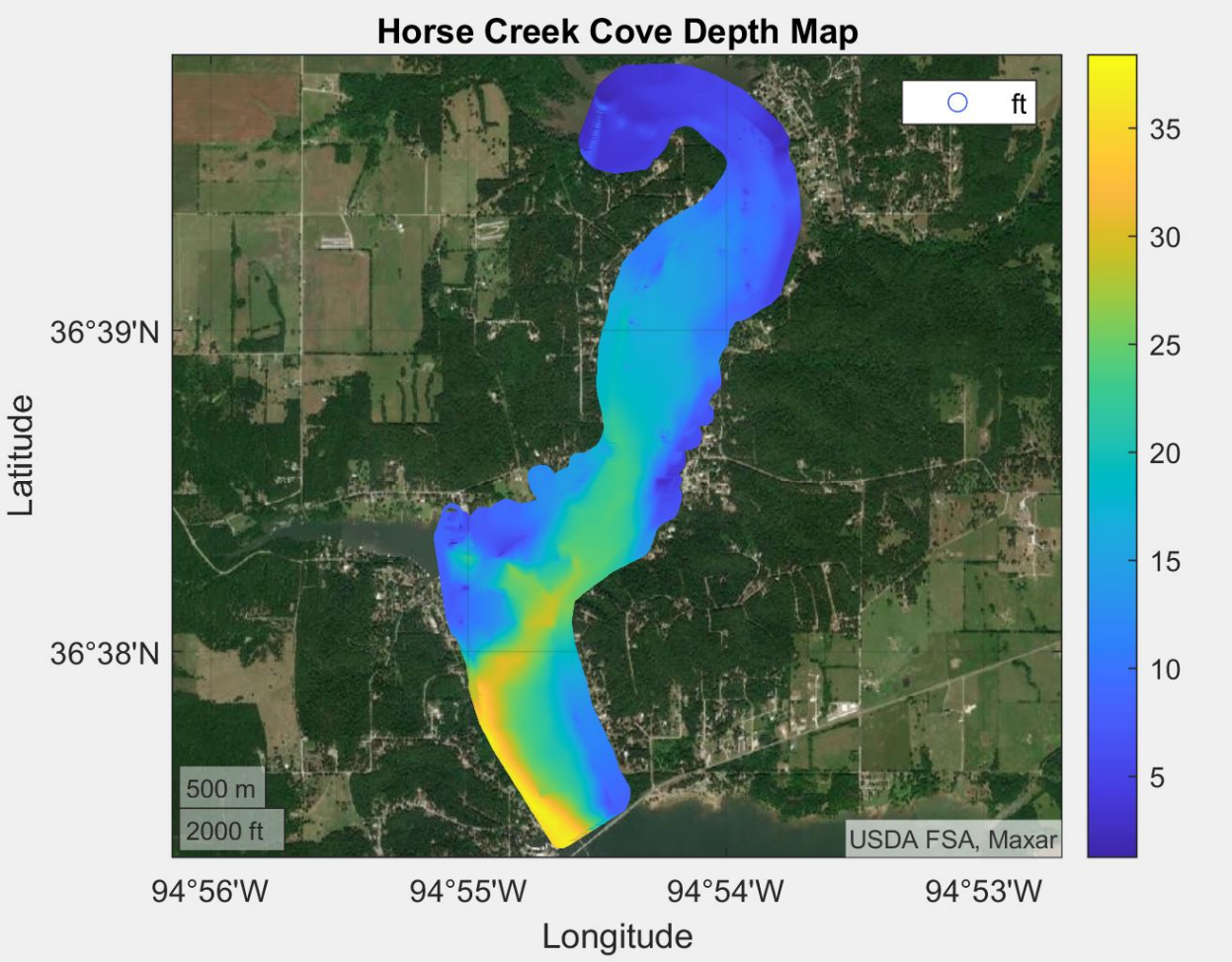

Figure 57: Depth Map of Horse Creek Cove

Temperature

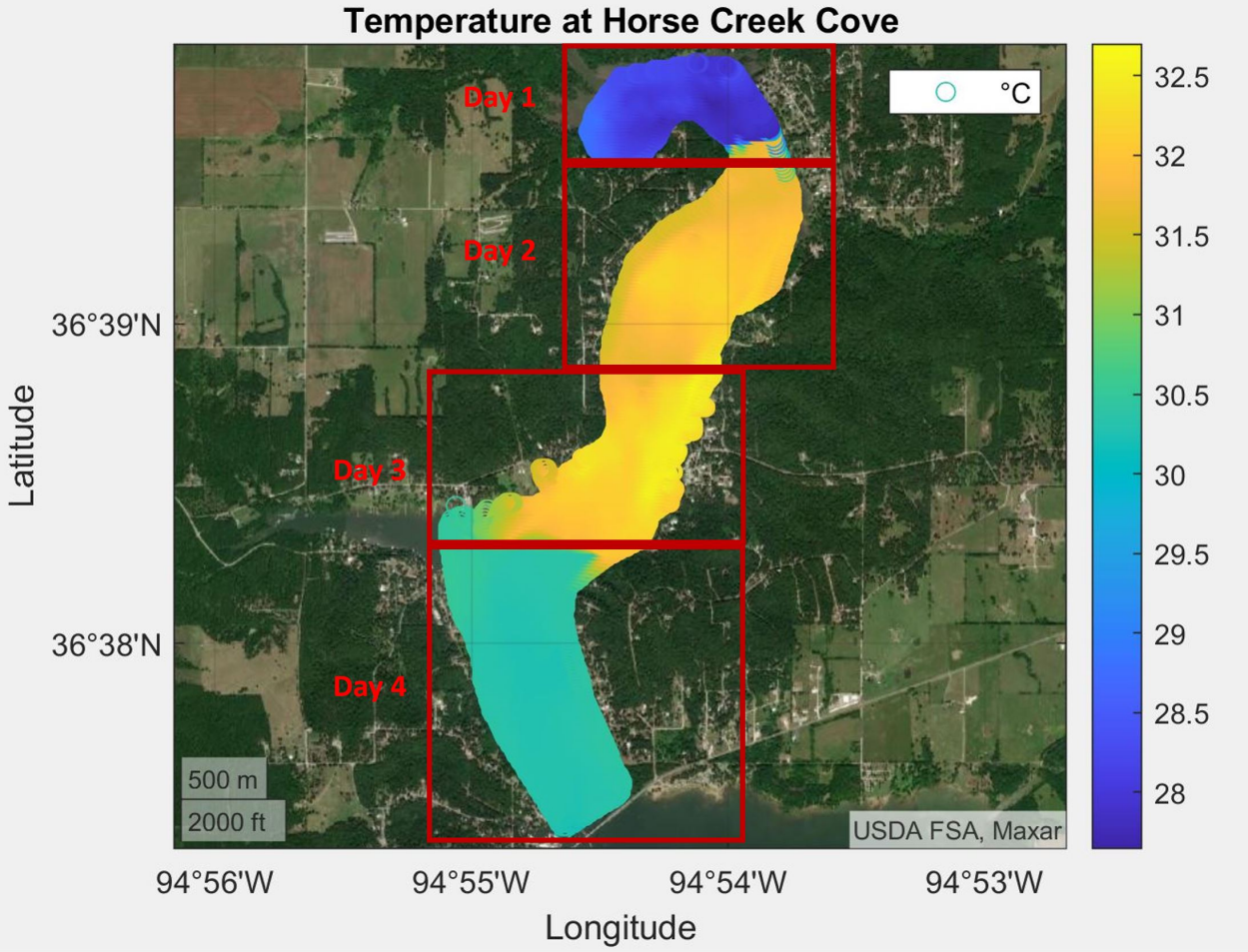

Figure 58: Temperature Map of Horse Creek Cove

pH

The collected pH data is plotted as shown in plot figure 59. From figure 59 of the entire Horse Creek is between 7.5 and 9.

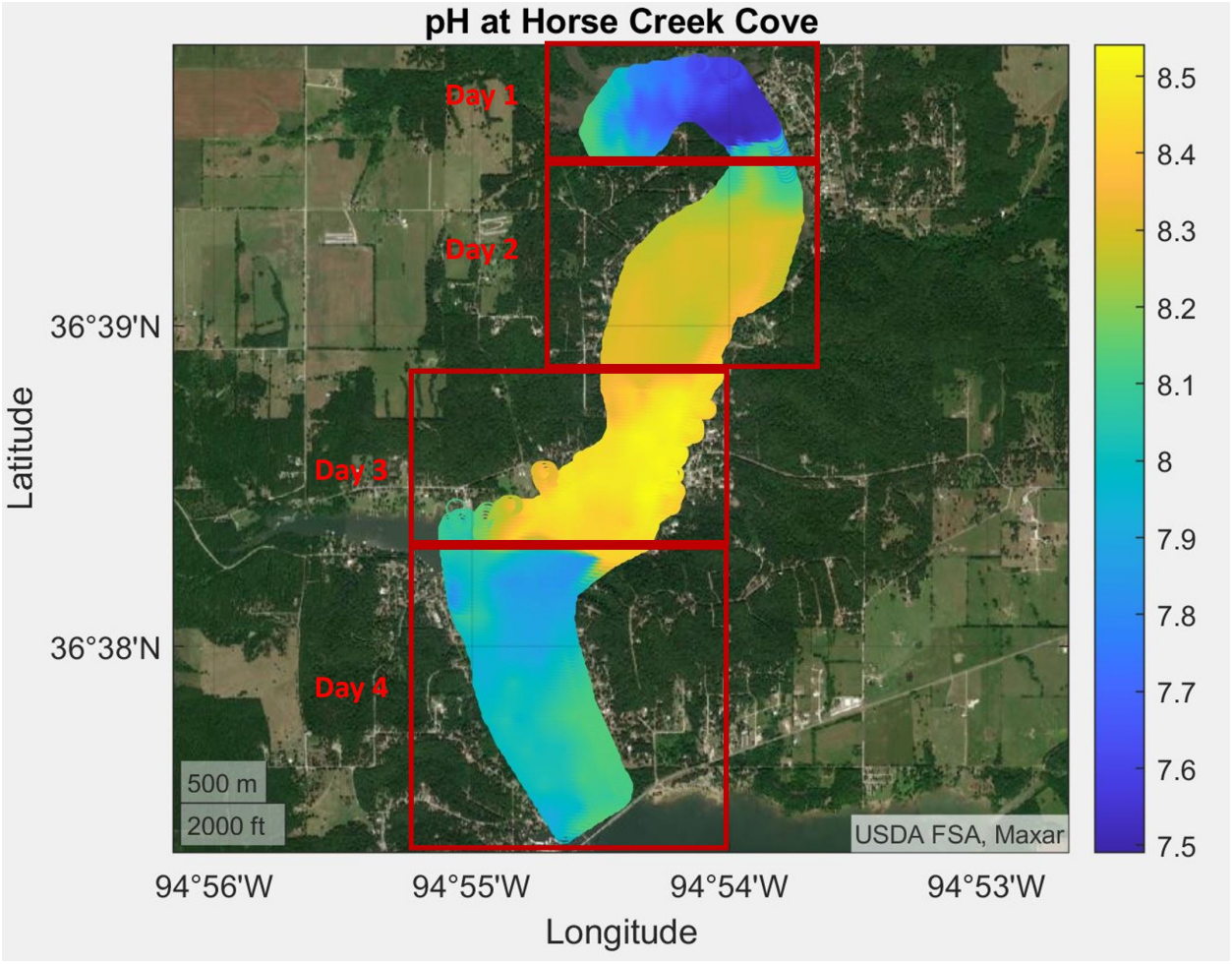

Figure 59: pH Map of Horse Creek Cove

Chlorophyll

Chlorophyll is one of the critical water quality parameter. The data collected with aid of MANUEL was processed as described earlier. The chlorophyll measurements were recorded in mill-grams per liter. The chlorophyll data is plotted and presented in figure 60.

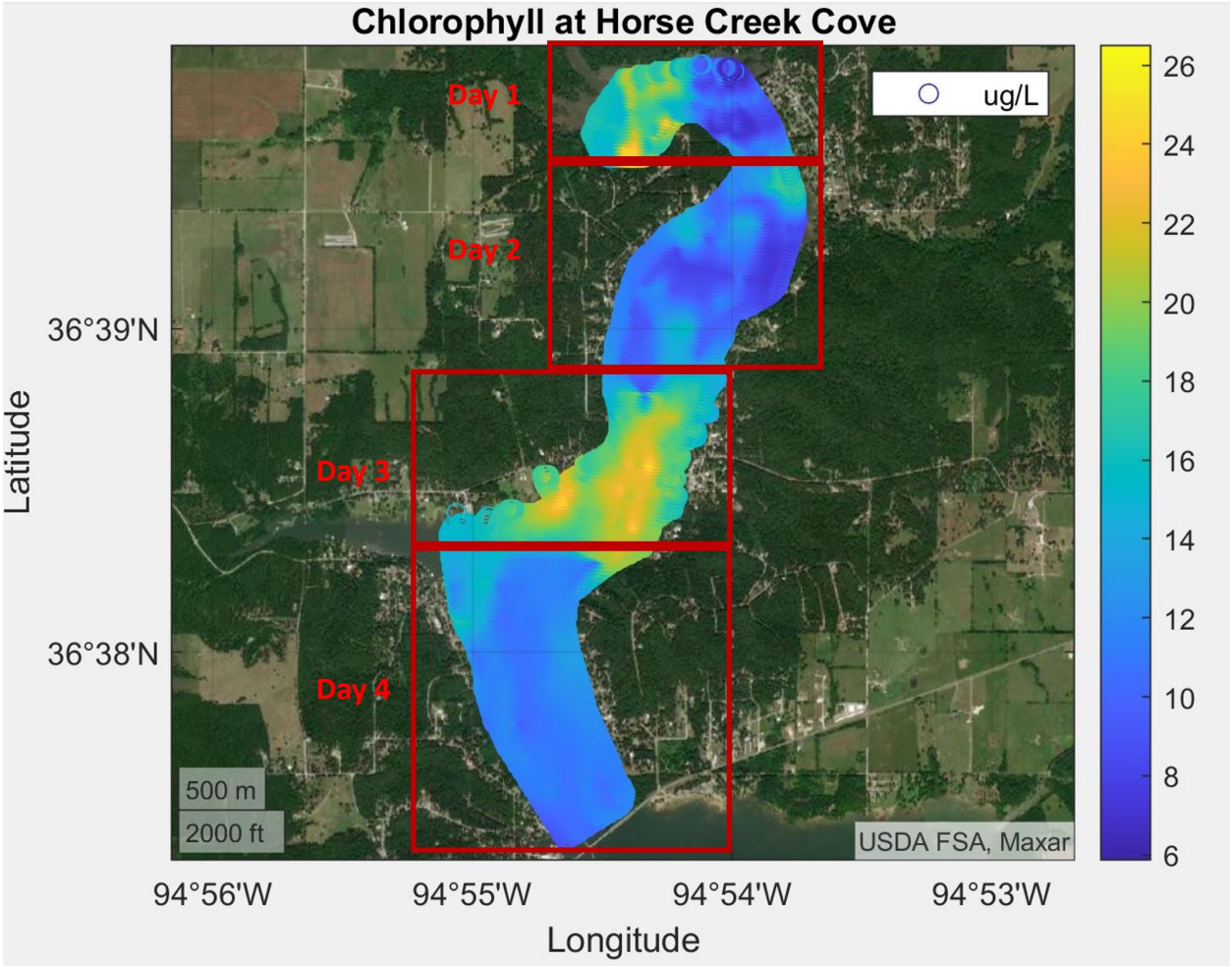

Figure 60: Chlorophyll Map of Horse Creek Cove

The chlorophyll data collected from the Horse Creek Cove is between 6 and 28 μg/L.

Dissolved Oxygen

The dissolved oxygen data was processed and plotted in figure 61

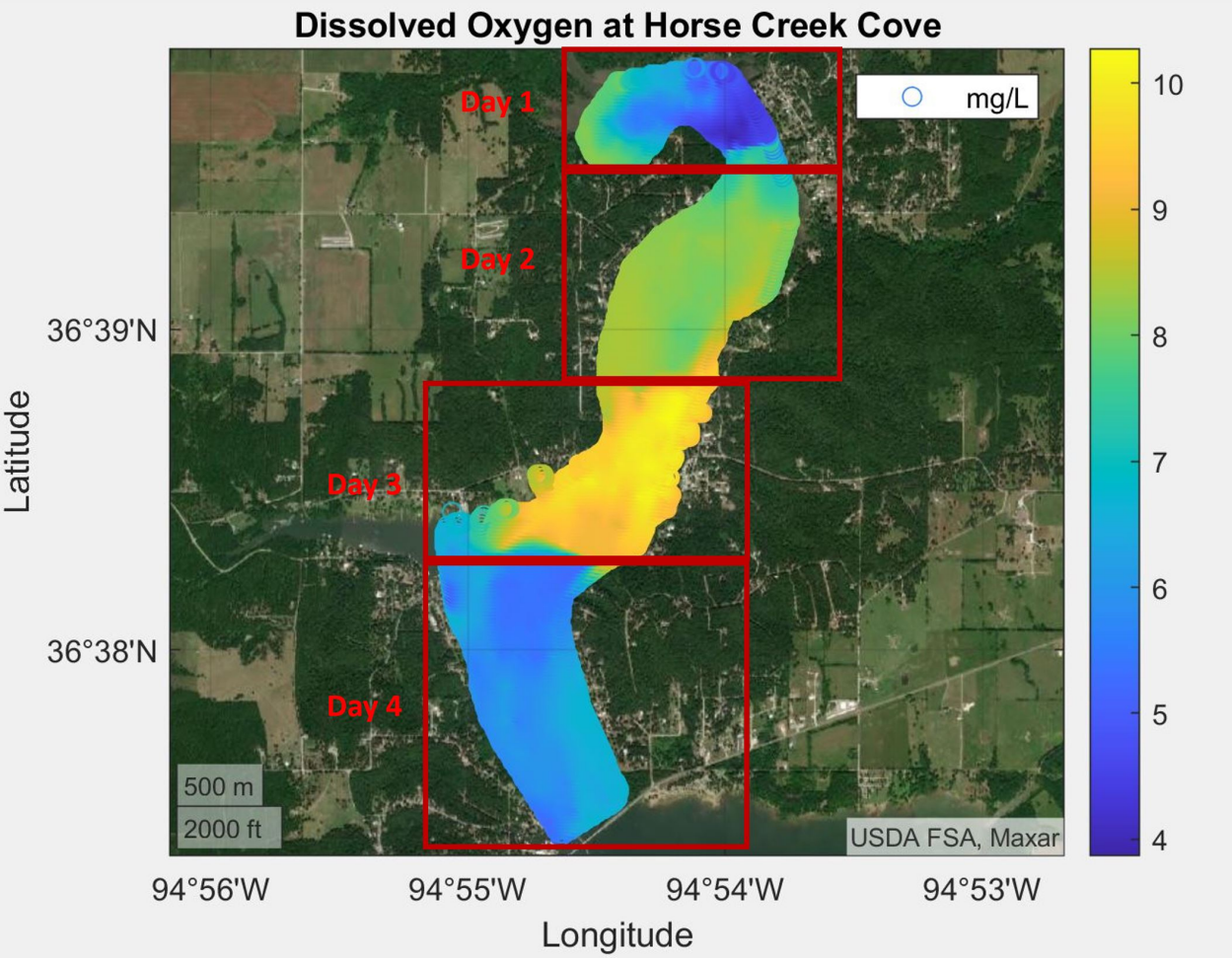

Figure 61: Dissolved Oxygen Map of Horse Creek Cove

Turbidity

The turbidity plot of the Horse Creek Cove is processed and plotted in figure 62.

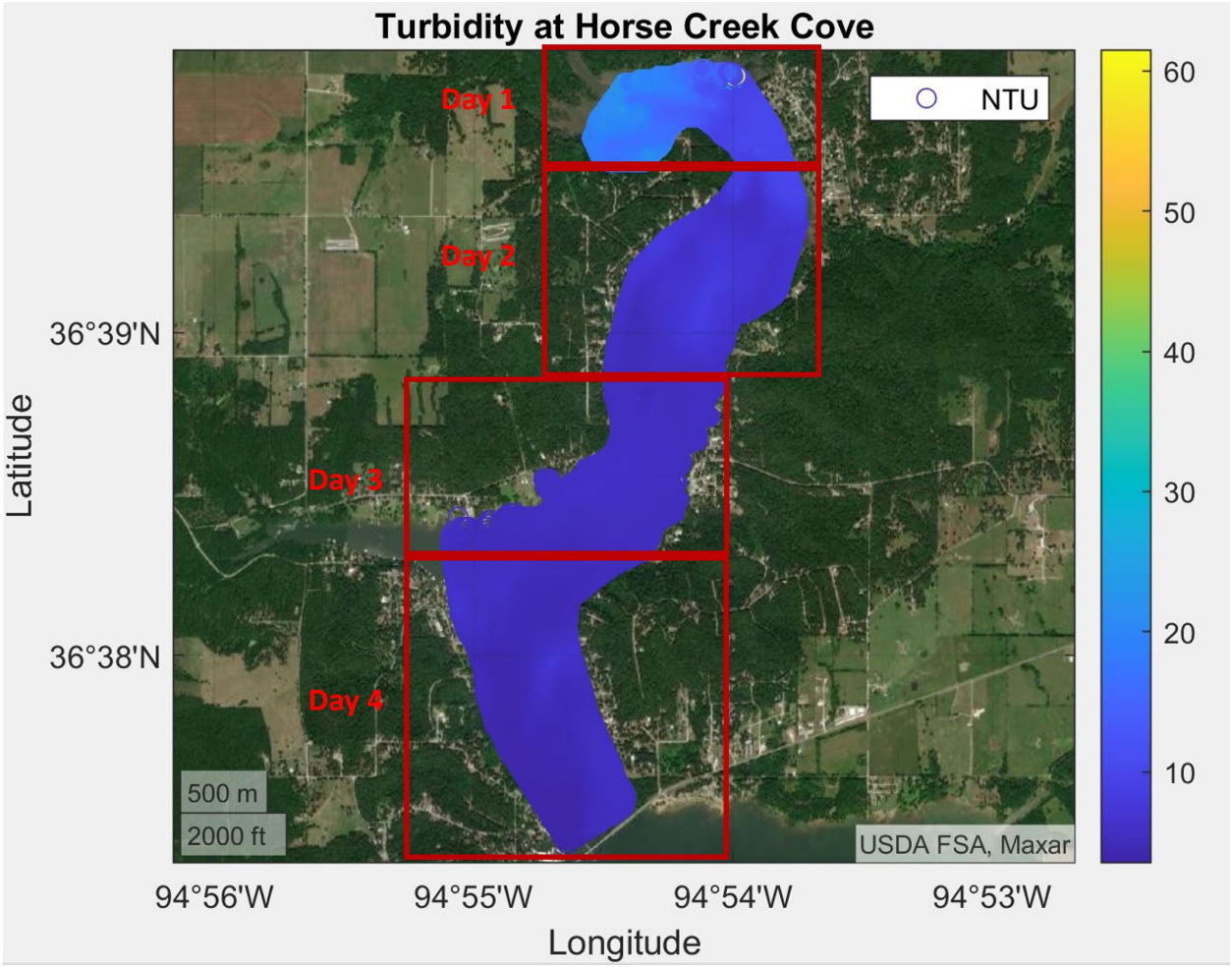

Figure 62: Turbidity Map of Horse Creek Cove

Conductivity

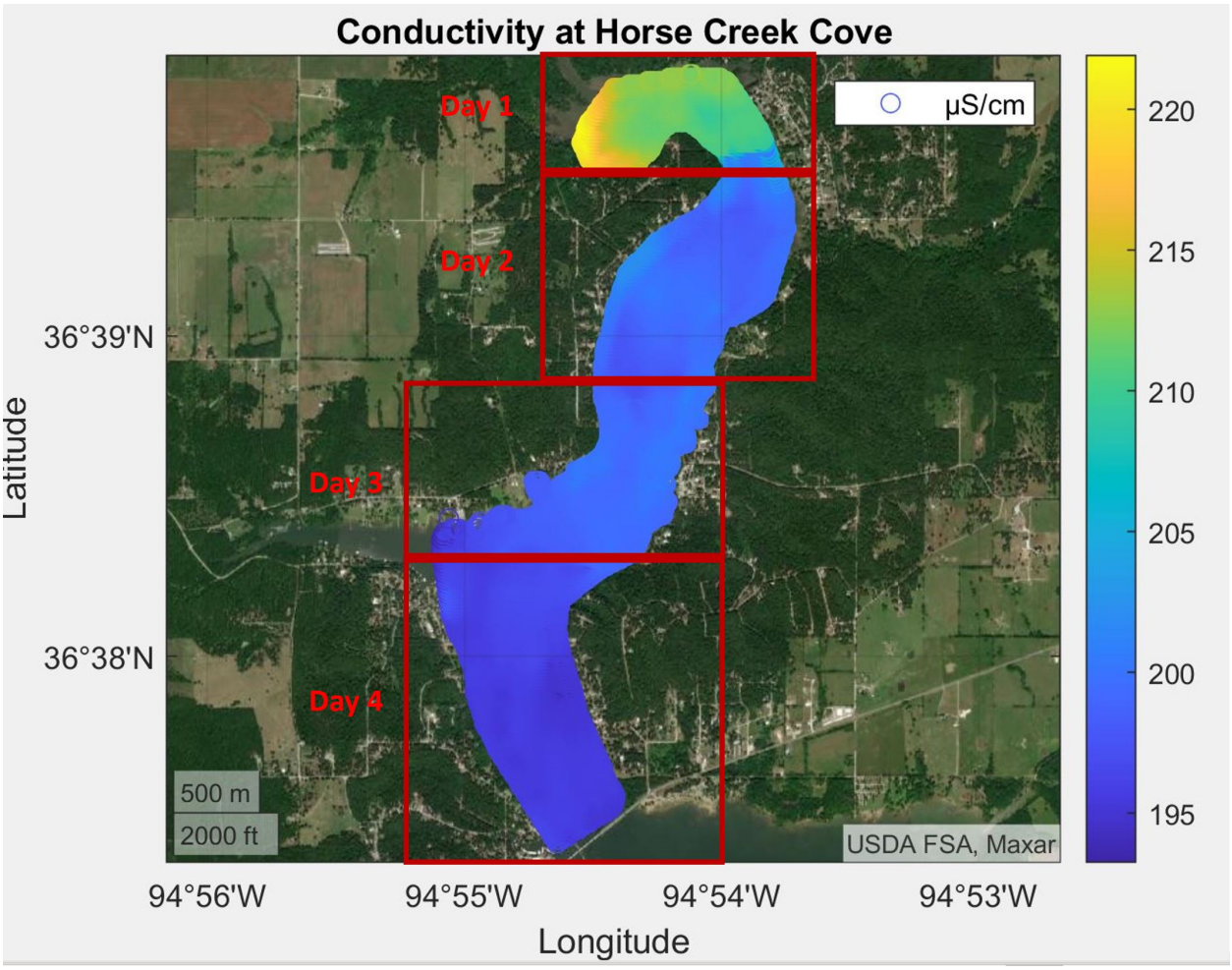

Figure 63: Conductivity Map of Horse Creek Cove

5.2.3 Lake McMurtry

Figure 64: Map of lake McMurtry

Lake McMurtry in figure 64 is located in Stillwater Oklahoma. Unlike many lakes in the State of Oklahoma, Lake McMurtry has no bathmeytric data readily available to the public or water scientist. Therefore, MANUEL was implemented at Lake McMurtry to collect bathmeytric data. Hence MANUEL producing the bathmetry data of Lake McMurtry for the first time. The plotted bathymetry data is in the figure 65.

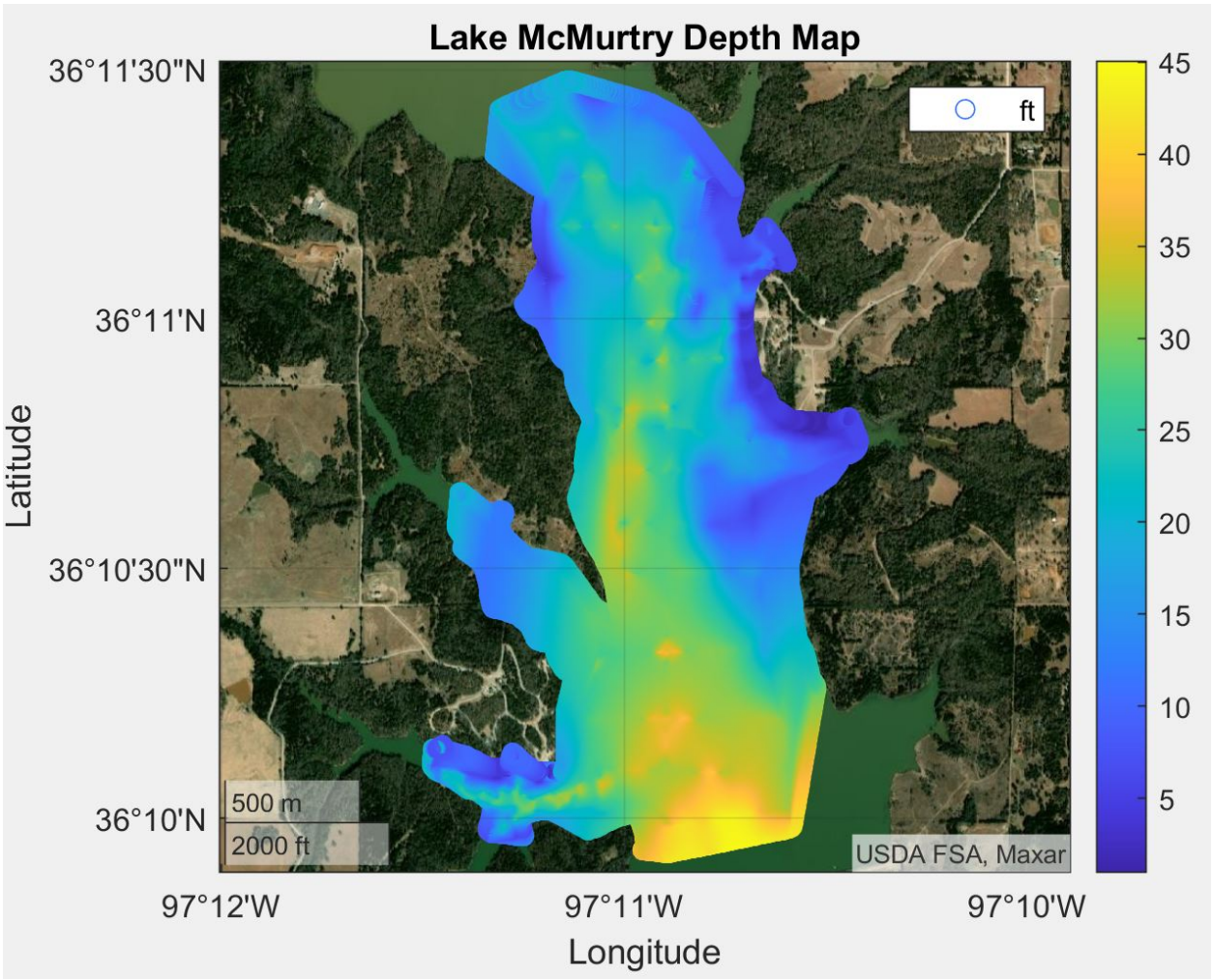

Figure 65: Lake McMurtry depth Map

5.2.4 Oklahoma State University Theta Pond Bathymetry

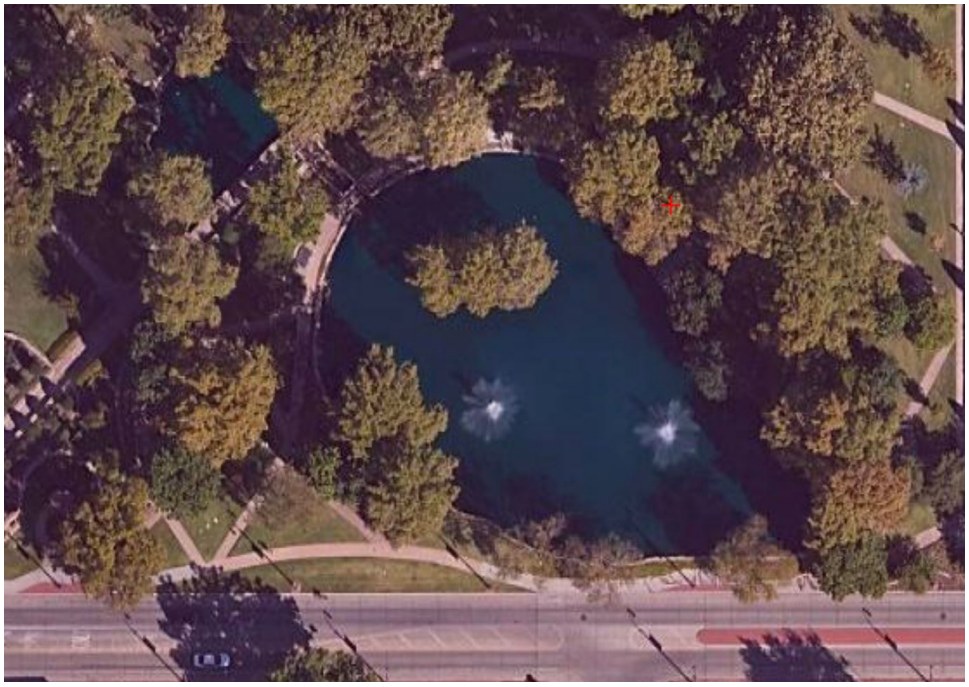

Figure 66: OSU Theta Pond Map

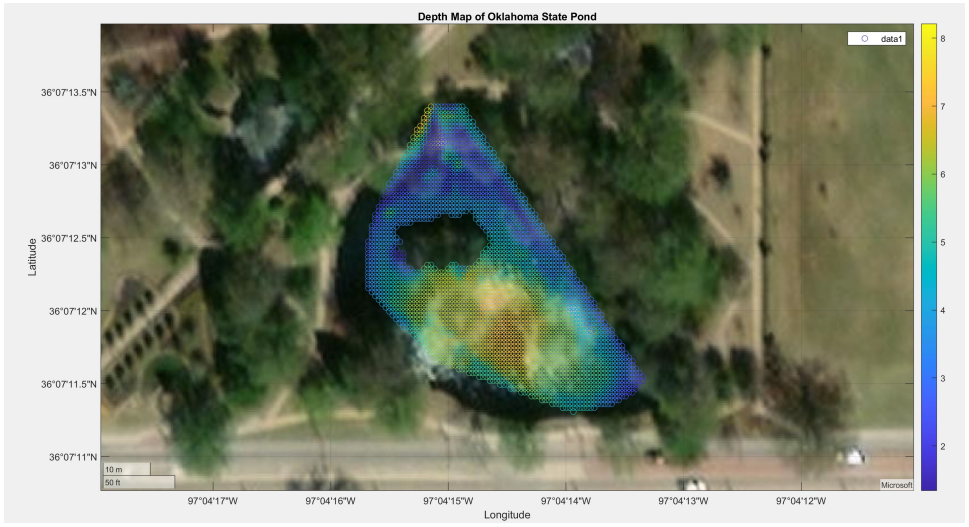

Figure 67: OSU Theta Pond depth Map

CHAPTER VI

Discussion

6.1 Bathymetry and Turbidity

The bathymetric data of the Horse Creek Cove collected by MANUEL is compared to the bathemytric data from the 2009 survey conducted by the Grand River Dam Authority.(GRDA) to study any differences or changes. The bathyemtry data was downloaded from the website as a shapefile. The shapefile was converted into a csv file to obtain the latitude, longitude and the depth of the Horse Creek Cove. The data collected was plot using the same MATLAB script used to plot results from the 2020 survey. Figure 68 is the bathemytric map of Horse Creek Cove from the 2009 survey.

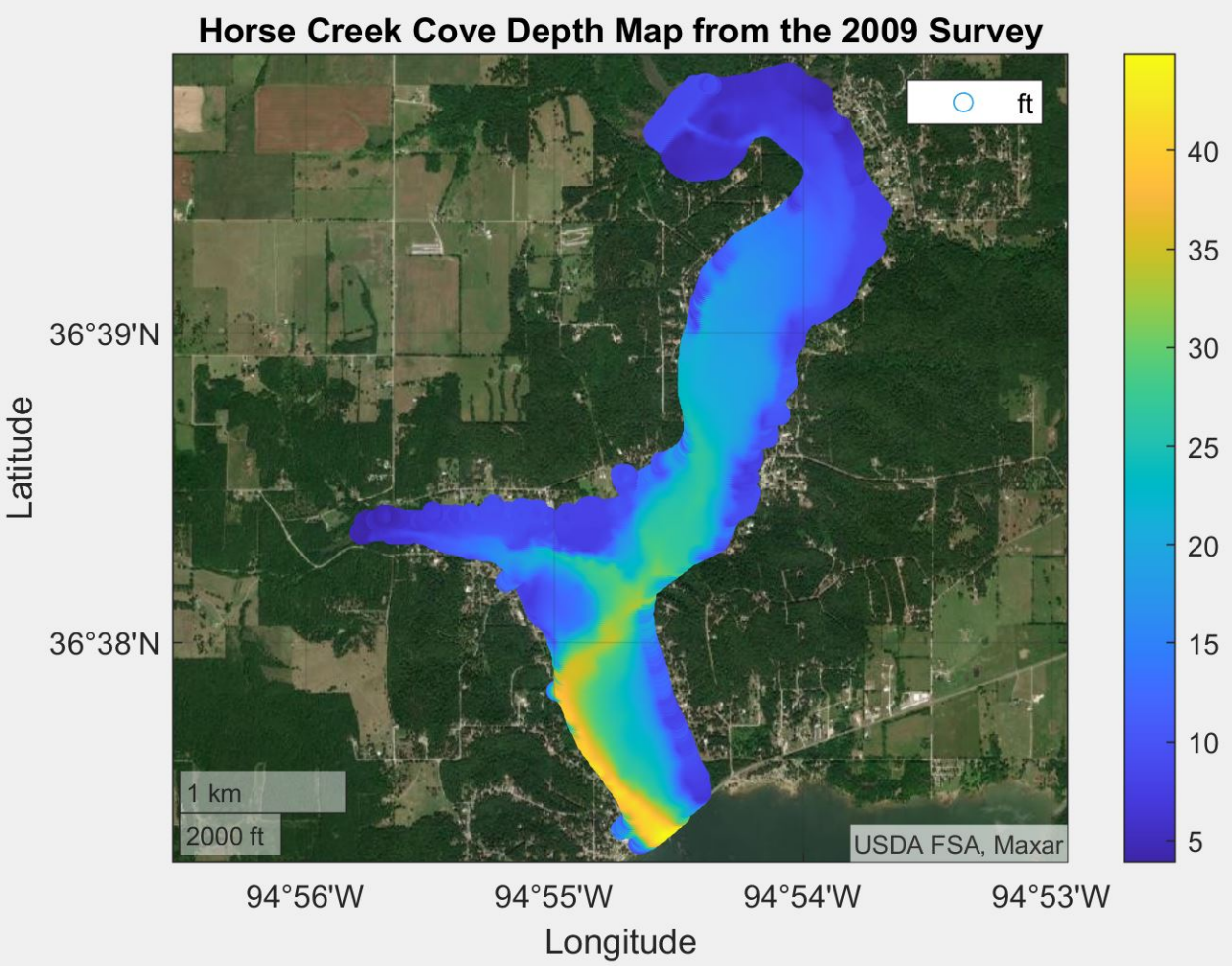

Figure 68: Horse Creek Cove Depth Map from 2009

The comparison between the 2009 and MANUEL 2020 bathymetric maps of Horse Creek Cove in figure 69, don't show significant difference. In figure 69, on the left is the 2009 bathymetric data plotted and on the right is the bathymetric data collected in 2020 by MANUEL.

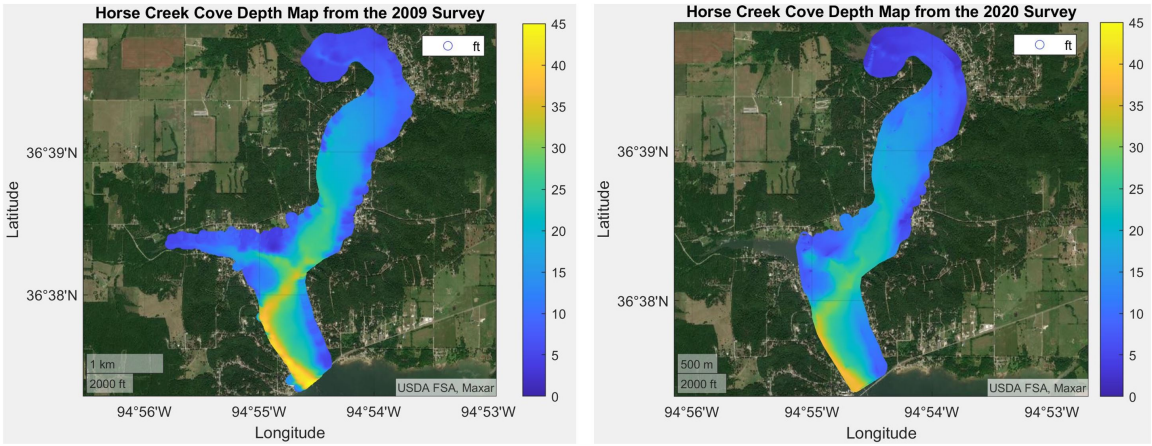

Figure 69: Depth comparison of Horse Creek Cove

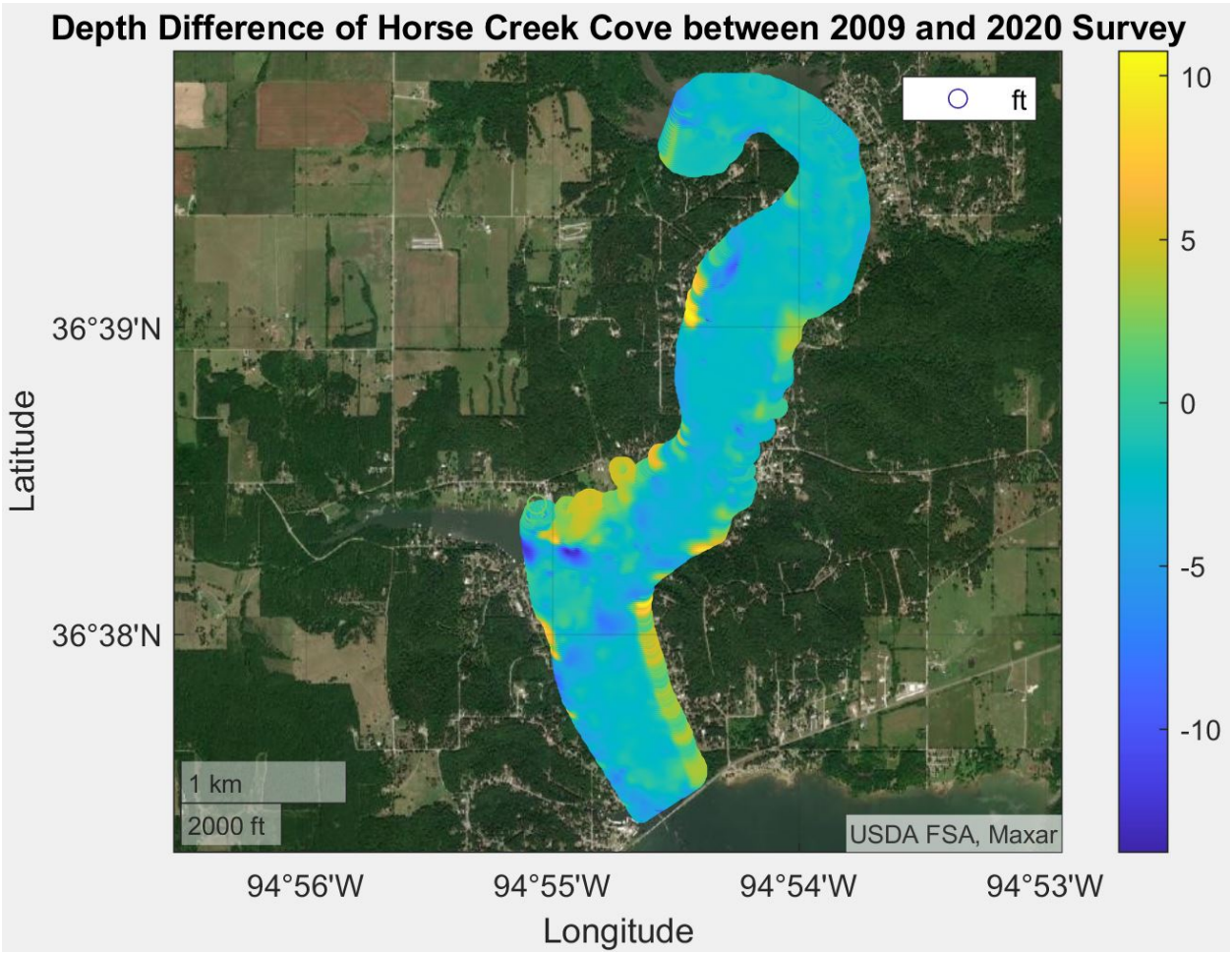

Figure 70: A map showing depth changes of Horse Creek Cove since 2009

The depth difference map is plotted by taking the difference between the depth data taken in 2009 and the data taken by MANUEL 2020. The difference between the depth

from the 2009 and 2020 survey are then plotted in figure 70. The positive value indicates the depth decreased while the negative value means the depth of Horse Creek Cove has increased since 2009 when the survey was conducted. However, from figure 70, the depth of Horse Creek Cove has generally decreased.

The slight percentage difference between the data collected by MANUEL in 2020 compared to the data collected from the manned survey in 2009 is due to the constant and continuous flooding, which transported the sediments into the Horse Creek Cove. Therefore, sediments running into the Lakes reduce the depth of the lake.

From the turbidity plot, the turbidity of the Horse Creek Cove is decreases from the north to the south of the creek. The depth is increasing as you move from the inlet/top(north) to bottom(south) of the creek. As the depth of the creek decreases, the water mixes with the sediments, increasing the cloudiness of the water hence increasing the turbidity of the creek. The increase in depth reduces sediments mix with water hence low turbidity as shown in the results plot. However, the turbidity of the creek is not only affected by the sediments mixing with the water but also chlorophyll-a, algae blooms and any other waste products discharged in the water.

6.2 Temperature, Chlorophyll, and Dissolved Oxygen

Horse Creek Cove was surveyed during day time with abundant sunlight. The average atmospheric ambient temperature as the measurements were recorded is averaged and compared to the average temperature of the water recorded indicated in table 10.

Table 10: Average Atmospheric and water Temperature at Horse Creek Cove.

Day	Avg. Atmospheric Temp °C	Avg. Water Temp °C
1	27.8	28.1
2	32.2	31.9
3	30	32.2
4	25.3	30.3

The average temperature of the water has a positive correlation with the average atmospheric ambient temperature. As the average atmospheric ambient temperature increased, it resulted in an increase in the average surface temperature of the water at Horse Creek. The increase in the water temperature is largely due to the sunlight and atmospheric heat. There was a abundant sunshine when surveying the Cove. Sunlight radiation transfer thermal energy to the water surface hence increasing the water surface temperature[7, 18]. The Temperature of the water is also increased due to the heat transfer from the atmosphere at the water surface from air; heat energy moves from regions of higher temperature to lower temperatures hence heating up and increasing the temperature of the water[10, 38].

From the results, the chlorophyll-A, is between 6 and 28 6 and 26 μg/L with patches of higher concentration at the inlet/beginning and in the middle of the Creek Cove. Chlorophyll-a concentration is classified in 3 different levels: Low concentration contains less amount of green pigment in water, medium concentration contains moderate amount of green pigment and the highly concentrated chlorophyll-a has a high amount of green pigment in

water. Chlorophyll-a is produced by phytoplankton, single celled like organisms in water. Chlorophyll-a estimates the quantity of the phytoplankton organisms in water[15]. Chlorophyll-a content in water has a relation to and affects the dissolved oxygen; the increase in chlorophyll increases dissolved oxygen in the presence of sunlight. To investigate the interactions between dissolved oxygen and other water quality parameters, the trends in the data were compared; from the data, it is observed that the dissolved oxygen, temperature, chlorophyll-a.

The amount of Dissolved oxygen in water is determined by numerous factors including temperature, pH, and chlorophyll. The relationship between temperature and dissolved oxygen is inverse. The increase in temperature reduces the solubility of oxygen in water, hence decreasing the amount of dissolved oxygen [32]. From the data collected at the Horse Creek Cove, the dissolved oxygen increased regardless of the increase in the temperature of the water. The increase in dissolved oxygen despite the increase in the temperature is due to the increase in chlorophyll and pH; The increase in chlorophyll, increases the amount of dissolved oxygen through photosynthesis [34]. Algae decay is also a very important process for dissolved oxygen levels. When the algae die, they are consumed, which lowers dissolved oxygen.

Photosynthesis is the major process that affects the dissolved oxygen. Photosynthesis involves the use of chlorophyll and sun light to produce oxygen and glucose hence producing more oxygen as demonstrated in the equation below. The water quality parameters including dissolved oxygen were collected in the afternoon when there was abundant sunlight (UV-light), a catalyst in the photosynthesis process. However, during night hours, in the absence of sunlight, the chlorophyll in water depletes the dissolved oxygen because of respiration of the green pigmented organism.

$$6CO_{2(g)} + 6H_2O_{(l)} \frac{Sunlight}{Chlorophyll} \rightarrow C_6H_{12}O_{6(aq)} + 6O_{2(g)} \tag{6.2.1}$$

6.3 pH, and Conductivity

The pH of the Horse Creek Cove is generally base-like with the pH between 7.5 and 9. At the shore, the average pH at shallow zones/inlet of Horse Creek Cove is approximately 7.7. The rest of the Creek Cove has an average pH of 8 as demonstrated in table 11. The pH has effects on the conductivity, and dissolved oxygen. However, the effect on conductivity is notable. The effect of the pH on conductivity is summarized in table 11 by evaluating and taking the average of the data collected on the different days.

Table 11: Average water pH and Conductivity at Horse Creek Cove.

Day	Avg. water pH	Avg. Water Conductivity μS/cm
1	7.7	212.6
2	8.3	199.1
3	8.5	199.4
4	8.0	196.0

The data indicates: the average conductivity decreases as the the pH of the water in-

creases. This is because as the pH increases, the ion concentrations in the water decreases. The decrease in the ion concentration in water reduces the water capability for electron flow [1]. The conductivity measurements collected are in the acceptable range of conductivity for freshwater. The conductivity of fresh water streams is between 100 to 2000 μS/cm [4] hence the conductivity of Horse Creek Cove is within the acceptable range.

6.4 Data Validation

During the data validation, the data collected by MANUEL was compared to the data collected by a scientist using a different sensor that measures the same water quality parameter. As MANUEL collected the data in a lawnmower pattern, the data collected by the scientist was taken in a transect randomly in the area surveyed by MANUEL. All the data validation was conducted using the data collected from Lake McMurtry. Both Sonde that measured the water quality parameters were produced by the same manufacturer YSI. The objective of the data validation was to evaluate the method of sampling water quality parameters. For example, collecting water quality measurements at 1 Hz while moving at 3.5 ft/s.

The randomly selected data from different GPS locations were compared in the tables below. The water quality parameters measured by the scientist using the second Sonde were geo-tagged. The water quality measurements were taken at average depth of 3.6 feet below the water surface.

The percentage difference and error between the water quality measurements collected by MANUEL Sonde probes were compared to those taken by the scientist using the traditional method. Equation 6.4.1 and equation 6.4.2 determine the percentage difference and error respectively for the recorded water quality parameters.

$$\%\text{Difference} = \frac{A - B}{\frac{A+B}{2}} * 100 \tag{6.4.1}$$

$$\%\text{Error} = \frac{A - B}{B} * 100 \tag{6.4.2}$$

Where A represents water quality parameter measured by MANUEL Sonde probe, and B represents the water quality parameter measured by the scientist.

A linear regression analysis was conducted to determine the correlation and demonstrate how well the data collected by MANUEL fits with the data collected by a scientist taking measurements stationary in the same location under the same environmental conditions. The R squared value produced in the linear regression is an indication of correlation between the parameters. For example, a higher R squared value is an indication of a strong correlation/relation between the parameters. the lower R squared value is an indicate or weak or no correlation between the parameters. Therefore, the R squared value is an indication of how the measurements taken by MANUEL change correlate with measurements taken scientist. When the R square value is 1, this means the data collected by both methodologies fits well

The Stationary Sonde uses pressure transducers to measure the pressure thus the depth of the Lake. The measurements collected were recorded and compared to MANUEL's ping sonar readings. The difference between the measurements are determined and tabulated in table 12. The depth measurements from the Sonar attached on MANUEL labelled (Depth

A) and the stationary Sonde labelled (Depth B). The percentage difference and error of the depth recording by MANUEL and the stationary Sonde are between 0.3% and 5%. Therefore, both methods of taking depth measurements produced close values.

Table 12: Depth Measurement Comparisons.

Location	Depth A	Depth B	Difference	%Difference	%Error
1	31.0	30.7	0.3	1.0	1.0
2	30.3	28.98	1.32	4.5	4.6
3	19.2	18.9	0.3	1.6	1.6
4	20.9	20.45	0.45	2.2	2.2
5	43.24	43.1	0.14	0.3	0.3

The linear regression analysis shows a strong positive correlation between the depth measured by MANUEL and that of the stationary Sonde. The R squared value is 0.996 thus measurements from the two methods agree with each other.

Regression Statistics	
Multiple R	0.998
R Square	0.996
Adjusted R Square	0.995
Standard Error	0.616
Observations	10

Figure 71: Depth Regression Summary Output

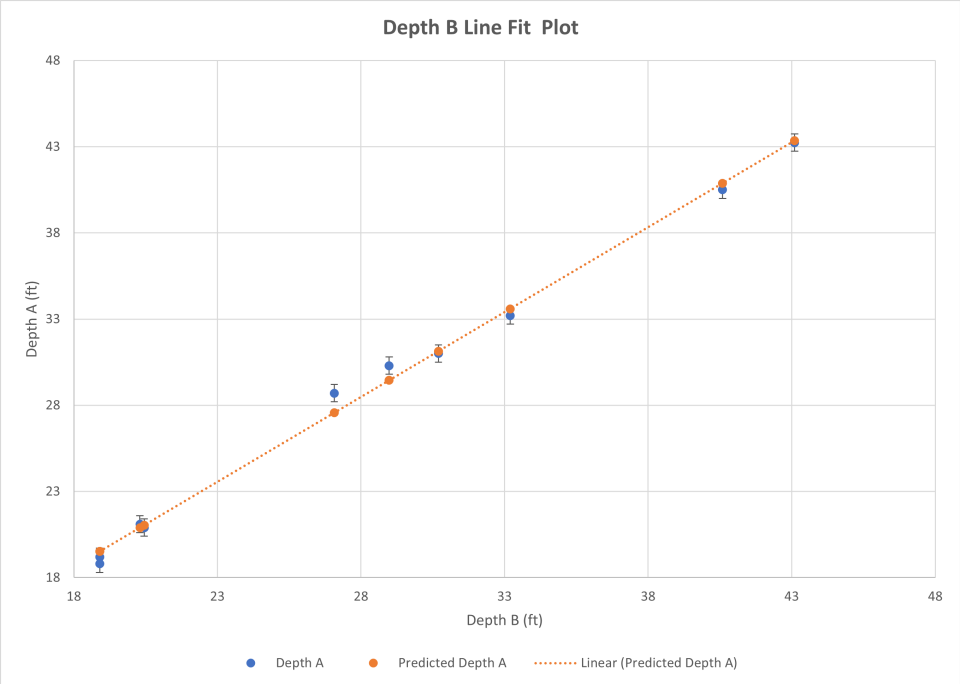

Figure 72: Depth line fit plots

Table 13: Turbidity Measurement Comparisons.

Location	TAL A	TAL B	Difference	%Difference	%Error
1	6.24	5.83	0.41	6.8	7.0
2	3.25	3.12	0.13	4.1	4.2
3	5.81	5.91	0.10	1.8	1.7
4	5.56	5.38	0.18	3.3	3.3
5	6.86	7.01	0.15	2.2	2.1

The turbidity measured by MANUEL(A) and stationary sensor(B) from five different positions are tabulated in table 13. The percentage difference is between 2% and 7% and the percentage errors are between 2% and 7%, assuming the scientist's stationary method of collecting data is more accurate than when it is in motion. According to the percentage difference and error, the sensor readings from MANUEL and the stationary Sonde are very close and therefore, collecting turbidity measurements with MANUEL did not distort the measurements. To further evaluate the measurements between the two different methods, a linear regression was performed using 10 different observations. The results indicate a strong correlation with an R square value of 0.94 with a confidence level of 95%. The summary of the results from the regression analysis are presented in figures 74, and 73.

Regression Statistics	
Multiple R	0.971
R Square	0.943
Adjusted R Square	0.936
Standard Error	0.272
Observations	10

Figure 73: Turbidity Regression Summary Output

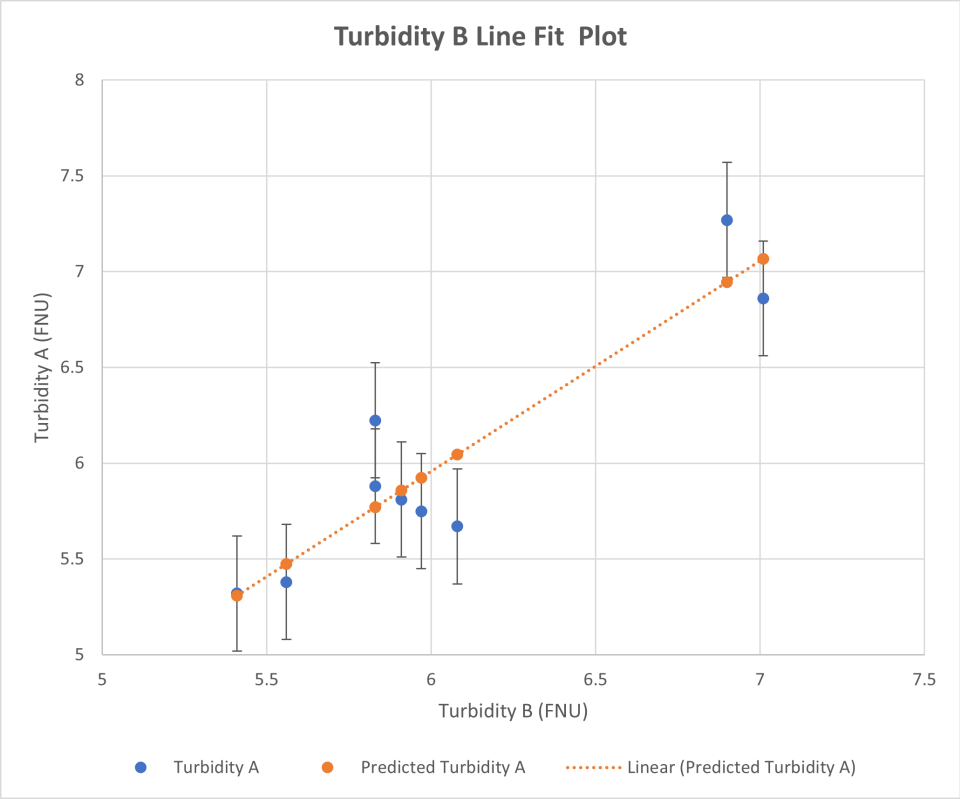

Figure 74: Turbidity line fit plots

From table 14, the percentage difference between the readings for the dissolved oxygen probes is between 7% and 9% and the the percentage error is between 7% and 8.5%. The tabular results indicate a minimal difference between the readings from the different methods of obtaining dissolved oxygen measurements. However, the dissolved oxygen(DO) measurements collected using the the stationary Sonde are on average slightly higher than the measurements when using MANUEL. The slightly higher DO B value is the depth at which Sonde B was placed verses the depth at which MANUEL Sonde probe collects the measurement.

Table 14: Dissolved Oxygen (DO) Measurement Comparisons.

Location	DO A	DO B	Difference	%Difference	%Error
1	6.18	6.75	0.57	8.8	8.4
2	8.73	9.37	0.64	7.1	6.8
3	6.51	7.07	0.56	8.2	7.9
4	6.27	6.74	0.47	7.2	7.0
5	6.38	6.95	0.57	8.6	8.2

Ten difference values were used in the linear regression analysis to evaluate correlation between the two different measurements. The R square value is 0.981. Dissolved oxygen measurements were not significantly altered. Therefore, there is a positive correlation between the measurements thus MANUEL collected reliable dissolved oxygen data.

Regression Statistics	
Multiple R	0.990
R Square	0.981
Adjusted R Square	0.978
Standard Error	0.109
Observations	10

Figure 75: Dissolved Oxygen Regression Summary Output

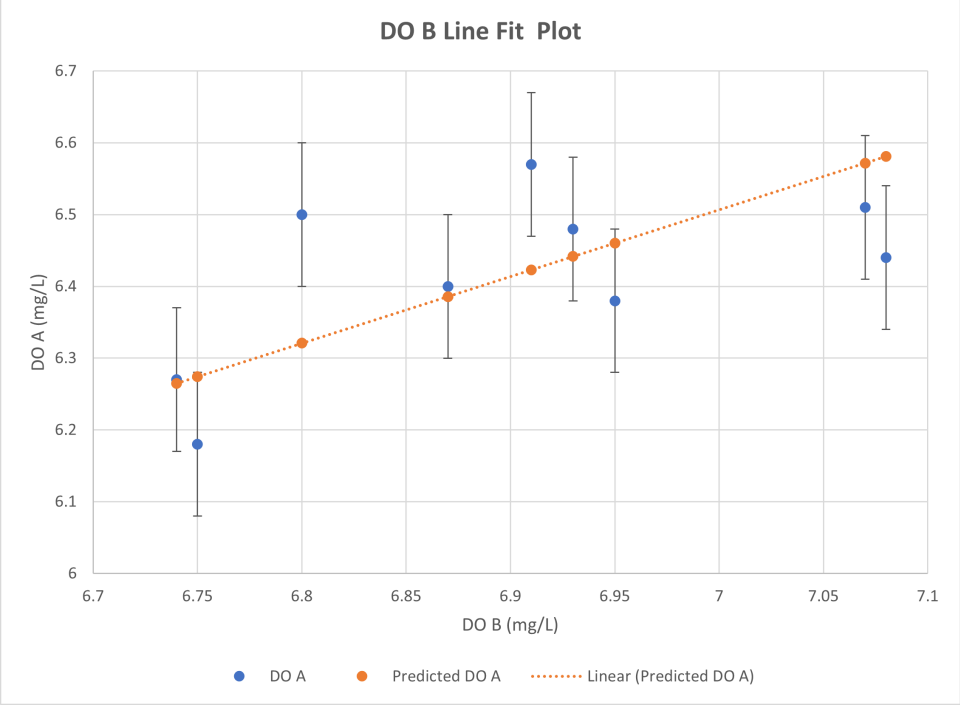

Figure 76: Dissolved Oxygen line fit plots

From the regression analysis, the R squared value is 0.917. Therefore, there is a correlation between the conductivity measurements obtained by MANUEL and the stationary Sonde readings as showed in figure 77. However, the conductivity measurements collected by the second Sonde(stationary), are relatively higher than those measured by MANUEL by approximately 100 μS/cm. The 100 μS/cm difference between the measurements is due to the depth at which the measurements were taken. MANUEL's Sonde probes are positioned to be less than a foot below the water surface thus surface measurements. The stationary Sonde was 3.6 feet deep thus slightly higher conductivity measurements. The trend between the two measurements coordinates as suggested by the regression analysis.

Regression Statistics	
Multiple R	0.958
R Square	0.917
Adjusted R Square	0.907
Standard Error	0.297
Observations	10

Figure 77: Specific Conductivity Regression Summary Output

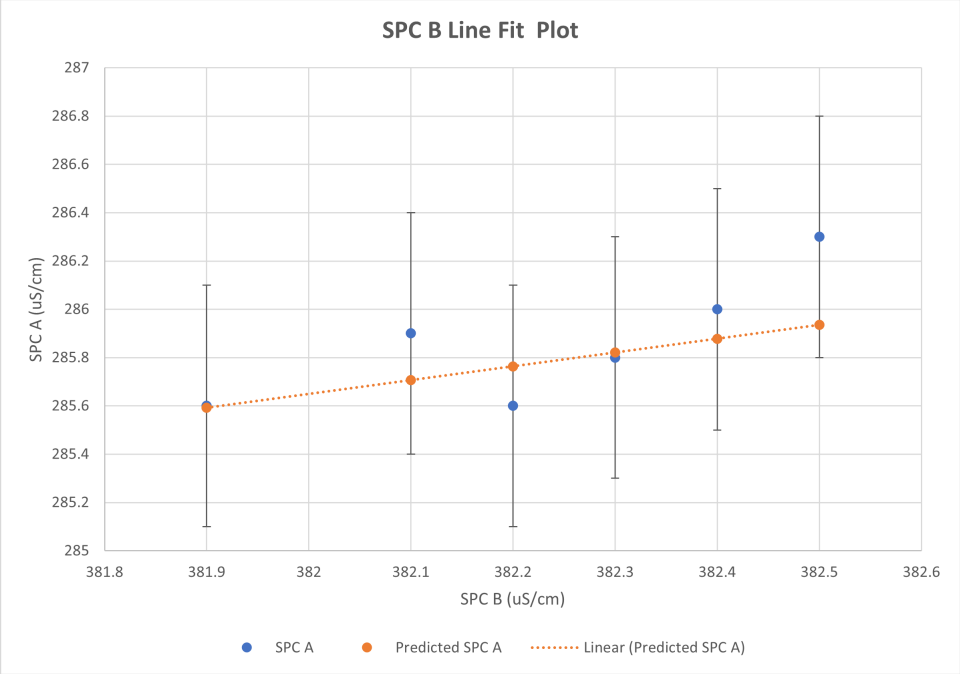

Figure 78: Specific Conductivity line fit plots

CHAPTER VII

Conclusions

7.1 Summary

The water quality parameter data collected by MANUEL, was not significantly affected by the movement of MANUEL as it was maneuvering through the water. The Sonde was strategically placed to enable measurements before the disturbance/mix up the water. The water quality parameters were sampled at 1 Hz with MANUEL moving at 3.5 ft/s. The data validation procedure showed a higher R square value for the water quality parameters measured by MANUEL and the stationary Sonde thus using MANUEL for water quality monitoring produces reliable data for scientist studying the water quality parameters.

The water quality parameter data collected during this study showed the relation and interactions between the water parameters. For example, the dissolved oxygen at Horse Creek Cove increased significantly with the increase in the chlorophyll-a content in the water. The average water temperature of the water had a positive correlation with the average ambient atmospheric temperature. The turbidity of the Horse Creek Cove was relatively high at the inlet of the Cove, this was also very shallow compared to the rest of the Cove. The pH at the Horse Creek Cove increased as you move from the inlet to outlet of the Cove. The Increase in pH affected conductivity. Increase in pH, decreased the conductivity.

The design and development of MANUEL is an autonomous potential solution to supplement and fills the gap between the already existing methods of water quality monitoring such as manned manual surveys and remote sensing. MANUEL presents enormous advantages. MANUEL provides an affordable way of water quality monitoring, provides a higher resolutions of data compared to the remote sensing. MANUEL's main goal is maintain a pristine environment and clean water as my system continuously monitors the quality of our lakes and rivers while reducing the risk and cost involved with current practices and to keep from exposing operators to unknown harmful water environments, for the benefit of all mankind. MANUEL is currently monitoring and surveying the water quality at Lake McMurtry and Grand Lake but hope to deploy this system across the state, nation, and world.

Figure 79: MANUEL during a survey at Grand Lake

7.2 Issues and Concerns

7.2.1 Obstacle Avoidance and Collision

Obstacle Avoidance and Collision was not implemented in the design and development of MANUEL. Obstacle Avoidance and Collision was a major limitation to the system as discovered later in the implementation phase as indicated in the figure 80. MANUEL collided a few times with obstacles above the water surface levels while in mission on AUTO; this is because it was not equipped with sensors to aid in the avoidance.

Figure 80: MANUEL on a collision course during an AUTO mission at Horse Creek Cove

The observable surface obstacles were not the only challenges to MANUEL. Some of the obstacles were below the surface of water and not visible; these included dead tree logs, and shallow waters. While surveying the Horse Creek Cove at Grand Lake in Oklahoma, MANUEL did not have capabilities to avoid shallow water. During one of the missions, some points of the lake were less than a foot deep which led to the damage of the sensor as showed in the picture below.

Figure 81: MANUEL's Sonde broke during an AUTO mission

During the implementation phase, on one of the occasions at the Horse Creek Cove, the Sonde broke into two pieces: One ended up at the bottom of Horse Creek Cove. After one month, a recovery mission was conducted using the sonar and MANUEL's capabilities to retrace it's previous mission path, the Sonde was retrieved. Figure 83, shows the recovery mission after MANUEL aided in the recovery of the Sonde. The Sonde probes in figure 82, recovered was fully immersed in the mud. However, it was cleaned and still functions well.

Figure 82: Recovered Sonde probes

In figure 83 is Muwanika Jdiobe, the Mechanical and Aerospace engineering graduate student, Levi Ross, a Research engineer and Pamula Abriham, a Ph.D., student in Civil and Environmental engineering. In the background is MANUEL after aiding to in the recovery of the lost Sonde.

Figure 83: After Recover of the Sonde probes, in at Horse Creek Cove, MANUEL in the background

7.2.2 Water plants

Water plants such as floating grass in the lakes and rivers hinder MANUEL's operations. MANUEL uses thrusters to maneuver through water. Therefore, any floating grass on the water surface that comes in close contact with MANUEL can easily be sucked into the thrusters. The water plants can significantly reduce the turning rate of the thrusters thus reducing the thrust propelling MANUEL. For example, MANUEL faced this challenge during the bathymetric mapping of Oklahoma State University Theta pond. However, water plants did not affect MANUEL's operations during the surveys at the Granda Lake, Boomer Lake and Lake McMurtry.

7.3 Future Work and Recommendations

In the future, MANUEL v2.1 will be modified with the lessons learned from MANUEL v2.0. These include:

1. To enhance obstacle detection, different options should be considered including the use of a camera, sonar and Lidar. Implementing sonar for obstacle detection under the water level and a Lidar for above the water surface would enable MANUEL to detect and avoid any obstacles and shallow parts thus maneuvering safely in dangerous parts of the lake. The sonar would constantly check any obstacles and shallow depths within MANUEL's pre-planned path.The on-board camera would provide a visual to the operator thus maneuvering MANUEL away from the obstacles.

2. Develop and build a custom sensor unit that can easily be integrated with MANUEL. The sensor unit would measures the pH, turbidity, chlorophyll-a, conductivity, dissolved oxygen, salinity, temperature, flow rates, depth and other lake nutrients.

3. MANUEL v2.0 currently has an endurance of 3.5 hours. However, to increase the endurance, more batteries will be added to MANUEL v2.1 hence extending the time of operation. For example, to survey Horse Creek Cove takes approximately 9 hours at a cruising speed of 3.5 ft/s.

4. Design a methodology to further investigate the error and uncertainty in the measurements from the sensor embedded in MANUEL as the speed of MANUEL changes. This would include altering the speed at which MANUEL is moving. This would determine the error in measurements vs speed of MANUEL thus determining the appropriate speed while sampling.

5. In order to reduce the time it takes to monitors larger lakes and rivers, more autonomous vehicles should be built and enabled to work together as a network thus reducing the time it takes monitor. The autonomous vehicles would be launched at different points to survey the lakes and rivers in a coordinated manner.

6. Design a protective shield for the thrusters to prevents water plants from interfering with the rotation.

REFERENCES

[1] United States Environmental Protection Agency, *Conductivity. In Water: Monitoring and Assessment.*, 2012.

[2] United States Environmental Protection Agency., *Online Source Water Quality Monitoring for Water Quality Surveillance and Response Systems*, 2016.

[3] E. Roberts Alley, *Water Quality Control Handbook, Second Edition*, The McGraw-Hill Companies, Inc, 2007.

[4] American Water Works Assoc. & Water Environment Federation. American Public Health Assoc., *Standard Methods for the Examination of Water and Wastewater (20th ed.).*, American Public Health Association., 1999.

[5] American Public Health Association, *Standard Methods for the Examination of Water and Wastewater*, vol. 21, American Public Health Association, American Water Works Association, Water Environment Federation, 2005.

[6] Bikram Pratap Banerjee, Simit Raval, Thomas J Maslin, and Wendy Timms, *Development of a uav-mounted system for remotely collecting mine water samples*, International Journal of Mining, Reclamation and Environment **34** (2020), no. 6, 385–396.

[7] UW Green Bay, *Temperature. watershed monitoring program*, (accessed Novermber 4, 2020).

[8] D. Becq, *Designing automatic water quality monitoring stations for lakes and rivers*, Proceedings of OCEANS'94, vol. 1, 1994, pp. I/469–I/474 vol.1.

[9] Blue-Robotics., *Ping echosounder sonar user manual*, (accessed October 16, 2020).

[10] The Concord Consortium, *Heat & temperature . in hands-on-physics.*, (accessed Novermber 4, 2020).

[11] M. Dunbabin and A. Grinham, *Experimental evaluation of an autonomous surface vehicle for water quality and greenhouse gas emission monitoring*, 2010 IEEE International Conference on Robotics and Automation (2010), 5268–5274.

[12] M. Dunbabin, A. Grinham, and J. Udy, *An autonomous surface vehicle for water quality monitoring*, ICRA 2009, 2009.

[13] EnviroDIY, *Getting started with the mayfly data logger*, October 2020.

[14] Wilde F.D., *Preparations for water sampling.*, In National Field Manual for the Collection of Water-Quality Data U.S. Geological Survey Techniques of Water-Resources Investigations, U.S. Geological Survey, 2005.

[15] Fondriest Environmental Inc., *"algae, phytoplankton and chlorophyll." fundamentals of environmental measurements. 22 oct. 2014*, (accessed September 8, 2020).

[16] Fondriest Environmental Inc, *"ph of water." fundamentals of environmental measurements. 19 nov. 2013.*, (accessed September 8, 2020).

[17] Fondriest Environmental Inc, *"turbidity, total suspended solids and water clarity." fundamentals of environmental measurements. 13 jun. 2014.*, (accessed September 8, 2020).

[18] Fondriest Environmental Inc, *"water temperature." fundamentals of environmental measurements. 7 feb.2014*, (accessed September 8, 2020).

[19] YSI Incorporated, *EXO3 Multiparameter Sonde*, October 2020.

[20] YSI Incorporated., *The basics of chlorophyll measurement. in ysi environmental tech note.*, (accessed September 10, 2020).

[21] Jacob, *Ping Echosounder Sonar User Manual*, October 2020.

[22] Amber Spackman Jones, Zachary T. Aanderud, Jeffery S. Horsburgh, David P. Eiriksson, Dylan Dastrup, Christopher Cox, Scott B. Jones, David R. Bowling, Jonathan Carlisle, Gregory T. Carling, and Michelle A. Baker, *Designing and Implementing a Network for Sensing Water Quality and Hydrology across Mountain to Urban Transitions*, JAWRA Journal of the American Water Resources Association **53** (2017), no. 5, 1095–1120.

[23] Cengiz Koparan, Ali Bulent Koc, Charles V. Privette, Calvin B. Sawyer, and Julia L. Sharp, *Evaluation of a uav-assisted autonomous water sampling*, Water **10** (2018), 655.

[24] Salih Külünk, *Lakebed characterization using side-can data for investigating the latest lake superior coastal environment conditions.*, 01 2017.

[25] Bureau of Reclamation California-Great Basin, *Water facts - worldwide water supply*, (accessed Novermber 10, 2020).

[26] World Health Organization, *Guidelines for drinking-water quality, fourth edition*, vol. 1, WHO, 2011.

[27] P. Prempraneerach and Pasan Kulvanit, *Autonomous robot boat for water sampling and environmental data acquisition tasks*, (2010).

[28] Blue Robotics, *Basic ESC*, September 2020.

[29] Blue Robotics, *T100 thruster (retired)*, September 2020.

[30] Blue Robotics., *T200 thruster*, May 2020.

[31] USGS United States Geological Survey, *Bathymetric surveys*, (accessed October 16, 2020).

[32] USGS United States Geological Survey., *Dissolved oxygen and water*, (accessed October 23, 2020).

[33] Stensel HD Tchobanoglous G, Burton FL, *Metcalf & Eddy Wastewater Engineering: Treatment And Reuse, 4Th Edn*, vol. 4, Tata McGraw-Hill Limited, 2003.

[34] J. Wallace, P. Champagne, and G. Hall, *Time series relationships between chlorophyll-a, dissolved oxygen, and ph in three facultative wastewater stabilization ponds*, Environ. Sci.: Water Res. Technol. **2** (2016), 1032–1040.

[35] J. Wang, W. Gu, and J. Zhu, *Design of an autonomous surface vehicle used for marine environment monitoring*, 2009 International Conference on Advanced Computer Control, 2009, pp. 405–409.

[36] AQUAREAD water monitoring instruments, *Nitrate test in water.*, (accessed October 7, 2020).

[37] Lake County Wateratlas, *Salinity*, October 2020.

[38] ROBERT G. WETZEL, *Limnology: Lake and River Ecosystems. Third Edition*, Academic Press, 2001.

APPENDICES

MATLAB Scripts for Data Processing.

The appendix includes the MATLAB script that merges the Sonde water quality data to the Autopilot GPS data. The second script plots the data.

```
%% User Settings
clc
clear all
close all

% 'Yes' or 'No'
SondeData = 'Yes';
Animation = 'No';

%% USGS Mapping Data
baseURL = "https://basemap.nationalmap.gov/ArcGIS/rest/services";
usgsURL = baseURL + "/BASEMAP/MapServer/tile/${z}/${y}/${x}";
basemaps = ["USGSImageryOnly" "USGSImageryTopo" "USGSTopo"
"USGSShadedReliefOnly" "USGSHydroCached"];
displayNames = ["USGS Imagery" "USGS Topographic Imagery" "USGS Shaded
Topographic Map" "USGS Shaded Relief" "USGS Hydrography"];
maxZoomLevel = 35;
attribution = 'Credit: U.S. Geological Survey';

%% ArduRover Parser
% Strips Pixhawk ArduRover log file down to GPS data and outputs as table

thrMinPWM = 1100;
thrMaxPWM = 1900;

ArduPilotType = 'Rover';

% Have user browse for a file, from a specified "starting folder."
% For convenience in browsing, set a starting folder from which to browse.
% Start in the current folder.
startingFolderDFL = pwd;
% Get the name of the file that the user wants to use.
defaultFileNameDFL = fullfile(startingFolderDFL, '*.mat');
[baseFileNameDFL, folderDFL] = uigetfile(defaultFileNameDFL, 'Select an
unparsed Pixhawk DFL file');
startingFolderDFL = folderDFL;
if baseFileNameDFL == 0
    % User clicked the Cancel button.
    return;
end

% Get the name of the input .mat file.
fullInputMatFileNameDFL = fullfile(folderDFL, baseFileNameDFL);
load(fullInputMatFileNameDFL,'GPS','GPS_label');

GPS =
[GPS(:,1),GPS(:,2),GPS(:,4),GPS(:,5),GPS(:,8),GPS(:,9),GPS(:,10),GPS(:,11),GP
S(:,6)];
GPS_label =
[GPS_label(1),GPS_label(2),GPS_label(4),GPS_label(5),GPS_label(8),GPS_label(9
),GPS_label(10),GPS_label(11),GPS_label(6)];
```

```
% Get filename without the extension, used by Save Function
[~, baseNameNoExtDFL, ~] = fileparts(baseFileNameDFL);

TO = find(GPS(:,9)>0, 1, 'first');
LND = find(GPS(:,9)>0, 1, 'last');

%%%%%%%%% GPS Logs Parsing %%%%%%%%%
% Latitude
x=GPS(TO:LND,5);
% Longitude
y=GPS(TO:LND,6);
% Altitude
z=GPS(TO:LND,7);
z_AGL = z(:)-z(1);

t_plot=(1:length(x));

%%%%%%%%% Airspeed and Windspeed Data %%%%%%%%%
% Ground speed
v_g=GPS(TO:LND,8);

% Parsed GPS data output
GPS_LN = GPS(TO:LND,1);
GPS_time = GPS(TO:LND,2);
GPS_ms = GPS(TO:LND,3);
GPS_wk = GPS(TO:LND,4);
GPS_time_out= (GPS_time-min(GPS_time))/1000000;
% Convert GPS timestamps to UTC time
leap_second_table = datenum(['Jul 01 1981';'Jul 01 1982';'Jul 01 1983';'Jul
01 1985';'Jan 01 1988';'Jan 01 1990';'Jan 01 1991';'Jul 01 1992';'Jul 01
1993';'Jul 01 1994';'Jan 01 1996';'Jul 01 1997';'Jan 01 1999';'Jan 01
2006';'Jan 01 2009';'Jul 01 2012';'Jul 01 2015';'Jan 01 2017'], 'mmm dd
yyyy');
gps_zero_datenum = datenum('1980-01-06 00:00:00.000','yyyy-mm-dd
HH:MM:SS.FFF');
days_since_gps_zero = GPS_wk*7 + GPS_ms/1e3/60/60/24;
recv_gps_datenum = gps_zero_datenum + days_since_gps_zero;
leapseconds = 18;
recv_utc_datenum = recv_gps_datenum - ((leapseconds)/60/60/24);
GPS_date=datestr(recv_utc_datenum,'mmm-dd-yyyy');
GPS_full_time=datestr(recv_utc_datenum,'HH:MM:SS.FFF');
tempGPS_date = datetime(GPS_date,'InputFormat','MMM-dd-
yyyy','TimeZone','Atlantic/Reykjavik');
tempGPS_time =
datetime(GPS_full_time,'TimeZone','Atlantic/Reykjavik','Format','HH:mm:ss.S')
;
tempGPS_comb = tempGPS_date + timeofday(tempGPS_time);
GPS_final =
datetime(tempGPS_comb,'TimeZone','Atlantic/Reykjavik','Format','MMM-dd-yyyy
HH:mm:ss.S');
tempGPS_time.TimeZone = 'America/Chicago';
GPS_final.TimeZone = 'America/Chicago';
GPS_final.Format = 'MMM-dd-yyyy HH:mm:ss';

% Output GPS table
```

```
GPS_label = {'Line No','Time since boot (us)','Time from Arming
(sec)','Date','Time (CST)','Lattitude','Longitude','Altitude (m,
MSL)','Altitude (m, AGL)','Groundspeed (m/s)'};
GPS_table = table(tempGPS_date,tempGPS_time, x, y, v_g, 'VariableNames',
{'Date','Time (CST)','Lat','Long','Groundspeed (m/s)'});
baseFileName = sprintf('%s_GPS.csv', baseNameNoExtDFL);
fullOutputMatFileName = fullfile(folderDFL, baseFileName);


% Write data to text file
writetable(GPS_table, fullOutputMatFileName);

%% Water Sensor Data Manipulation
% Merge Pixhawk GPS data with data logged from water sensor using timestamps

if(strcmpi(SondeData,'Yes'))
    startingFolder = pwd;

    % Get the name of the file that the user wants to use.
    defaultFileName = fullfile(startingFolder, '*.csv');
    [baseFileName, folder] = uigetfile(defaultFileName, 'Select a 5HP/TPH
.CSV file');
    if baseFileName == 0
        % User clicked the Cancel button.
        return;
    end

    % Get the name of the input .mat file.
    fullInputMatFileName = fullfile(folder, baseFileName);
    % Get filename without the extension, used by Save Function
    [~, baseNameNoExt, ~] = fileparts(baseFileName);

    try
        sensorData = readtable(fullInputMatFileName);
    catch
        fid = fopen(fullInputMatFileName, 'rt', 'n', 'UTF16LE');
        fread(fid, 2, '*uint8');
        filecontent = fread(fid, [1 inf], '*char');
        datacell = textscan(filecontent,
'%s%s%s%s%s%s%s%s%s%s%s%s%s%s%s%s%s%s%s%s%s%s%s%s', 'Delimiter', ',',
'HeaderLines', 1);
        allData = vertcat(datacell{:});

        newCount=0;
        for i=1:24;
            for j=1:length(datacell{1,1}(:,1))
                newCount=newCount+1;
                data(j,i) = allData(newCount);
            end
        end
        sensorData = array2table(data);
    end
```

```
    locVars=cellfun('isempty', sensorData{3:end,1} );
    startLocVars = find(locVars == 0,1,'first')+3;
    locStats=cellfun('isempty', sensorData{3:end,4} );
    startLocStats = find(locStats == 0,1,'first')+2;

    ncols = width(sensorData);
    nrows = height(sensorData);

    modData = table2array(sensorData(startLocVars:nrows,:));

    % Convert CSV data to general table to datetime array
    Sensor_date_ref = sensorData(startLocVars:nrows,1);
    Sensor_date_conv = table2array(Sensor_date_ref);
    Sensor_date =
datetime(Sensor_date_conv,'InputFormat','MM/dd/yyyy','Format','MMM-dd-
yyyy','TimeZone','America/Chicago');
    Sensor_time_ref = sensorData(startLocVars:nrows,2);
    Sensor_time_conv = table2array(Sensor_time_ref);
    Sensor_time =
datetime(datevec(Sensor_time_conv),'Format','HH:mm:ss','TimeZone','America/Ch
icago');

    % Convert datetime arrays into datetime vectors
    [S_y, S_m, S_d] = datevec(Sensor_date(:,1));
    [ no, no, no,S_h, S_M, S_s] = datevec(Sensor_time);
    Sensor_vec = [S_y S_m S_d S_h S_M S_s];

    GPS_vec = datevec(GPS_final);

    % Convert datetime vectors datetime serials
    GPS_serial = datenum(GPS_vec);
    Sensor_serial = datenum(Sensor_vec);

    zero1=(zeros(length(Sensor_serial),1));
    zero2=(zeros(length(Sensor_serial),1));
    zero3=(zeros(length(Sensor_serial),1));
    Pix_use = table(zero1,zero2,zero3);

    %     Pix_use.Properties.VariableNames = {'Lat','Long','Groundspeed'};

    for i=1:length(Sensor_serial)
        for j=1:length(GPS_serial)
            if(Sensor_serial(i)==GPS_serial(j))
                Pix_reduce(i,1)=GPS_table(j,1); % Date
                Pix_reduce(i,2)=GPS_table(j,2); % Time
                Pix_use(i,1)=GPS_table(j,3); % Lat
                Pix_use(i,2)=GPS_table(j,4); % Long
                Pix_use(i,3)=GPS_table(j,5); % Groundspeed
            end
        end
    end
```

```
    zero4 = string(zeros(1,(ncols+3)));
    DateTime = modData(:,1:3);
    Remaining = modData(:,4:ncols);
    merge = [DateTime Pix_use Remaining];
    names = zero4;
    tempNames = sensorData((startLocVars-1),:);
    sensorNames = table2array(tempNames);
    names(1,1:3) = sensorNames(1,1:3);
    names(1,4) = 'Lat';
    names(1,5) = 'Long';
    names(1,6) = 'GroundSpeed (m/s)';
    names(1,7:(ncols+3)) = sensorNames(4:ncols);
    merge.Properties.VariableNames = names;


    zero5 = string(zeros(5,(ncols+3)));
    stat = zero5;
    tempStat = sensorData((startLocStats):(startLocStats+2),1:ncols);
    newCol=repmat({''},size(tempStat(1,:)));
    tempStat = [newCol; tempStat];

    sensorStat = table2array(tempStat);
    stat(2:5,1:ncols) = sensorStat;
    stat(1,:) = '';
    stat(1:5,(ncols+1):(ncols+3)) = '';

    final_stat = array2table(stat);
    final_stat.Properties.VariableNames = names;

    final_merge = [merge;final_stat];
    final_merge(ismember(final_merge.Lat,'0'),:)=[];


    % Get the name of the input.mat file and save as input_Parsed_TPH.csv
    baseFileNameDFL = sprintf('%s_Parsed.csv', baseNameNoExtDFL);
    fullOutputMatFileNameDFL = fullfile(folderDFL, baseFileNameDFL);
    % Write data to text file
    writetable(final_merge, fullOutputMatFileNameDFL);
end

%% Animation Function
% Animation of the Pixhawk Log from recorded GPS coordinates

if(strcmpi(Animation,'Yes'))

    % Get the name of the intput.mat file and save as input_parsed.mat
    baseFileName = sprintf('%s_animation', baseNameNoExtDFL);
    fullParsedMatFileName = fullfile(folderDFL, baseFileName);
    app.LocationofOutputFilesEditField.Value = fullParsedMatFileName;
    % Save file with parsed data as the original filename plus the added
portion
```

```
    animVid = VideoWriter(fullOutputMatFileName,'MPEG-4');
    animVid.FrameRate = 20;  %can adjust this, 5 - 10 works well for me
    animVid.Quality = 100;

    fig.Position = [5 360 560 420];
    fig.Resize = 'off';

    xAnim=x;
    yAnim=y;
    lx = length(xAnim);
    ly = length(yAnim);
    ax = geoaxes();
    geoplot(ax,[min(xAnim) max(xAnim)],[min(yAnim) max(yAnim)]);
    geolimits([min(xAnim) max(xAnim)],[min(yAnim) max(yAnim)]);
    geobasemap('colorterrain')
    basemapx = basemaps(2);
    url = replace(usgsURL,"BASEMAP",basemapx);
    legend('Depth in ft')
    title('Depth of lake')
    view(ax,2)

    open(animVid);

    for jj=1:length(xAnim);
        geoplot(ax,xAnim(1:jj),yAnim(1:jj),'LineWidth',1.5)
        %geolimits([min(xAnim-.0001) max(xAnim+.0001)],[min(yAnim-.0001)
max(yAnim+.0001)]);
        geobasemap('satellite')
        pause(.0000001);
        frame = getframe(gcf);
        writeVideo(animVid,frame);
    end

    close(animVid);
end
```

```
%% Clear workspace
clear all
%close all
clc

%% Convert or load pre-converted MP waypoint file
ConvertMPfile = 'load';
% convert - select MP file and run convert
% load - select CSV file previously run through convert
% anything else (or blank) - do nothing and proceed with no null zones

%% USGS Mapping Data
baseURL = "https://basemap.nationalmap.gov/ArcGIS/rest/services";
usgsURL = baseURL + "/BASEMAP/MapServer/tile/${z}/${y}/${x}";
basemaps = ["USGSImageryOnly" "USGSImageryTopo" "USGSTopo"
"USGSShadedReliefOnly" "USGSHydroCached"];
displayNames = ["USGS Imagery" "USGS Topographic Imagery" "USGS Shaded
Topographic Map" "USGS Shaded Relief" "USGS Hydrography"];
maxZoomLevel = 21;
attribution = 'Credit: U.S. Geological Survey';

%% Execute
[baseFileName, folder]=uigetfile('*.csv','Select MANUEL GPS DATA FILE');

% Convert naming character array to string
baseFile = cellstr(baseFileName);

% Load waypoint files iteratively
fullInputMatFileName = fullfile(folder, baseFile);
ManuelData = load(char(fullInputMatFileName));
%dataTable1 =
table(ManuelData(:,1),ManuelData(:,2),ManuelData(:,3),ManuelData(:,4),'Variab
leNames',{'Lat','Long','Speed','Depth'});

if (strcmpi(ConvertMPfile,'convert'))

    [baseFileName, folder]=uigetfile('*.waypoints','Select Mission Planner
.WAYPOINT file');

    % Convert naming character array to string
    baseFile = cellstr(baseFileName);

    % Load waypoint files iteratively
    fullInputMatFileName = fullfile(folder, baseFile);
    data = readmatrix(char(fullInputMatFileName),'FileType','text');

    % Parse out the relevant portions of the waypoint file
    % Lat, Long, Alt (AGL), use airspeed (as read by UgCS, not MP)
    % Removes home location and home alt
    WaypointData = data(2:end,9:10);
```

```
    % Get filename without the extension, used for output file naming
    [~, baseNameNoExt, ~] = fileparts(char(baseFile));

    % Get the name of the input.mat file and save as input_GPS.csv
    UgCS_output = sprintf('%s_converted.csv', baseNameNoExt);
    fullOutputMatFileName = fullfile(folder, UgCS_output);
    % Write data to text file
    writematrix(WaypointData, fullOutputMatFileName);
    clear data baseFile baseFileName baseNameNoExt folder
fullInputMatFileName fullOutputMatFileName UgCS_output

end
if (strcmpi(ConvertMPfile,'load'))

    [baseFileName, folder]=uigetfile('*.csv','Select Null Zone GPS Boundary
File (*_converted.csv)');

    % Convert naming character array to string
    baseFile = cellstr(baseFileName);

    % Load waypoint files iteratively
    fullInputMatFileName = fullfile(folder, baseFile);
    WaypointData = load(char(fullInputMatFileName));

    clear baseFile baseFileName folder fullInputMatFileName

end


%% Null Zoning
latGrid = linspace(min(ManuelData(:,1)), max(ManuelData(:,1)),
length(unique(ManuelData(:,2))));
longGrid = linspace(min(ManuelData(:,2)), max(ManuelData(:,2)),
length(unique(ManuelData(:,2))));

[X,Y] = meshgrid(latGrid, longGrid);
clear latGrid longGrid

if(exist('WaypointData')==1)
% Determines what data points (X,Y) are inside null zone (data2)
in = inpolygon(X,Y,WaypointData(:,1),WaypointData(:,2));

X_red = X(in);
Y_red = Y(in);
clear X Y in
Z = griddata(ManuelData(:,1), ManuelData(:,2), ManuelData(:,3), X_red,
Y_red,'natural');
T = griddata(ManuelData(:,1), ManuelData(:,2), ManuelData(:,4), X_red,
Y_red,'natural');
```

```
X_fin = X_red(~isnan(T));
Y_fin = Y_red(~isnan(T));
T_fin = T(~isnan(T));
clear Y_red X_red

figure(1)
gx1=geoaxes();

% Adding the ~ before "in" plots all data OUTSIDE the null zone
% Removing the ~ before "in" plots all data INSIDE thelp he null zone
geoscatter(gx1,X_fin,Y_fin,[],T_fin);
geobasemap('satellite')
%gx1.ZoomLevel = 19;
title('Horse Creek Cove Depth Map');
legend('ft');
colorbar();

else
Z = griddata(ManuelData(:,1), ManuelData(:,2), ManuelData(:,3), X,
Y,'natural');
T = griddata(ManuelData(:,1), ManuelData(:,2), ManuelData(:,4), X,
Y,'natural');

figure(1)
gx1=geoaxes();


% Plots without regard for null zones
geoscatter(gx1,X(:),Y(:),[],T(:));
geobasemap('satellite')
%gx1.ZoomLevel = 14;
title('pH of Lake McMurtry');
end
```

VITA

Muwanika Jdiobe

Candidate for the Degree of

Masters of Science

Thesis: DESIGN AND DEVELOPMENT OF A WATER OBSERVATORY: AN AUTONOMOUS ENVIRONMENTAL SAMPLING SYSTEM FOR IN-SITU SENSING OF LAKES AND RIVERS.

Major Field: Mechanical and Aerospace Engineering

Biographical:

Education:

Completed the requirements for the Master of Science in Mechanical and Aerospace Engineering at Oklahoma State University, Stillwater, OK in 2020.

Completed the requirements for the Bachelor of Science in Mechanical and Aerospace Engineering at Oklahoma State University, Stillwater, OK in 2020.

Professional Membership:

American Institute of Aeronautic and Astronautic